Functional Analysis of a Supersoluble Fish Antifreeze Protein

(高溶解性魚類不凍タンパク質の機能解析)

By

SK. MAHATABUDDIN

(March 2017)

北海道大学
HOKKAIDO UNIVERSITY

Functional Analysis of a Supersoluble Fish Antifreeze Protein

(高溶解性魚類不凍タンパク質の機能解析)

A dissertation submitted to Division of Life Science, Graduate School of Life Science, Hokkaido University, for the fulfillment of the Degree of Doctor of Philosophy in Life Science

By

SK. MAHATABUDDIN

(March 2017)

Transdisciplinary Life Science Course
Division of Life Science
Graduate School of Life Science
Hokkaido University
Sapporo 060-0810, Japan

Contents

List of Tables

List of Figures

List of Abbreviations

IBP	Ice binding protein
AFP	Antifreeze protein
CD	Circular dichroism
native bpAFP	Isoform mixture of the antifreeze protein purified from fish muscle
rbpAFP	Recombinant protein of the dominant isoform of barfin plaice AFP
FIPA	Fluorescence-based ice plane affinity
T_f	Freezing point
T_m	Melting point
TH	Thermal hysteresis
CISC	Critical ice shaping concentration
nfeAFP	AFP from *Zoarces elongatus Kner*
lpAFP	AFP from *Brachyopsis rostratus*
AFGPs	Antifreeze glycoproteins
*Tm*AFP	*Tenebrio molitor* AFP
wfAFP	Type I HPLC6 isoform of *Pleuronectes americanus*
*Cf*AFP	AFP from *Choristoneura fumiferana*
IBS	Ice binding site
RiAFP	AFP from *Rhagium inquisitor*
iwAFP	AFP from *Campaea perlata*
sfAFP	AFP from Hypogastrura harveyi
*Mp*AFP	AFP from *Marinomonous primoryensis*
DcAFP	AFP from *Daucus carota*
LpIBP	AFP from *Lolium perenne*
*Tis*AFP	AFP from *T. ishikariensis*
Cn-AFP	AFP from *Chaetoceros neogracile*
FfIBP	IBP from F*lavobacterium frigoris*
ColAFP	AFP from *Colwellia* sp. SLW05
*Tis*AFP8	Isoform of *Tis*AFP
NagAFP	AFP from *Navicula glaciei*
Maxi	Type Ih AFP from *Pleuronectes americanus*
lpAFP	AFP from *Brachyopsis rostratus*
srAFP	AFP from *Hemitripterus americanus*
FIPA	Fluorescence-based ice plane affinity
nfeAFP6	6th isoform of the AFP from *Zoarces elongatus Kner*
Trx	Thioredoxin
NTA	Nitrilotriacetic acid
AFP9	Type I AFP from *Pleuronectes americanus*
LS-12	Type I AFP from *Myxocephalus octodeceimspinosis*
LpAFP	AFP from *Lolium perenne* grass
nfeAFP2	2nd isoform of the AFP from *Zoarces elongatus Kner*

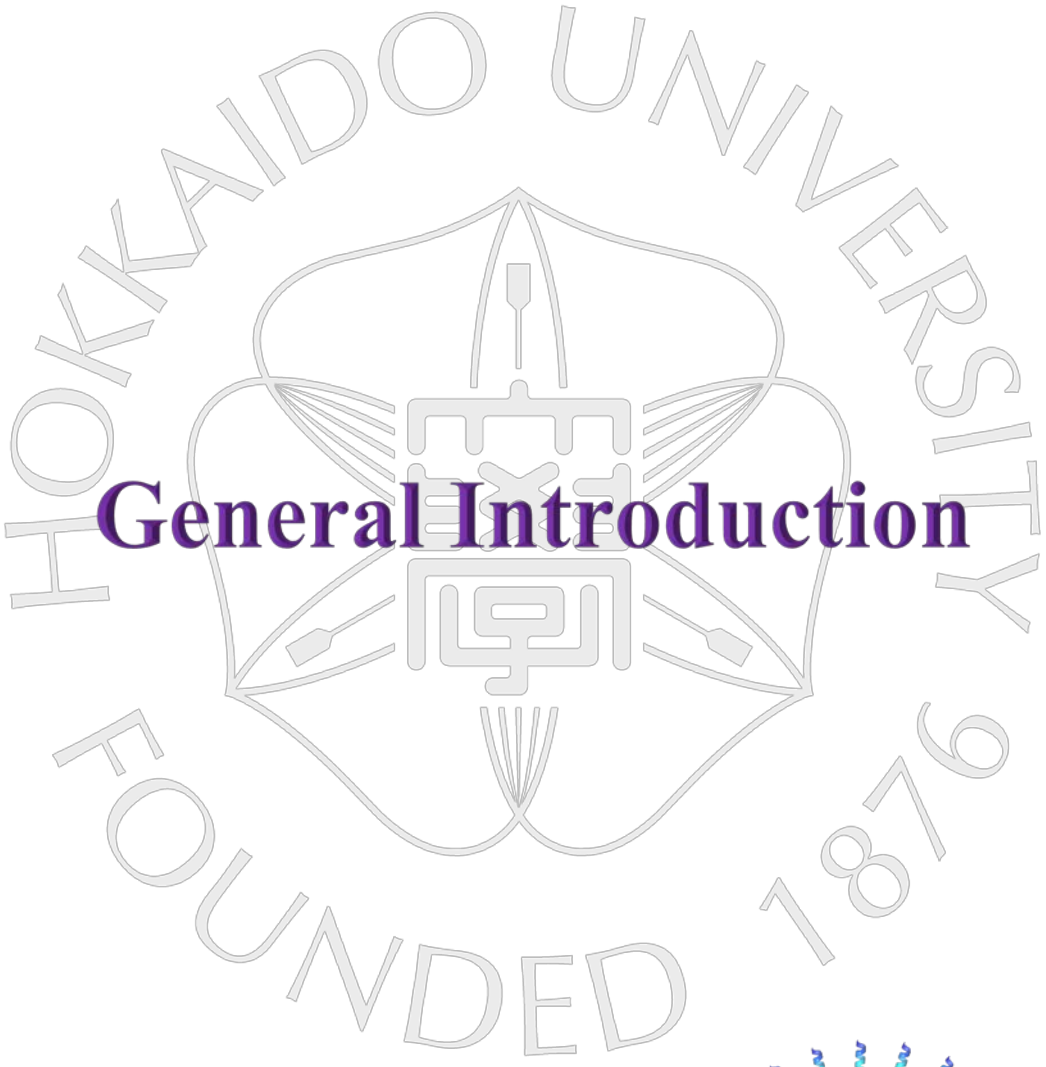

General Introduction

Chapter: 1

1.1 Proteins

Proteins are the most abundant biopolymers among all the macromolecules found in living systems. They are linear polymer of amino acids. Amino acids combine with each other through peptide bond to form these macromolecules. Proteins folded up into three-dimensional structure. Their three-dimensional structures are determined by the sequence of the amino acids (Berg et al. 2002). Such one to three dimensional structures make proteins extremely plastic. It helps them to adopt variety of shapes. They also can interact with one another and other biological macromolecules to form different complex assemblies. All these properties provide the prerequisite abilities to the proteins to perform crucial functions essentially in all biological processes.

1.1.1 Functional Proteins

It is not true that all proteins played crucial functions in the biological processes. Proteins having the biological activity are known as functional proteins. For example, immunoglobulins serve as the cell-surface receptor for antigens and soluble effector molecules, which can individually bind and neutralize antigens at a distance (Schroeder and Cavacini, 2010). Human lithostathine, a protein synthesized by the pancreas, inhibits the growth of calcium carbonate crystals through binding onto the grain crystal surfaces to prevent lithiasis (Gerbaud et al., 2000). Another calcite binding protein ovocleidin-17 found in the ovaries of hens (Freeman CL et al, 2012). Materially, functional proteins are synthesized by any living systems depending on their necessity to accomplish different biological activities *in vitro* or *in vivo*. Some of them are synthesized to carry out the ordinary processes and some to facilitate their survival in extreme environments.

1.2 Life at extreme environments

The environments other than sustainable for common organisms can be called as extreme environments. Salt lakes (high salinity), deep sea (high pressure), hot springs (high temperature), Polar regions (icy environments) and high acidic or basic water are the representative environments could be designated as extreme environments. The organisms living in extreme environments are known as extremophiles (Wharton, 2002). Extremophiles have the capacity to adapt with such unusual environments. Enzymes expressed by some archaea and eubacteria living in hot spring are active at high temperatures around 100°C. Such type of extremophiles are denoted as “thermophiles” (Koga, 2012). In contrast, extremophiles living in icy environments are referred as “psychrophiles” (Feller and Gerday, 2003). They have the ability to perform their biological processes even in sub-zero temperatures which is a prerequisite condition to survive in such harsh environment. Consequently, extremophiles need to survive by adopting not only to temperatures but also to further environmental constraints.

1.2.1 Strategies of cold adaptation in different organism

Earth is mostly cold and the major portion of ecosystem exposed to temperatures below 5°C. The Polar Regions covered 15% of the earth surface which covered with ice all over the year (Feller and Gerday, 2003). In addition to this, earth surface has notable regions that experience sub-zero temperatures during winter season. The processes that are utilized by the habitant of such harsh environments to adopt themselves with surroundings are known as cold adaptation. Cold adaptation not only assists the psychrophiles to maintain internal biological reactions but also help to maintain fluidity of the body fluids or membranes. To keep the fluidity they need to prevent formation of ice crystals *in vivo* and/or *in vitro*. Ice crystals can rapture the cell membranes or create a pseudo-scarcity of liquid water, the necessary solvent as well as reactant of many biochemical reactions. Formation of ice crystals also increases the solute concentrations that generate excessive osmotic pressures. Such osmotic pressure induces the dehydration of cells leading to the critical damage for the cells. Consequently, controlling of the ice crystal growth is an important strategy adopted by psychrophilic organisms. These organisms evolved a set of powerful physiological and molecular level adaptations to counter the effects of cold stress. Production and utilizations of polyols, ice nucleators, antifreeze proteins (AFPs) and any other molecules are referred as molecular level adaptations (Doucet et al., 2009). These molecules act in two different manners, colligative and non-colligative, to lower the freezing temperature of the body fluids. AFPs belong to the group of macromolecules named ice binding proteins (IBPs) depresses the freezing temperature in non-colligative manner (Yeh and Feeney, 1996).

1.3 Ice binding proteins (IBPs)

IBPs are special class of proteins that can interact specifically with ice crystals at temperatures below the melting point of the solution. These proteins have important roles for molecular level cold adaptation in psychrophilic organisms. IBP was first discovered in 1969 from Antarctic Notothenioid fish (DeVries and Wohlschag, 1969). Since then IBPs have been identified and characterized in variety of organisms (Fletcher et al., 2001; Duman, 2001; Duman and Olsen, 1993). IBPs are not only structurally diverse proteins but they also showed different functions. Binding of IBPs to ice change the morphology and growth kinetics of the ice crystals. Therefore, understanding the functional activities and physicochemical properties of these ice crystal growth modifiers could offer to develop innovative strategies for cryoprotection, cryopreservation, hypothermic preservation, anti-icing and deicing technologies.

1.3.1 Classification of IBPs

IBPs are divided into at least four different groups, ice structuring proteins (ISPs), ice adhesion proteins (IAPs), ice nucleation proteins (INPs) and antifreeze proteins (AFPs), depending on their functional activities. ISPs consists a group of proteins that can structured the ice crystal in different shapes to halt Ostwald ripening

or particularly ice recrystallization. Ice structuring activity of plant extracts were first reported by Griffth et al. in 1992. ISPs were synthesized by different overwintering plants (Griffith and Yaish, 2004). Guo et al. recently reported about an extraordinary large (1.5-MDa) protein in an Antarctic bacterium that act as adhesive to transiently bind the host bacteria to ice. These type of proteins are referred as IAPs. On the other hand, INPs act nearly opposite to the ISPs. These proteins catalyze ice formation at the temperatures ranging from -2 to -12 °C to impose frost injury to the frost-sensitive plants (Gurian-Sherman and Lindow, 1993). The last type of proteins are known as AFPs for their ability to shape the ice crystal by adsorbing onto the ice crystal surfaces and inhibit its growth.

1.4 Antifreeze proteins (AFPs)

AFPs adsorbed to the ice nuclei formed in supercooled solutions and arrest their growth. These proteins have been discovered from diverse class of organisms (such as, fish, insect, fungi, bacteria, fly and plants) since 1969 (DeVries and Wohlschag, 1969). Their non-colligative depression of freezing temperature of the blood or the body fluids facilitate the cold survival of psychrophiles at extremely cold environments. This depression of the freezing temperature is 100~1000 times higher than that of colligative depression based on molar concentrations, especially, at lower concentrations (Yeh and Freeney, 1996). The combination of colligative and non-colligative depression of freezing point assisted marine fishes to survive in such harsh environments (Jia and Davies, 2002) (Fig. 1.4.1). This non-colligative depression of the freezing temperature of the fluids consisting AFPs is denoted as thermal hysteresis (TH). AFPs from different organisms exhibits different range of TH activities (Jia and Davies, 2002; Fletcher et al., 2001; Duman, 2001). In addition to ice-binding ability they are capable to interact with different substrates other than ice. As for example, Wang et al. reported that AFPs naturally bind to nucleoside crystals other than ice nuclei. These proteins also bind to the cell membrane to prolong the storage of cell at hypothermic conditions (at 4 °C) (Kamijima et al., 2013). The outcomes of these studies extending the possibilities of application of AFPs in myriad research fields without altering their amino acid sequences.

1.4.1 Evolutional background of AFPs

Though AFPs are evolved to accomplish similar functions although their 3D structures showed remarkable divergence. The reason of such remarkable diversity has been explained as convergent evolution in which organisms evolved their own AFP independently from different origins to protect themselves from glacial damages (Cheng, 1998; Scott et al, 1986). Appearance of the ice in the sea level dates back to 10-30 million years ago in the southern hemisphere and 1-2 million years ago in the northern hemisphere (Kerr, 1984; Shackleton et al., 1984). The inhabitants of this ice laden environments, at least the fishes, has been claimed to evoked to produce AFPs to survive in this extreme conditions (Cheng, 1998; Fletcher et al., 2001). However, AFPs

interact with ice crystal irrespective of their origin. Though different AFPs recognize different set of oxygen atoms at distinct planes of ice crystals (See details at Chapter 1.5) (Basu et al., 2014). Consequently, the diversity of ice structures has been proposed as another ingredient to diversify their 3D structures (Fletcher et al., 2001; Jia and Davies, 2002).

1.4.2 Classification of AFPs

Since 1969 to date more than dozens of AFPs have been identified from different organisms. They can be classified depending on two different categories, classification based on origin and classification based on functional activities. The classification based on origin can described as follows:

Fish AFPs

About five decades before marine researchers discovered that the marine fishes express a high concentration of antifreeze substances to keep fluidity of their body fluids (DeVries and Wohlschag, 1969). These antifreeze glycoproteins (AFGPs) present in millimolar concentrations in fish blood to stop ice crystal growth in Antarctic Notothenioid fishes. Following the discovery of AFGPs, a notable types of AFPs have been characterized in a variety of fishes from both the Polar regions and nearby temperature zones (Fletcher et al., 2001). More detail about fish AFPs are discussed in chapter 1.4.3.

Arthropod AFPs

The territorial arthropods experienced more severe cold temperatures (~-30°C) than polar fishes (Grather and Sykes, 2004). Naturally they produce antifreezes to survive in this harsh environments. The common yellow meal-worm beetle, *Tenebrio molitor*, AFP is the first arthropod AFP reported by Graham et al. in 1997. This Thr- and Cys-rich AFP (*Tm*AFP) (Fig. 1.4.2a, A) with more than double molecular weight (8.4-kDa) of winter flounder AFP (wfAFP) exhibited up to 100 times of the specific activity of common fish antifreeze proteins. It folds into right-handed β-helix structure (Liou et al., 2000). The Thr-X-Thr (T-X-T) pattern in the ice binding site (IBS) of this AFP was reported as the reason for its hyper TH activities (Liou et al., 2000).

A 9-kDa arthropod AFP *Cf*AFP has been identified and characterized from a moth, spruce budworm (*Choristoneura fumiferana*) (Tyshenko et al., 1997). It has been characterized as Thr- and Cys-rich protein with an IBS consisting of T-X-T pattern similar to *Tm*AFP in spite of its left-handed β-helix structure (Gauther et al., 1998; Graether et al., 2000; Li et al., 2005) (Fig. 1.4.2a, B).

An AFP (RiAFP) was discovered in a freeze-avoiding longhorn beetle, *Rhagium inquisitor* (Kristiansen et al., 1999). This 13-kDa RiAFP shows TH of around 6.5°C and forms a silk-like β-helical (solenoid) structure (Kristiansen et al., 2011).

The homogenate of an inchworm, larvae of the pale beauty moth *Campaea perlata*, shows a high TH activity of 6.4°C. This TH activity was contributed by two Thr-Ala rich AFP (iwAFP) isoforms having molecular weight 3.5 and 8.3-kDa (Lin et al., 2011). The silk-like β-helical structure has been proposed for the 8.3-kDa isoform of iwAFP.

A member of primitive arthropods snow fleas, *Hypogastrura harveyi*, body extract displays a TH activity of 5.8°C. The biochemical analysis revealed that this TH activity came from two different glycine rich isoforms of snow flea AFP (sfAFP) having 6.5 and 15.7-kDa molecular weight (Graham and Davies 2005). The X-ray structure of the smaller isoform exhibited that it composed of six antiparallel left-handed polypropline type II (PPII) helices, stacked in two sets of three, to form a compact brick-like structure with one hydrophilic face and one hydrophobic face (Pentelute et al., 2008). The structure of the less abundant larger isoform has been predicted as strictly amphipathic in nature with a hydrophilic surface on one side and a hydrophobic, putative ice-binding surface on the other. It consists of 13 PPII helices connected by proline-containing loops stacked into two flat sheets oriented antiparallel to one another (Mok et al., 2009).

An antifreeze protein in the larvae of a fly named midges, *Thecodilosis japonesis*, has been identified and partially characterized by Li Y et al (2000). The major isoform of the Lake Ontario midges has a 10 residue tandem repeating sequence xxCxGxYCxG, with regularly spaced cysteines, glycines and tyrosines comprising one half of its 79 residues. Its structure has been predicted as tightly wound left handed solenoid fold in which the cysteines form a disulfide core to brace each of the eight 10-residue coils (Basu et al., 2015).

Bacterial AFPs

Identification of bacterial AFPs began with the name Duman and Olsen (1993). They reported the presence of antifreeze proteins in *Rhodococcus erythropolis* and *Micrococcus cryophilus*. An AFP with approximately 164-kDa was identified from *Pseudomonas putida* (Sun et al. 1995). This glycine and alanine rich protein consists both carbohydrate and lipid moiety. It exhibited unusual ice nucleation ability that is absent in other AFPs. The removal of the 92-kDa carbohydrate moiety diminish the ice nucleation ability without altering the antifreeze activity of this protein (Xu et al. 1998). A 52-kDa bacterial AFP with a lipid moiety has been identified and characterized from *Moraxella sp* (Yamashita et al., 2002). It alters the ice crystal morphology to hexagonal bipyramid. In addition, an 80-kDa AFP with very low TH activity has been identified in a *Pseudomonas fluorescens* (Kawahara et al., 2004). This bacteria also produce an ice-nucleating protein.

A bacterial AFP (*Mp*AFP) (Fig. 1.4.2a, C) with higher TH activity (2°C) has recently been identified and characterized from an arctic lake bacterium,

Marinomonous primoryensis (Gilbert et al., 2005). MpAFP is a calcium dependent 34-kDa protein. It is a part of 1.5-MDa adhesion protein localized in the cell surface of the bacterium (Granham et al., 2008; Guo et al., 2012). It contains β-helical fold containing xGTGND repeat motif in every turns of its IBS. Its IBS also consists an array of Ice-like surface waters that are anchored by hydrogen bonds directly to the polypeptide backbone and adjacent side chains (Granham et al., 2011). A gram negative bacterium *Colwellia* strain SLW05 from Antarctic sea ice produces an extracellular protein (*Col*AFP) with ice binding activities (Raymond et al., 2009). Its crystal structure has been solved by Hanada et al. (2014).

Plant AFPs

Plants are one of the essential and largest member of the living organisms. They also have to face extreme environments like ice-laden environments. Freezing is unavoidable for the plants at such environments. Plants experienced freezing injury caused by dehydration for the formation of ice crystals in their intercellular spaces (apoplast) (Pearce et al., 2001). Such detrimental effects of ice formation have been believed to be minimized by using AFPs (Griffith and Yaish, 2004). The antifreeze activity in plants was first reported in 1992 (Urrutia ME et al., 1992). The plant AFPs not only supports them to tolerate freezing temperatures but also provide protection against psychrophilic pathogens. A plant AFP from a common vegetable, carrot (*Daucus carota*), has been characterized as a leucine rich AFP (DcAFP, Mw = 36-kDa) (Worrall et al. 1998). It composed of 24-amino acid tandem repeats and inhibits ice recrystallization effectively at 1 μg/mL concentration. Its recombinant protein has been prepared and characterized (Zhang et al., 2004). Another plant AFP (LpIBP) has been identified and characterized from a forage grass, perennial ryegrass (*Lolium perenne*). This 11-kDa LpIBP is extremely heat-stable protein consists of 118 amino acid residues (Sidebotttom et al., 2000). It folds as a left β-roll structure with eight 14- and 15-residue coils (Middelton et al., 2012) (Fig. 1.4.2a, D).

AFPs from other sources

Fungi possess the enormous capability to adopt with and survive in different extreme environments. They are found in everywhere of this earth even in the frozen Polar regions. Consequently, they utilize cold adaptation process to survive in such harsh environment. Presence of AFP in fungi was first reported by Duman and Olsen (1993). It was also reported that the culture medium of the snow mold fungi display antifreeze activity (Snider et al., 2000). The fungal AFP was first time purified and recombinantly prepared by Hoshino et al (2003). They also characterize this fungal AFP (TisAFP) at the molecular level. The TisAFP composed of 223 amino acid residues and exhibited TH activity approximately 1°C at 20 $mg \cdot mL^{-1}$. Its crystal structure has been determined by Kondo et al. at 0.95-Å resolution (2012) (Fig. 1.4.2a, E). It consists an irregular β-helix with six loops of 18 or more residues that lies alongside an α-helix. A 28-kDa fungal AFP has been identified in *Antarctomyces psychrotrophicus* (Xiao et al. 2010).

The IBPs has also been identified from Antarctic sea ice diatoms, *Navicula glaciei* and *Fragilariopsis cylindrus* (Janech et al., 2006). Another Antarctic diatom, *Chaetoceros neogracile*, produce an AFP (Cn-AFP) of Mw 29.2-kDa (Gwak et al., 2010). The Cn-AFP changed the ice crystal morphology to elongated hexagonal shape. In contrast, ice crystal morphologies alter to snowflake and dendritic patterns in the presence of the isoforms Pg-1-AFP and Pg-2-AFP from an Antarctic chlorophyte, *Pyramimonas gelidicola* (Jung et al., 2014), respectively.

Hitherto, several homologues macromolecules containing ice-binding activity have been identified in diatoms (Raymond and Morgan-Kiss, 2013), unicellular algae (Raymond and Kim, 2012), bacteria (Raymond et al., 2007; 2008; and Do et al., 2012), a copepod (Kiko, 2012) and other fungi (Raymond and Janech, 2009; Lee et al., 2010). Though, the exact route for evolution of the common gene encoding these AFPs/IBPs in those organisms is still mysterious although convergent evolution of the AFP carrying gene has been proposed (Basu K et al., 2015). In addition, horizontal transfer from bacterial origin also been proposed (Bayer-Giraldi et al., 2010; Raymond and Kim, 2012). However, discovery and characterization of different AFPs have been enriched our knowledge about the evolution of these unique ice crystal modifiers.

The classification based on activities are described below-

The activities of ordinary AFPs have been evaluated using two concentration dependent physicochemical properties, TH and ice recrystallization inhibition (IRI). Accumulation onto the ice surfaces is the major functional activities of AFPs, while they exhibit different numerical values of TH activities at molar concentration after bound to the embryonic ice crystals. Therefore, they are divided into two different groups, hyperactive and moderate active AFPs (Scotter et al., 2006 and Bar-Dolev et al., 2012) (Fig. 1.4.2b). The moderate active AFPs can exhibit TH values 0.5 to 1°C at their mM concentrations. Almost all fish AFPs, Midge AFP, plant AFPs and antifreeze glycoproteins are categorized as moderate active AFPs. Whereas, the hyperactive AFPs could display similar TH values at hundredth times lower peptide concentrations and extended to 6°C at a maximum. The AFP from meal-worm beetle, *Tm*AFP, has documented as first hyperactive AFP (Graham et al., 1997). In addition, the arthropod AFPs, *Cf*AFP, iwAFP, sfAFP and RiAFP, a fish AFP (type Ih, Marshall et al., 2004), bacterial AFP (*Mp*AFP, FfIBP and *Col*AFP) (Raymond et al., 2007; Do et al., 2012 and Hanada et al., 2014), a fungal AFP, *Tis*AFP8 (Xiao et al., 2010) and a diatom AFP, NagAFP (Janech et al., 2006) have been regarded as hyperactive AFPs.

These two group of AFPs are not only differ in their observed TH activities but also in exhibition of the ice crystal bust patterns rapid growth of the ice crystal at the lowest range of TH. The ice crystals busted along *c*-axis in the presence of moderate AFPs (Raymond et al., 1989) whereas, bust patterns are perpendicular to the *c*-axis were observed in the presence of hyperactive types (Graether et al., 2000). The reason

for such difference in the activities of AFPs from different origin have been advancing by research based on their concentration-dependent physicochemical properties.

1.4.3 Fish AFPs

Presence of a non-colligative freezing-point-depressant in the serum of the Antarctic marine fishes has been reported more than four decades before (DeVries and Wohlschlag et al, 1969). Since then, AFPs have been identified in different fishes living in the Polar region and its proximal temperature area (Fletcher et al., 2001). To date, five types of fish AFPs have been identified and characterized: type I, α-helical alanine rich (Mw: 3.3-4.5-kDa) proteins (Fig. 1.4.3A); type II, ~14-kDa proteins having high level of structural similarities with C-type lectins (Fig. 1.4.3B); type III, ~7-kDa globular proteins containing short β strands (Fig. 1.4.3C); type IV, predicted as helix bundle protein with 12-kDa molecular weight; type Ih, four helix bundle protein consisted of 65% alanines (Harding etal., 1999, Fletcher et al., 2001; Nishimiya et al., 2008 and Sun et al., 2014). The type Ih (Maxi) is only known hyperactive AFP has recently been characterized from a flat fish winter flounder, *Pleuronectes americanus* (Marshall et al., 2004, 2005 and Sun et al., 2014) (Fig. 1.4.3D). Maxi can surmounted the ice crystals entirely to change their morphologies to lemon shaped and protect this fish from freezing.

Lemon shaped ice crystal was also observed in the presence of a Ca^{2+} independent type II AFP, lpAFP (Nishimiya et al., 2008). It was identified and purified from longsnout poacher, *Brachyopsis rostratus*. Another Ca^{2+} independent type II AFP (srAFP) has also been identified and characterized from a cottid fish, sea raven (*Hemitripterus americanus*) (Ng NF et al., 1986). It is notable that type II AFP has two different subclasses of peptides, Ca^{2+} dependent and Ca^{2+} independent. The Ca^{2+} dependent type II AFPs have been identified from Japanese smelt (*Hypomesus niponensis*) (Yamashita et al., 2003), rainbow smelt (*Osmerus Mordax*) and Atlantic herring (*Clupea harengus harengus*) (Ewart and Fletcher, 1990). A glutamine rich Type IV fish AFP has been identified from longhorn sculpin, *Myoxocephalus octodecimspinosis* (Deng G et al, 1997).

The type III AFPs have been identified in Arctic and Antarctic eelpouts (*Austrolycicthys brachyeephalus, Lycodes Polaris* and *Lycodichthys dearborni*), Atlantic ocean pout (*Macrozoarces americanus*), Atlantic wolffish (*Anarhichas lupus*) and Notched-fin eelpout (*Zoarces elongatus Kner*) (Cheng and DeVries, 1989; Schrag et al., 1987; Hew et al., 1984; Scott et al., 1988 and Nishimiya et al., 2005) These globular shape AFPs characterized by internal twofold symmentry of the 'pretzel' fold that provides a flat amphipathic IBS (Jia et al., 1996, Graether et al., 1999 and Granham et al., 2010). However, irrespective of the source all these type III AFPs altered the hexagonal ice crystal morphology to hexagonal bipyramidal shape.

The bipyramidal ice crystals were also observed in the presence of the type I AFPs. These type of polypeptides have been identified and characterized from Winter flounder (*Pseudopleuronectes americanus*) (Duman and DeVries, 1974), Yellowtail flounder (*Limanda ferruginea*) (Scott et al., 1987), Alaskan plaice (*Pleuronectes quadritaberulatus*) (Knight et al., 1991), Shorthorn sculpin (*Myoxocephulus scorpius*) (Hew et al., 1985), Grubby sculpin (*Myoxocephulus aenaeus*) (Chakrabartty et al., 1988), Arctic sculpin (Yang et al., 1988) and cunner (*Tautogolabrus adspersus*) (Hobbs et al., 2011). The HPLC6 isoform from winter flounder has been extensively studied among all type I AFPs (Davies and Hew, 1990; Knight et al., 1991; Sicheri and Yang, 1995; Gronwald et al., 1996 and Sönnichsen et al, 1998). A new α-helical 40 residual polypeptide (bpAFP) has recently been identified and characterized from barfin plaice (*Liposetta pinnifasciata)* (ii, this thesis).

1.5 Structure of the ligand of AFPs: Ice

The ice, target ligand of AFPs, is a lattice arrangement of water molecules with a particular geometry (Hobbs, 1974). It exists in numerous crystalline forms depending on the temperature and the pressure in which they are formed. Therein, hexagonal ice (I_h) (Fig. 1.5A) is the most common formation of ice available to the organisms. The hexagonal ice crystal forms under normal atmospheric pressure and at around 0°C temperature. Its structure was determined using X-ray diffraction. Its hexagonal symmetry resulted from the tetrahedral coordination of the oxygen atoms in the lattice. It possesses different patterns of oxygen atoms that presented on the surface of distinct planes defined by Miller-Bravais indices. These planes are designated by the reciprocal of the distances from the center of the unit cell to where they intersect each axes (a_1, a_2, a_3 and c). The line above the distance represents that it is in negative direction. It always satisfy the expression $-a_3 = a_1 + a_2$ for the hexagonal plane defined by the three *a*-axes. In the hexagonal lattice the basal plane intersects the *a*-axes at infinite distance and the *c*-axis at 1. The reciprocals of infinity and 1 are 0 and 1, respectively. Therefore the Miller-Bravais index ($a_1\ a_2\ a_3\ c$) for the basal plane is (0001) (Fig. 1.5B). On the other hand, both the primary and secondary prism planes are perpendicular to *c*-axis, hence, they cut this axis at infinity. The former planes are parallel to the sides of the hexagonal unit cell and have indexes, such as, (01-10) (Fig. 1.5C). The latter one, secondary prism planes, perpendicular to *a*-axes can also be represented with the indexes, for example, (2-1-10) (Fig. 1.5D). Similarly, the pyramidal planes intersect the unit cell at different angels and have the indexes, for example (1-101) (Fig. 1.5E) or (1-102) of which last one will be closer to basal plane. The ability of the AFPs to recognize the arrangement of water molecules in different planes is an important aspect of any structure-function analysis of these ice crystal modifiers. The interactions of these polypeptides with ice has been summarized by Hew and Yang (1992).

1.5.1 Ice plane specificity of fish AFPs

The fact of having different surfaces in the ice crystal lattice have been accounted as one of the reason for AFPs structural diversity (Davies et al., 2002). Therefore, the investigation of the ice plane specificity is one of the essential information for characterization of AFPs. The experimental method for the determination of ice plane specificity was developed by Knight et al (1991) and defined as ice-etching technique. The ice-etching technique has been improved by Garnham et al. (2010). They replace the ordinary AFP solutions with fluorescent labeled AFP solution that can visualize the ice-binding planes of these proteins through UV-illumination. It was defined as fluorescence-based ice plane affinity (FIPA) analysis (see details in chapter 4.3).

The ice plane specificity of different AFPs has been examined using both the ice-etching and FIPA analysis. The type I winter flounder HPLC6, wfAFP, and Alaskan plaice AFP adsorbed onto the (20-21) pyramidal planes (Knight et al., 1991; Basu et al. 2013). In contrast, another type I AFP, sculpin AFP, bind onto the (2-1-10) secondary prism planes (Knight et al., 1991). A type II AFP, lpAFP, adsorbed onto the prism and pyramidal planes (Nishimiya et al., 2008; Basu K et al. 2013). The type III AFP from Notched-fin eelpout, nfeAFP, can bind onto the pyramidal and/or prism planes of the ice crystals (Garnham et al., 2010; Basu et al., 2013). The multiple ice plane specificity including basal planes has been reported for the type Ih AFP from winter flounder, Maxi (Sun et al., 2014).

Entirely fluorescent ice hemispheres are also observed as concentration-dependent manner in the presence of fluorescently labeled bpAFP (iii, in this thesis). It is notable that this is the first report of concentration-dependent ice plane specificity and to date bpAFP is the sole type I AFP molecule to exhibit such specificity.

1.5.2 Ice-shaping ability of AFPs

The modification of the ice crystal morphology and growth kinetics are the primitive characteristics of AFPs. In the absence of ice crystal modifiers, such as AFPs, the uniform growth of all the planes except for the basal planes provide a disc like ice crystal (Fig. 1.6). In the presence of AFPs, AFP molecules get adsorbed onto specific planes and impeded this uniform growth of those planes. The AFP adsorbed planes converted to the plane consisting microcurvatures between the ice-bound-AFP molecules that is energetically less favorable for ice formation. These growth-terminated surfaces become crystal facets, which is a sign of growth inhibition effect of AFPs (Davies and Hew., 1990; Hew and Yang 1992). Such terminated growth towards prism and/or pyramidal planes alters the ice crystal morphology to bipyramidal in the presence of type I and II AFPs (Davies et al., 2002; Takamichi et al., 2007, i). In contrast, lpAFP and Maxi changed the ice crystal morphology to lemon shaped, while rice-grain-like ice crystal was observed in the presence of sfAFP, AFP from snow flea (Graham and Davies, 2005). Lemon shaped ice crystals were also observed in the solution containing *Tm*AFP (Graham et al., 1997).

1.6 Physicochemical activities of AFPs

Crystallization depends largely on the surface phenomenon as a growing crystal has contact with its mother liquor. Growing of ice crystal also follow the similar mechanism in which water molecules from bulk solution migrate to the ice water interface and accumulate into the ice crystal lattice. Arresting the ice crystal growth and such migration of the water molecules are the fundamental properties of the AFPs. Therefore, activity of AFPs mainly been evaluated by two concentration dependent physicochemical parameters, TH and IRI. The mechanism proposed as "adsorption inhibition" is still generally accepted mechanism by which AFPs inhibit the ice crystal growth and depress the freezing temperature (Raymond and DeVries 1977). According to this hypothesis, the AFP molecules get absorbed onto the relatively flat ice fronts that makes curved ice fronts between the adsorbed AFP molecules. Curved ice fronts obstacle new water molecules to be ordered and stops the formation of new ice (Fig. 1.6a). Adsorbed AFPs also decrease the free energy of the surface to make the ice formation procedure thermodynamically unfavorable even at supercoiling temperatures (Raymond and DeVries 1977; Knight et al. 1991). Such adsorption depress the freezing temperature (T_f) and elevates the melting temperature (T_m) slightly to create a significant gap between melting and freezing temperature of an AFP adsorbed embryonic ice crystals (Celik et al., 2010). This depression (T_m - T_f) of freezing temperature is defined as TH (Fig. 1.6b). The rapid growth of the ice crystals were observed at the last limit of TH (T_f) which also known as busting temperature.

The impedimental growth of ice crystal changed the morphology to different shapes, for example bipyramidal shape. Almost all fish AFPs usually exhibited significant TH activities at the minimum concentration approximately 0.5 mg·mL^{-1}. On the other hand, there are some AFPs, such as isoform 2 and 6 of AFP from Notched-fin eelpout (nfeAFP6, nfeAFP2), has no significant TH activities even at 14 mg·mL^{-1} concentration (Nishimiya et al. 2008). It is notable that Notched-fin eelpout produce at least 13 isoforms of AFPs (nfeAFP). Takamichi et al. (2009) reported that the defective isoform, nfeAFP6, can obstacle burst ice growth of the ice crystal. Irrespective of the type or source AFPs inhibit the migration of water molecules to ice. The grain boundary migration is a spontaneous process in all crystalline to decrease the grain boundary area per unit volume that decrease the total energy of the system (Knight et al., 1995). The AFPs inhibit such grain boundary migration after adsorption onto the ice crystals. It stops the formation of large ice crystals at the expense of small crystals, Ostwald ripening. This phenomenon is termed as IRI. The IRI activity has been described as a dominant characteristics of plant AFPs (Smallwood et al., 1999; Jia and Davies, 2002). It should be noted that, it has not been subjected a parameter or mathematical correlation to show a relationship between the TH and IRI. Recently Olijve et al. (2016) reported the first comprehensive evaluation of TH and IRI using cryoscopy, sonocrystallization and recrystallization assays. They could not found any significant correlation between TH and IRI activities. However, the basic criteria to exhibit TH or IRI activity is the binding of AFP onto the ice surface has been widely

accepted and future studies might correlate these two physicochemical parameters in near future.

1.7 Ice-binding mechanism of AFPs

AFPs are remarkable for recognizing the embryonic ice crystals in vast excess (55M) of liquid water to adsorb onto them and arrest their growth (Sharp, 2014). The mechanism of this irreversible binding has been difficult to deduce. However, scientist proposed different adsorption mechanism to explain binding of AFPs to ice at molecular level based on experimental and computational studies. These are-

Hydrogen bonding

The X-ray crystal structure determination of the wfAFP at 2.5Å resolution provided the first mechanistic insight into antifreeze activity (Yang et al., 1988). They proposed a mechanism of antifreeze protein binding to ice surfaces that requires: firstly, the dipole moment from the helical structure dictates the preferential alignment of the peptide to *c*-axis of the ice nuclei; secondly, amphiphilicity, regularly spaced-polar side chain groups (mainly Thr), of the helix; and thirdly, torsional freedom of the side chains to facilitate hydrogen bonding to ice surfaces. This model further supported by Sicheri and Yang (1995) et al. by a series of docking models between AFP and ice based on the refined crystal structure of same AFP (Fig 1.7 A).

Hydrophobic interaction

In 1996 Sönnichsen et al. reported that the IBS of type III AFP is planner and encompasses with relatively non polar residues. Hydrophobic IBS has also been reported for a bacterial AFP, *Mp*AFP (Granham et al., 2008). On the other hand, the mutational analysis of wfAFP displayed that the replacement of the four Thr to Val cannot altered the antifreeze activity significantly. These analysis provide the information that hydrophobic interaction is important than hydrogen bonding (Wen and Laursen, 1992; Haymet et al., 1998; Baardsnes et al., 1999). In addition, the importance of the surface planarity of the IBS of type III AFP was proposed based on its numerous IBS mutants and X-ray structure (DeLuca et al., 1998) (Fig 1.7 B).

Anchored clathrate water

Anchored clathrate water hypothesis was proposed by Nutt and Smith (2008) and experimentally established by Garnham et al. (2011). The authors proposed that, there is a hydration layer around the AFP in aqueous solution. This layer assists the AFP molecule to bind to the molecularly rough ice surfaces. This solvation shell around the IBS of the AFPs become more structured and experiences slowed dynamics at sufficiently low temperatures. It creates a “pre-ordered” region of water molecules in which the barrier to ice formation is reduced (Fig. 1.7). This arranged water molecules are in ice-like arrangement and thought to be directly incorporated into an ice plane with a similar molecular arrangement. Subsequently, these clathrate waters merge with the quasi-liquid layer waters and converted to ice to facilitate the binding of AFPs.

Arrangement of the solvent water molecules in such an order are carried out by the hydrophobic IBS which could be stabilized through hydrogen bonding with the hydrophilic residues on the IBS. In addition, X-ray structure analysis visualized that there are some AFPs that have ice-like surface water molecules on their IBS, such as *Mp*AFP (Granham et al., 2011), *Col*AFP (Hanada et.al, 2014). At present, this model is generally accepted and believed to be true (Sharp, 2011; Hakim et al., 2013; Sun et al., 2014) (Fig 1.7 C).

1.8 Purpose and Scope of this dissertation

The biological ice crystal modifiers, antifreeze proteins (AFPs), can bind onto the surface of ice crystals to alter their morphology and change their growth kinetics. Such ice growth inhibition protects the organisms living in icy environments from glacial damage that facilitate their cold survival. Since 1969 AFPs have been identified in variety of organisms ranging from bacteria to fish. The functional activities and the structure-function relationships have been studied to elucidate the detailed mechanism of ice-binding followed by TH or IRI activities. The knowledge about their detailed mechanism is still under development. Therefore, understanding the functional activities and physicochemical properties of these ice crystal modifiers could offer to develop innovative strategies for cryoprotection, cryopreservation (Pegg, 2010), hypothermic preservation (Kamijima et al. 2013), anti-icing and deicing technologies.

The discovery of new species of AFPs and their characterizations have been led us to a new insight of knowledge about their functional activities and physicochemical properties. The AFPs have been identified from different fishes and characterized as moderately active AFPs except Maxi and ApAFP (Marshall 2005; Gautheir 2005; Scotter et al., 2006; Middleton et al., 2012). Most of these AFPs were purified from blood serum that obstacle mass purification, a prerequisite condition for scientific and technological application of AFPs. The mass purification of type III nfeAFP has only been reported by Nishimiya et al. (2004). The mass purification methodology of a new AFP from the fish muscle homogenate is developed in this dissertation. The author group succeeded to isolate 95% purified AFP from fish muscle. This purified AFP showed ultra-high solubility in pure water, to date it the highest solubility of any AFP. Such distinctive property offer author to characterize this newly found AFP up to very high concentrations. The goal of this dissertation was to examine physicochemical behavior and functional activities of this AFP. The author also aimed to elucidate the concentration dependency of FIPA, IRI and TH activities of this AFP and correlate a new concertation-dependent parameter with two fundamental (TH and IRI) parameters used to evaluate AFP activities. The specific purposes in each chapter of this dissertation are as follows:

Chapter two: *Mass preparation of bpAFP and expression and purification of recombinant bpAFP (rbpAFP)*. The methodology of purification of native protein from fish muscle was established. Its sequence and secondary structure were determined. A

recombinant peptide consisting this sequence was prepared and characterized to ensure homogeneity of sequence.

Chapter three: *The ice plane specificities of bpAFP and rbpAFP were examined in this chapter*. The concentration-dependent ice plane binding ability of bpAFP and rbpAFP and a recombinant type III AFP, nfeAFP6, were examined using FIPA analysis.

Chapter four: *The TH activity and dependence of the TH activity on temperature and pH were investigated in this chapter*. The TH activities of bpAFP and rbpAFP at different protein concentration were measured. The effect of temperature and pH on the secondary structure followed by the TH activity was investigated. The effect of pH on the ice plane specificity of bpAFP was also examined in this chapter.

Chapter five: *Expression, purification and characterization of mutated bpAFP*. Mutant of BpAFP was prepared to investigate the role of the threonine at the C-terminal end. The TH activities and ice binding specificity of this mutant was evaluated with the native and recombinant BpAFP. The CD spectra at different temperature and pH were recorded to observe the effect of temperature and pH on the secondary structure of this mutant.

Chapter six: *Examined the critical ice shaping concentrations (CISC) of type I, II and III fish AFPs and their recombinant proteins to correlate CISC with their effective IRI concentrations.* The CISC and IRI of native and recombinant type I, II and III fish AFPs were examined. A correlation between this initial concentrations of TH measurement and IRI were established for active AFPs. Evaluated the CISC and IRI of a defective isoform of nfeAFP (nfeAFP6) and hypothesized two step adsorption mechanism based on these experimental results.

Figures

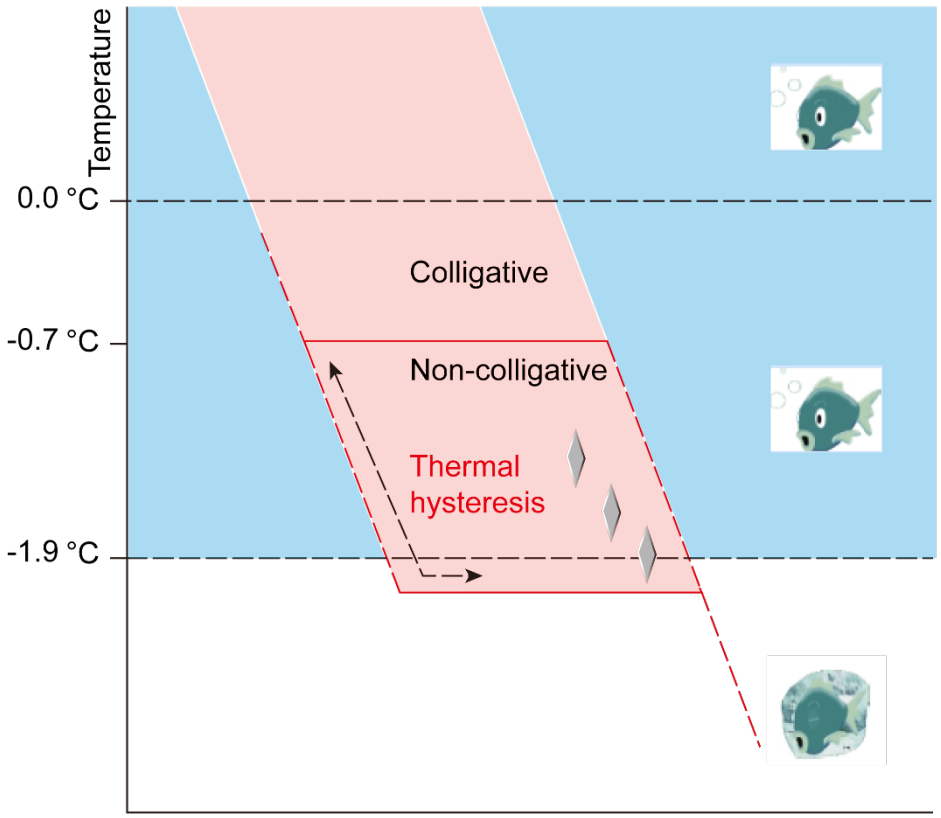

Figure 1.4.1.
Mechanism of protection from freezing by marine fishes. Marine fishes are protected from freezing by a combination of colligative and non-colligative mechanisms. The blue areas represent seawater, which freezes at −1.9°C (indicated by the transition to white). Pink signifies fish blood, which freezes just below −1.9°C (marked by the lower horizontal red line). The freezing point depression of the blood is the sum of two components: a colligative depression from 0°C to −0.7°C owing to blood solutes (marked by the upper horizontal red line), and a non-colligative effect caused by binding of the antifreeze protein (AFP) to ice crystals. The latter is referred to as thermal hysteresis, which is a separation of the freezing and melting temperatures (lower and upper red horizontal lines, respectively). Within the thermal hysteresis gap, ice crystals will neither grow nor melt. Reproduced from Jia Z and Davies PL (2002)

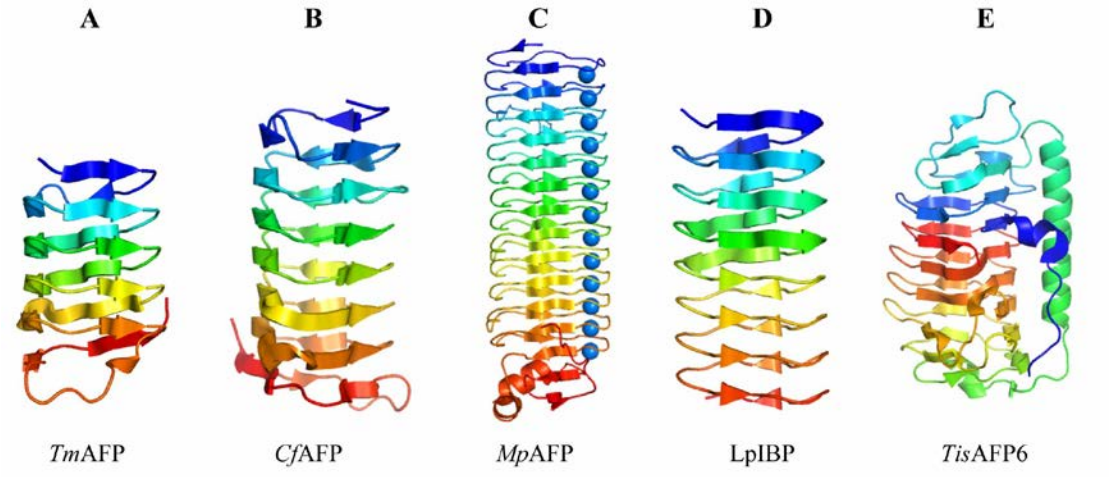

Figure 1.4.2a
Structures of AFPs. (A) X-ray crystal structure of Tenebrio molitor AFP (regenerated from PDB ID: 1L0S), (B) Solution structure (NMR) of AFP from *Choristoneura fumiferana* (regenerated from PDB ID: 1Z2F), X-ray crystal structure of (C) *Marinomonas primoryensis* AFP (*Mp*AFP), cyan balls are Ca^{2+} (regenerated from PDB ID: 3P4G), (D) *Lollium perenne* IBP (LpIBP) (regenerated from PDB ID: 3ULT) and (E) *Typhula ishikariensis* AFP 6th isoform (TisAFP6) (regenerated from PDB ID: 3VN3). These structures were regenerated using PyMOL.

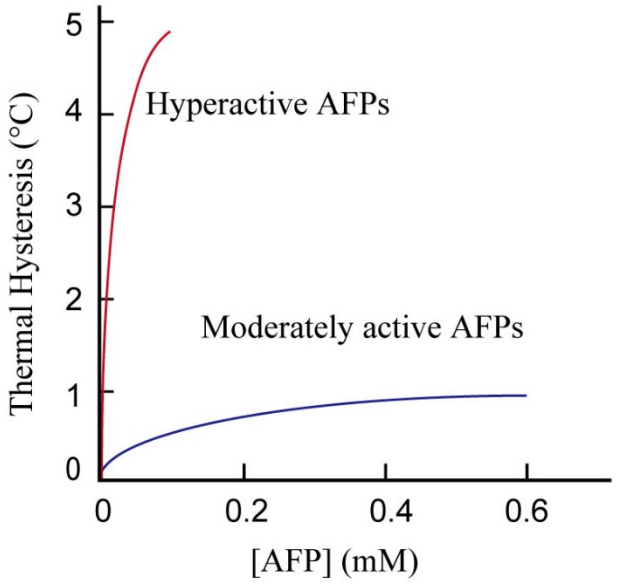

Figure 1.4.2b.
Schematic representation of TH vs concentration of AFPs profile for hyperactive and moderately active AFPs.

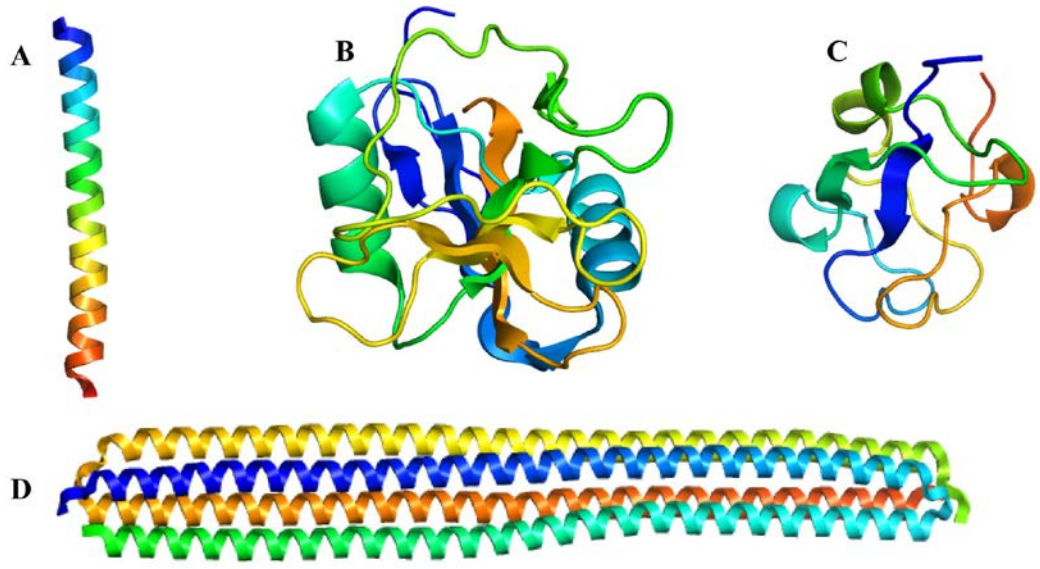

Figure 1.4.3.
X-ray crystal structure of type I, II, III and Ih fish AFPs. X-ray crystal structure of (A) type I AFP (wfAFP) from *Pseudopleuronectes americanus* (regenerated from PDB ID: 1WFB), (B) calcium independent type II AFP (lpAFP) from *Brachyopsis rostratus* (regenerated from PDB ID: 2ZIB), (C) type III AFP from *Zoarces americanus* (regenerated from PDB ID: 1AME) and (D) type Ih AFP from *Pseudopleuronectes americanus* (regenerated from PDB ID: 4KE2). These structures were regenerated using PyMOL.

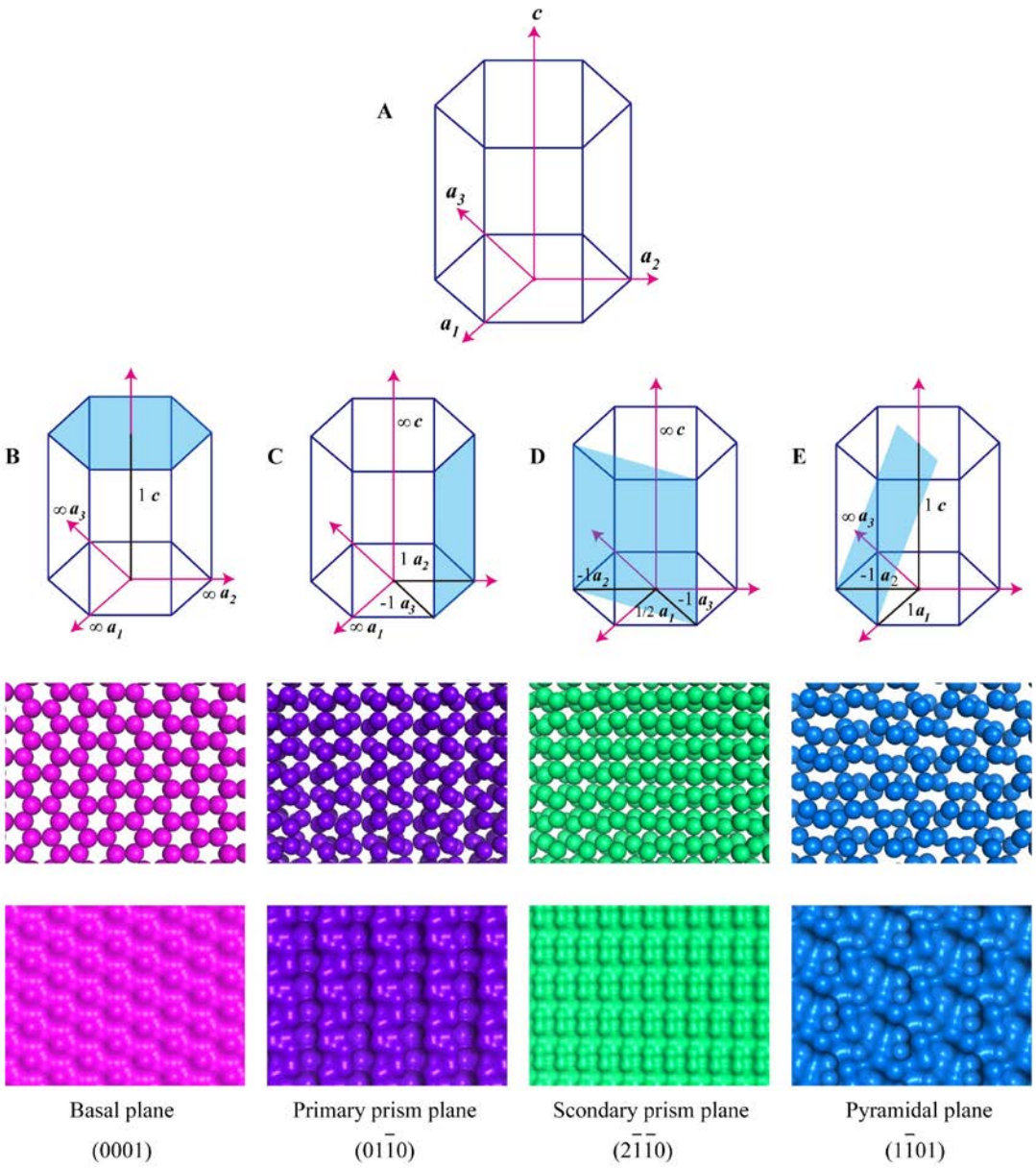

Figure 1.5.
Unit cell of hexagonal ice crystal (I_h) and representative ice planes involving in AFP interactions. (A) The unit cell with *c* and *a*-axes. The representative ice planes involving in AFP interaction represented in hexagonal lattice (Upper), space filling (middle) and surface (lower) with their Miller-Bravais indexes. The ice planes were generated by VESTA (Momma and Izumi, 2008) and visualized with PyMOL.

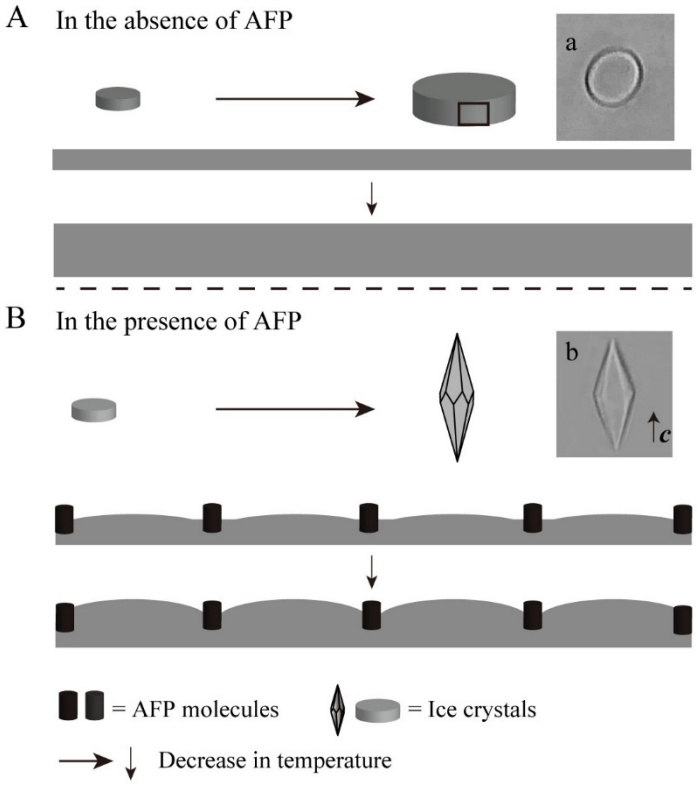

Figure 1.6a.
Schematic representation of adsorption and inhibition mechanism. (A) Uniform growth of flat ice crystal fronts in the absence of AFPs, typical image spherical shape of ice crystal (a). (B) Adsorption of AFPs convert the flat ice fronts to curve and obstacle uniform growth that results different shape of ice crystal for example, bipyramidal, a representative ice crystal shape observed in the presence of fish AFP (b).

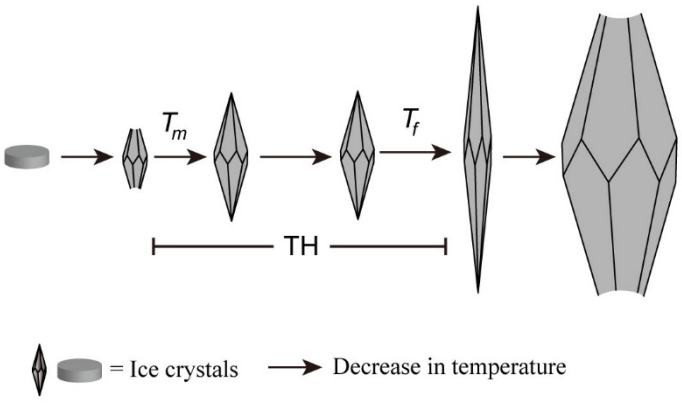

Figure 1.6b.
Schematic representation of thermal hysteresis activity (TH) of AFPs.

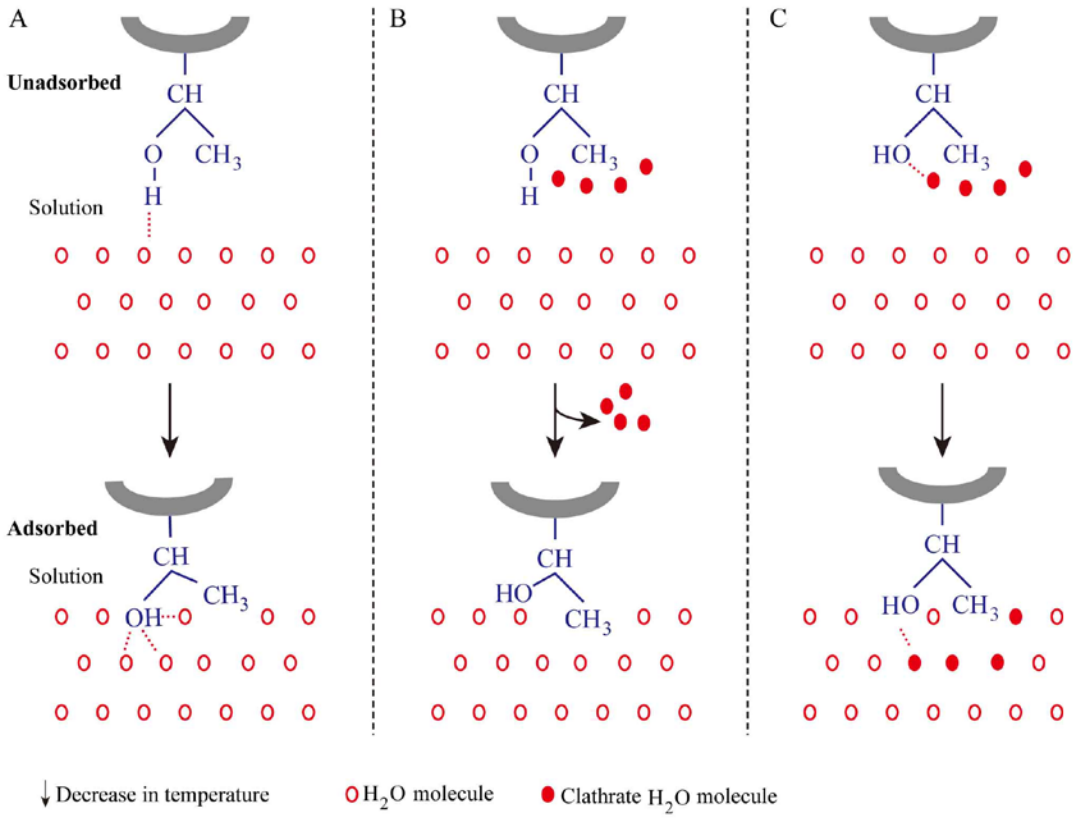

Figure 1.7.
Schematic representation of the proposed mechanisms for binding of the AFPs onto the crystal surfaces. The proposed mechanisms for ice binding (panels A, B and C) are illustrated in the preadsorbed (upper) and adsorbed (bottom) states. The ice binding site of an AFP are represented by the single threonine residue in blue. Water molecules in the ice lattice or quasi-liquid layer above ice are shown as red circles. Clathrate waters around IBS are shown in filled red circles. (A) Hydrogen bonding hypothesis. Threonine representing the IBS initially hydrogen bonds (broken line) to ice (top) and progresses to have the threonine hydroxyl occupy an ice lattice O atom site to make additional hydrogen bonds. (B) Hydrophobic effect. Constrained waters around hydrophobic groups on the IBS (top) are released into the solvent on IBP binding to ice with an intimate fit (bottom). (C) Anchored clathrate hypothesis. Ice-like clathrate waters around hydrophobic groups on the IBS hydrogen bond to the protein backbone and side chain groups (top). These clathrate waters merge with the quasi-liquid layer waters and become ice (bottom). This figure is regenerated from PL Davies (2014).

Discovery of a Supersoluble AFP from Fish and Expression and Purification of its Recombinant Protein (rbpAFP)

Chapter: 2

2.1 Summary

Abstract

A supersoluble antifreeze protein (bpAFP) is identified from a flounder fish barfin plaice, *Liposetta pinnifasciata*. BpAFP was purified from the fish muscle homogenate through a succesfully developed method as mixture of isoform. Among them, sequence of the major isoform was determined. It is a 40-residue single polypeptide, for which α-helical structure was assumed based on the CD measurement. It contains three 11-residue repetitive sequence described as Thr-Ala-X-Y-Ala-Ala-Z-Ala-Ala-Ala-Ala (X-Z are either Ala, Ser, Lys, Asp, or Glu) which is a typical feature of fish type I AFP (AFPI). A recombinant protein (rbpAFP) consisiting this sequence was pepared to ensure homogeneity of sequence. rBpAFP showed similar physicochemical properties of bpAFP. It is notable that, though this peptide contains 75% of alanine although it solublized at least 650 mg in 1mL of pure water.

Outlines

In this chapter the author described the contents of an unpublished manuscript entitled "Concentration-dependent oligomerization of an α-helical polypeptide makes it hyperactive" by Sheikh Mahatabuddin, Yuichi Hanada, Yoshiyuki Nishimiya, Ai Miura, Hidemasa Kondo, Peter L Davies and Sakae Tsuda. The authors contributions are S.M. and S.T. designed research; P.L.D. contributed new analytic tools; S.M., Y.H., Y.N., A.M., and H.K. performed Research and analyzed data; S.M., P.L.D., and S.T. wrote the paper. Here, the mass purification of native protein, the protein sequencing of its major isoform and purification of its recombinant peptide have been reported. The author also examined the secondary structure of the protein using circular dichroism spectroscopy.

2.2 Introduction

Type I fish AFPs are exist as single amphipathic α-helices. The 37-residual type I AFP from winter flounder was the first to have its three-dimensional structure determined (Sicheri and Yang, 1995). Irrespetive of the origin, all type I AFPs conssisted a concensus sequence of $ThrX_2AsxX_7$, where X is usually alanine or any other aminoacid that favors α-helix formation. They consist terminal cap that asists the helix to be stablize (Sicheri and Yang, 1995). The sequence of the type I AFPs identified from winter flownder, yellowtail flounder and Alaskan plaice started with aspartic acid residue (D). On the other hand, type I AFP from shothorn sculpin, gurby sculpin, arctic sculpin and cunner has a metihionine at their N-terminal end (Harding et al., 1999; Hobbs et al., 2011). However, the discovery and physicochemical studies of these proteins have been advanced our understanding of the functional activities of AFPs.

The inhibitory function of type I AFPs are classified as moderate scale, they can inhibit ice crystal busting up to 1°C at their mM concentrations (Bar-Dolev et al., 201). This inhibition effect further reduced the freezing temperature of their body fluid below the colligative depression (-0.7°C) to facilitate their survival. It is notable that, sea water with its high saline content freeze at -1.9°C. A right eye founder fish living at similar temperature zone is Barifin plaice, *Liposetta pinnifasciata*. This fish produce a new type I antifreeze protein (bpAFP) to facilitate its survival at subzero temperatures. The bpAFP has been purified and characterized (in this thesis).

Characterization of native type I proteins from at least seven different fishes have been reported (Duman and DeVries, 1974; Scott et al., 1987; Knight et al., 1991; Hew et al., 1985; Yang et al., 1988; Hobbs et al., 2011). Multidimensional studies have also been reported to elucidate the relationship of structure and function of the type I AFPs (Fletcher et al., 1982; Davies and Hew, 1990; Chakrabartty and Hew, 1991; Sicheri and Yang, 1995; Gronwald et al., 1996 and Sönnichsen et al, 1998). Among them, majority studies were carried out using their recombinat proteins. Recombinant expression of these proteins fascilitate the studies based on mutational analysis (Haymet et al., 1998; Wen and Laursen, 1992,1993), X-ray crystallography (Sicheri and Yang, 1995), NMR (Gronwald et al., 1996 and Sönnichsen et al, 1998), effect of chain length on their activities (Chakrabartty et al., 1989) and so on. On the other hand, mass purification of AFPs from reombinant source is somewhat difficult, which is a prerequisite condition to study the cell or organ preservation abilities of AFPs (Kamijima et al., 2013). To date, this thesis is the first report about the mass purification of type I AFP from fish muscle (ii).

In this chapter, the author describe about the development of mass purification methodology of the bpAFP from fish muscle homogenate and determination of the amino acid sequence of that protein. A recombinant protein encompassing this sequence are expressed and purified from a fusion protein tagged with thioredoxin

(Trx). Both the bpAFP and rbpAFP adsorbed ice crystal changed its morphology to bipyramidal hexagonal trapezohedron with a fixed *c* to *a* axis ratio 3.6:1.

2.3 Materials and methods

Preparation of fish muscle homogenate

The fish was captured from Okhotsk coastal area of Hokkaido. Captured fishes were cut into fillets and ground to make a muscle paste. A homogenize fluid consisting of 2 kg of this paste in 2 liter water was prepared. This homogenate was centrifuged at 9000×g for 30 minute and supernatant was subjected for initial activity measurement. The supernatants were ultrafiltrated (Pellicon XL biomax 30 kDa, Merck Millipore, Germany). The filtrates were lyophilized to obtain approximately 6g of proteins with a molecular weight less than 30 kDa. These mixture of proteins were used for further purification of the bpAFP (see details in the results section). The purity of the prepared sample was examined using 15% Tris-Glycine SDS-PAGE.

Expression and purification of recombinant bpAFP

The cDNA encoding bpAFP tagged with thrombin cleavage site followed by histidine (six) and thioredoxin in the N-terminal was cloned into the expression vector pET32α in *Escherichia coli* BL21 (DE3) Rosetta2 (Novagen) to express rbpAFP. Cells were cultivate in Luria-Bertani medium with 100 μgmL^{-1} ampicillin and expression of target protein was induced by 0.5 mM isopropyl-β-D-thioglactopyranoside (IPTG). Expression of the target peptide was confirmed by 15% Tris-Glycine. The cultivated cells were collected and suspended in 50 mL (per 1L culture medium) 50 mM Tris/HCl, pH 8.0. Cells were disrupted by sonication and centrifuged to remove insoluble fractions from this mixture. Supernatants of this centrifuged mixture were then applied to affinity chromatography using Ni-NTA column. Histidine tagged peptides were eluted with isocratic flow with 60% A buffer (50 mM Tris-HCl and 0.5 M NaCl) and 40% B buffer (10mM Tris-HCl, 0.5 M NaCl, 0.5 M Imidazole (Fig. 2.3C). Purification of recombinant protein from this Trx-tagged fusion protein described in results section.

Measurement of antifreeze activity

The antifreeze activity was assayed using a photomicroscope system consisting of a Leica DMLB 100 photomicroscope equipped with Linkam LK600 temperature controller and a CCD camera. The sample solution was placed as a droplet (≈5 μL) on a circular cover slip (13 mm radius) and then sandwiched using another cover slip. This sandwiched sample was then placed on the stage of the microscope and frozen to -20°C at a rate 40 °C/min and incubated for two minutes. It was heated to -1°C at the same rate. It was slightly warmed up at the rate of 5 °C/min to create small ice crystals at their melting temperatures. After that the temperature was decreased slightly below the melting temperature to create directed shape of ice crystals and photographed using the CCD camera. The protein solution was prepared using 10 mM ammonium bicarbonate (ABC) buffer as solvent.

HPLC analysis of native protein

The purified native bpAFP sample was dissolved in PBS buffer (137 mM NaCl, 2.7 mM KCl, 4.3 mM Na_2HPO_4, 1.47 mM KH_2PO_4 and pH 7.4) and further chromatographed using reversed phase HPLC with a TSKgel ODS-80Ts column (TOSOH, Tokyo, Japan) by a linear gradient of 0-100% acetonitrile in 0.1% trifluoroacetic acid (Fig. 2.2 A).

Measurement of CD spectrum

Protein solutions were prepared at 0.45 mg·mL^{-1} concentration in 10 mM sodium phosphate buffer of pH 7.4. CD spectrum were recorded using JASCO J-725 CD spectrophotometer equipped with JASCO PTC-348WI temperature controller (Jasco Analytical Instruments, MD, USA). CD data in degrees then converted to mean residue ellipticity (deg·cm^2·dmol^{-1}) using the following equation.

$$[\boldsymbol{\theta}]_{\boldsymbol{mrw},\lambda} = \frac{\boldsymbol{MRW} \times \theta_\lambda}{\boldsymbol{10} \times \boldsymbol{d} \times \boldsymbol{c}} \mathbf{deg}\, \boldsymbol{cm^2\, dmol^{-1}}$$

Where, $\boldsymbol{MRW} = \frac{\textbf{Molecular Wight of protein in Da}}{\textbf{Number of amino acid (N)} - \mathbf{1}}$, θ_λ = CD data in degrees at λ wavelength, c = concentration in g·mL^{-1} unit.

2.4 Results

2.4.1 Purification of native protein

Barfin plaice belongs to small group of psychrophilic flounders that do not avoid icy environments. Its survival in this harsh environments does indeed facilitated by the native bpAFP. The crude native bpAFP powder obtained from muscle homogenate was dissolved in 20 mM Tris-HCl buffer (pH =8.5) containing 0.2 M NaCl at 0.2 g·mL^{-1} concentration and centrifuged at 9000×g rpm for 20 minutes. Supernatants of this centrifuged solution were then loaded onto a Sephadex G-25 size exclusion column (XK 50/30, 500 mL, GE healthcare, USA). The effluent of void-volume fractions that exhibited ice-shaping ability further loaded onto a DEAE Sepharose anion exchange column (XK 50/20, 80 mL, GE healthcare, USA) equilibrated with 20 mM Tris-HCl buffer (pH 8.5). Its initial flow through fractions (Fig 2.1A) were then collected and dialyzed against distilled water to remove the Tris buffer. Lyophilization of this dialyzed protein solution provides approximately 1 g of 90-95% purified native bpAFP (Fig. 2.1B). Above procedures were repeated successively for mass-purification of native protein for which muscle homogenate act as a key source. The electrophoretogram of 15% Tris-Glycine gel showed the purity of bpAFP, which always visualized as asparagus shape (Fig. 2.1C). It also notable that position of the protein band migrated downward from its actual position similar to 7-kDa type III AFP.

2.4.2 Solubility of native protein

Solubility of bpAFP was measured by dissolving AFPs in 25mM $(NH_4)_2CO_3$ (ABC) buffer at room temperature. Dissolution limit was obtained (Fig. 2.2B) 650 $mg \cdot mL^{-1}$. Similar result was obtained by using milliQ as solvent. To date, bpAFP is the sole molecule that gives such high concentrated of AFP solutions. Therefore, it can be denoted as supersoluble AFP.

2.4.3 Sequence of the major isoform

The native AFP was separated into several fractions with reversed-phase HPLC (Fig. 2.2A). The effluents of the peak containing highest UV absorbance was digested into two fragments (Fr I and Fr II) (Fig. 2.3A) with trypsin and sequenced. The N-terminal fragment is 26 residues long, and the C-terminal fragment, with an amidated c-terminus is 14 residues long (Figure 2.3A) D^{1}TASDAAAAAAAATAAAAAAAAAATAKAAAEAAAATAAAAR^{40}-NH_2 is the full primary sequence of this isoform. It exhibited the typical type I AFP sequence with three tandem repeats of the 11-residue i.e. TX10 where X is mostly alanine along with a few another amino acids that favors formation of α-helix. However, bpAFP is more alanine-rich (75%) than other type I AFP isoforms that are typically only two thirds are alanine. The extra alanines, up to 10 in a row take the place of Asn amd Leu that are not though to play a critical role in either structure or function of type I AFP. The N-terminal D^{1}TASD sequence and C-terminal amidation that form the α-helix capping strctures are well conserved (Sicheri and Yang, 1995; Harding et al., 1999; Patel and Graether, 2010).

2.4.4 Purification of recombinant bpAFP

The affinity chromatogram of fusion protein visualized a peak at 214 nm confirmed the ellusion of the histidine tagged fusion protein (Fig. 2.4 B, lane 1). Effluents containing this peak were diyalyzed (against milliQ) and lyophilyzed to obtain fusion protein. Approximately, 125 mg of fusion protein obtained per litre culture mediuam. Of which, 50 mg was dissolved in 30 mL of PBS solution and allowed to be digested with thrombin protease (GE Healthcare) in the ratio 1 unit per 100 μg of fusion protein. This digested protein solution then loaded to a Ni-NTA column. It chelated the histidine containing Trx. Therefore, the flow through fractions (Fig. 2.4D) were collected and lyophilized to obtain crude recombinant protein including thrombin protease after dialysis (Fig. 2.4B, lane 4). This thrombin protease and other higher molecular weight contaminant were removed from tag free AFP using reversed-phase HPLC purification.

10 mg of crude lyophilized protein was dissolved in 5 mL of PBS buffer (pH 7.4). This solution was applied for the reversed-phase HPLC using TSKgel ODS-80Ts column (TOSOH, Tokyo, Japan) with a linear gradient of 0-100% acetonitrile in 0.1% trifluoroacetic acid. Effluents containing pointed peak in the chromatogram (Fig.2.4 A) were collected and lyophilized after dialysis against milliQ. The purity of this

lyophilized bpAFP was confirmed with Tris-Glycine native PAGE (Fig. 2.4C). These proteins were 97-98% pure (calculated with ImageJ).

2.4.5 Antifreeze activity

The AFP molecules get adsorbed onto the embryonic ice crystals and stop their uniform growth. Such impeded growth results hexagonal trapezohedron shaped of ice crystal in the presence of bpAFP and rbpAFP with a fixed *c* to *a* axis ratio of 3.6:1 (Fig. 2.1E and 2.3D). In contrast, spherical shape of ice crystals were observed in absence of native protein (Fig. 2.1F). Here, it is notable that the bipyramidal crystals became less faceted at higher protein concentrations such as above 1 $mg \cdot mL^{-1}$. The detail of the TH and IRI activities of the natural protein will be discussed latter.

Secondary structure of the native protein

Irrespective of the source all of the type I AFPs folded as an amphipathic α-helix. Which is another prerequisite criteria of the AFP sequences along with the typical repetitive sequences. Therefore, the secondary structure of the native protein was determined using CD spectroscopy at 20°C. The native protein visualize a typical spectrum with two minima at 208 and 222 nm, which is represents of simple α-helical secondary structure (Fig. 2.5A). Similar spectrum was obtained from the rbpAFP confirmed that it also folded into amphipathic α-helical secondary structure. These results classify bpAFP as a new member of type I AFP family.

2.5 Discussion

A supersoluble 40-residual protein is discovered from a right flounder, barfin plaice. It has the ability to bind onto the ice crystal surfaces to alter their growth kinetics. Such altered growth changed the ice crystal shape from normal hexagon to hexagonal trapezohedron shape. This alteration of ice crystal morphology and significant TH activity (see detail in chapter 5) of this protein classify it as a biological ice crystal modifier or AFP. The extreme water solubility (650 $mg \cdot mL^{-1}$) of this peptide represent it as a sole AFP molecule that exhibit such ultra-solubility in pure water though it composed of 75% alanines.

The sequence information of bpAFP also revealed that it consists 4 repetitive threonines after every 11 consensus repeats. The α-helical structure of the native and recombinant protein were confirmed from their CD spectra with considerable confidence. Although its crystal structure is not determined, the sequence and α-helical protein fold highly suggest that bpAFP construct a secondary structure similar to wfAFP. WfAFP's high resolution X-ray structure revealed that elaborate N- and C-terminal capping structures, which together with internal salt bridge and high alanine content have important role to stabilize its long α-helical structure (Ananthanarayanan and Hew, 1977; Sicheri and Yang, 1995). Similar biochemical properties presumably be stabilize the secondary structure of extremely high alanine content bpAFP. The

author introduce an arginine residue in the C-termini of the recombinant protein that assumed to facilitate the stabilization of its α-helix through formation of the capping structure at that region. It is notable that the alanine content in other type I AFPs are less than bpAFP, such as wfAFP (62%), Alaskan plaice AFP (65%), and yellow tail flounder 69% (Fig. 2.6A, B, C, D). Additionally, bpAFP contains only 5 polar residues (D^1, S^4, D^5, K^{26} and E^{30}) excepting the 4 threonines and the C-terminal arginine. The sidechains of the residues of K^{26} and E^{30} in the model structure are at 4.8Å distance from each other (Fig. 2.6G). They will presumably form a slat-bridge similar to the salt bridge formed between between K^{18} and E^{22} in wfAFP. Therefore, the four threonines and the residual 30 alanines are the principal constituent of bpAFP, implying that assembly of only methyl groups with four equally spaced hydroxyl groups construct an extremely regular surface of this molecule. In addition, it is the type I AFP with lowest polar amino acid residues whereas other type I AFP molecules composed with more polar residues to acquire the amphipathic nature (Fig. 2.6). This extreme occupancy of hydrophobic methyl groups on its molecular surface evoked a sparingly soluble nature of this peptide, while it showed 650 $mg \cdot mL^{-1}$ of supersolubility in pure water. It also get oligomerized in solution (see detain in chapter 3). One may speculate that bpAFP sequence has some water holding capacity from such ultra-high solubility and oligomerization. The water holding capacity has been found in a 33-kDa AFP, Maxi, that organizes 400 water molecules in the interior of its four helix bundle structure, although its maximal solubility was not reported (Sun et al., 2014). Both Maxi and bpAFP are largely composed of the 11-residue repetitive unit TX_{10} (where X is mostly alanine), and the repetitive unit of Maxi forms three helical turns with an average of 3.7 residues per turn, as opposed to 3.6 residues per turn in the classic α-helix (Sharp et al., 2014; Sun et al., 2014). As shown by the Maxi crystal structure this deviation in the peptide bond facilitates hydrogen bonding between the backbone carbonyl groups and the solvent water molecules. Moreover, the small size of the Ala side chain also helps water to access the peptide backbone. These two factors contribute the extraordinarily high solubility of bpAFP.

It was reported in the recent studies that the IBS of the type I AFPs encompass with the conserved hydrophobic alanine rich face and the regularly spaced threonines (i thr, i+4 ala and i+8 ala) (shown in blue parallelograms in their helical net representation in Fig. 2.6) (Bardnes et al., 1999). This conservation was evident from the helical wheel representation of wfAFP (Fig. 2.6F). The helical wheel representation of bpAFP also shows the conservation of this alanine rich face. Though further studies are necessary to elucidate the IBS of bpAFP. However, the mass purification method of a new type I AFP was developed by the author group. They also developed the expression and purification methodology of the recombinant protein which is indispensable to elucidate the structure and function relationship of any peptide.

Figures

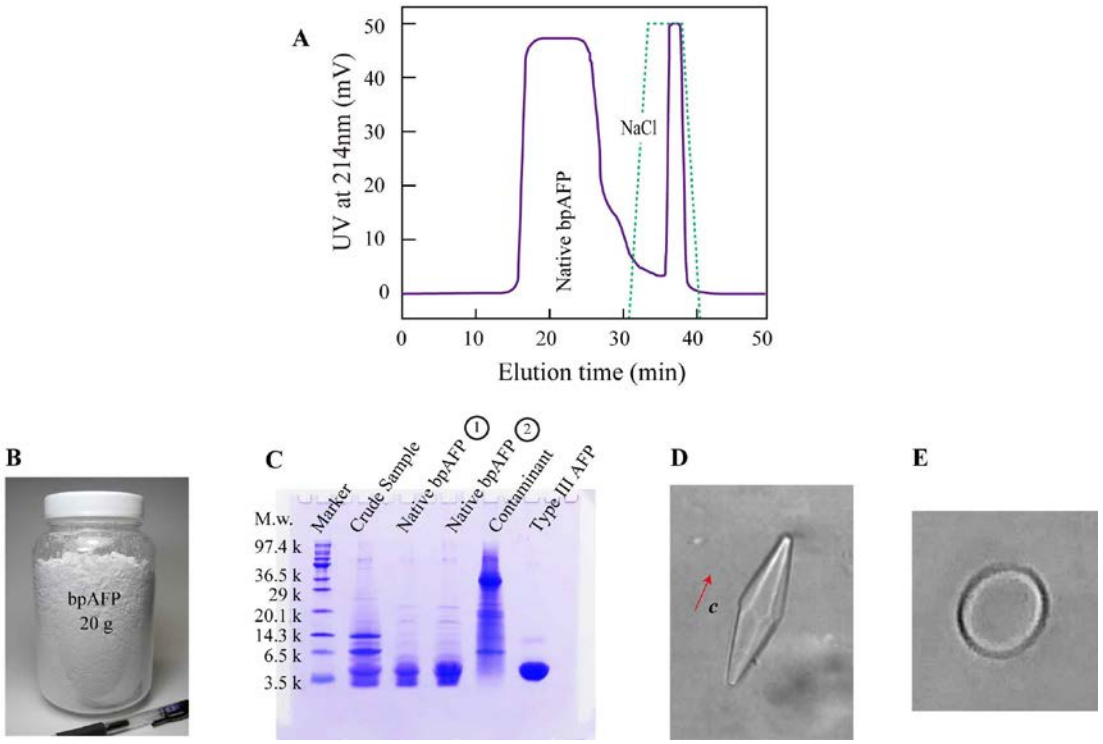

Figure 2.1.
Fish muscle homogenate supplies bpAFP. (A) DEAE anion exchange chromatography of bpAFP, where contaminates were separately eluted with NaCl, the cyan dotted line represents NaCl gradient. (B) Gram-quantities of native bpAFP as a lyophilized powder of 95% purity. (C) Electrophoretogram of fractions from the anion-exchange chromatography (A) separated by 15% Tris-Glycine SDS-PAGE, 1 and 2 represents 3 and 6 $mg \cdot mL^{-1}$ of purified native bpAFP, respectively. (D) Hexagonal trapezohedron ice crystal observed in 0.5 $mg \cdot mL^{-1}$ of purified bpAFP solution. (E) The circular disc shape ice crystal observed in the absence of AFPs.

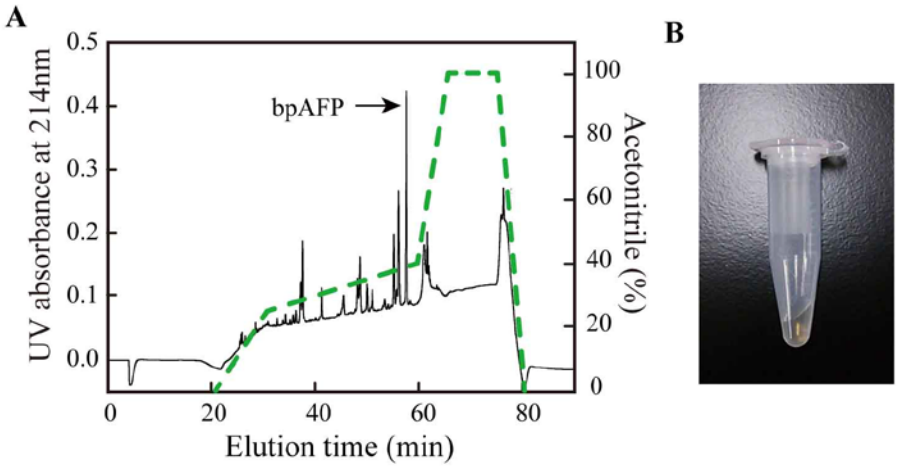

Figure 2.2.
Isolation of the bpAFP isoform and the solubility of bpAFP. (A) The HPLC chromatogram containing separated peak for the isoform bpAFP, chromatogram was obtained from reverse phase HPLC using TSKgel ODS-80Ts column (TOSOH, Tokyo, Japan) with a linear gradient of 0-100% acetonitrile in 0.1% trifluoroacetic acid (green dashed line). (B) Approximately 650 $mg \cdot mL^{-1}$ of native bpAFP solution represents its supersolubility.

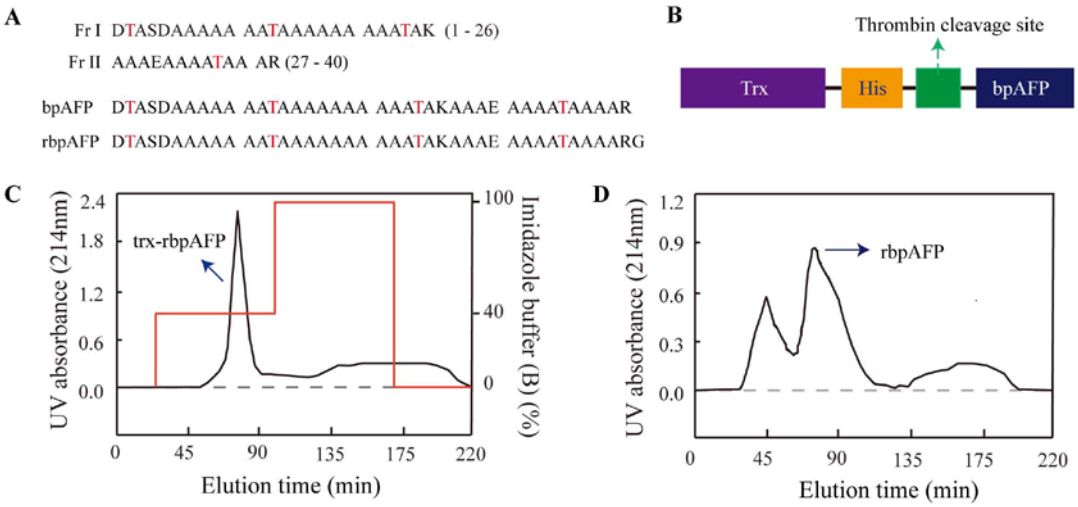

Figure 2.3.
Determination of the sequence of bpAFP and expression of rbpAFP. (A) The sequence of the fragments from trypsin digestion, bpAFP and rbpAFP. (B) Illustration of the fusion protein composed of thioredoxin (Trx), His-tag, and a thrombin cleavage site used for the expression of rpAFP. (C) Ni-affinity chromatogram of the supernatant of cell lysates, percent of imidazole buffer shown in red line. (C) Flow through peak obtained in Ni-affinity chromatography, the effluents containing second peak were collected and lyophilized after dialysis to obtain crude recombinant sample without Trx tag.

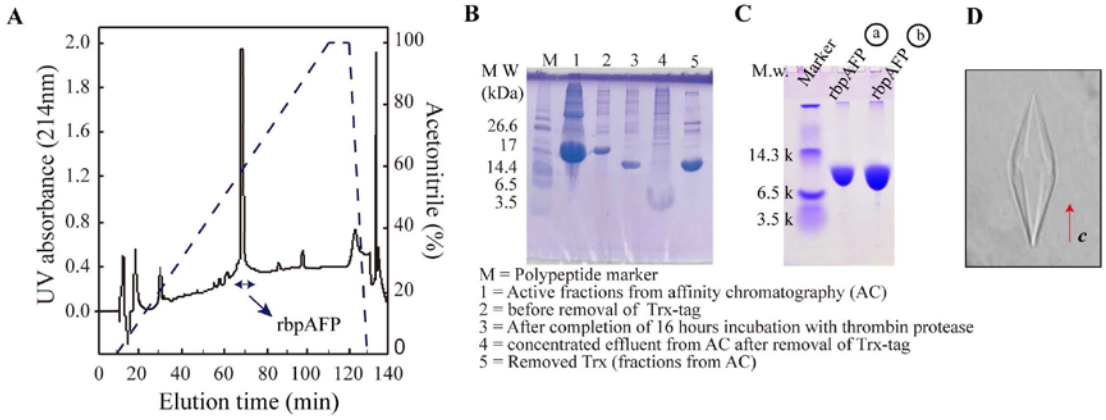

Figure 2.4.
HPLC purification of rbpAFP and ice crystal morphology in purified ebpAFP. (A) HPLC chromatogram containing peak of the purified rbpAFP at 214 nm, chromatogram was obtained from reversed-phase HPLC using TSKgel ODS-80Ts column (TOSOH, Tokyo, Japan) with a linear gradient of 0-100% acetonitrile in 0.1% trifluoroacetic acid (blue dashed line) (B) Electrophoretogram of rbpAFP at different steps of purification separated by Tris-glycine SDS-PAGE. (C) Electrophoretogram of bpAFP after HPLC purification separated by Tris-Glycine native PAGE, a and b represents 5 and 10 mg·mL^{-1} of 98% purified rbpAFP. (D) Hexagonal trapezohedron ice crystal observed in 0.5 mg·mL^{-1} of purified rbpAFP solution.

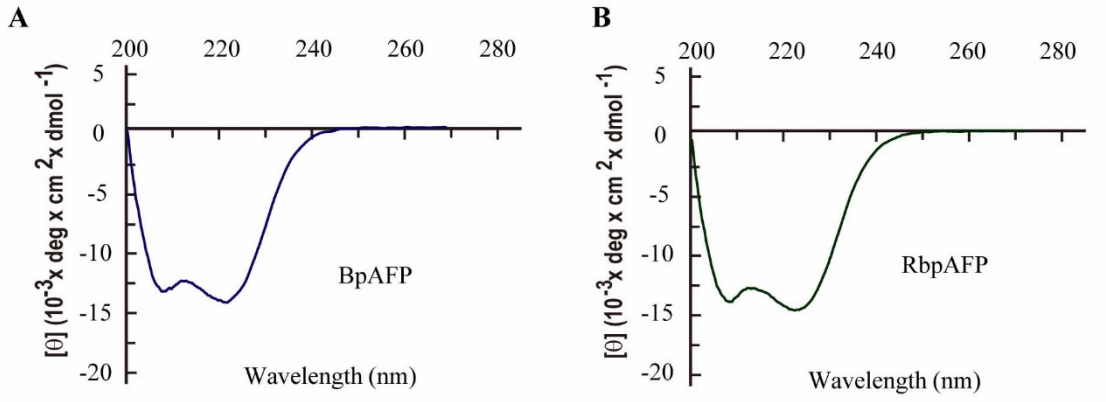

Figure 2.5.
CD spectrum of bpAFP (A) and rbpAFP (B). Protein concentration was 0.45 mg·mL^{-1} in 10 mM phosphate buffer.

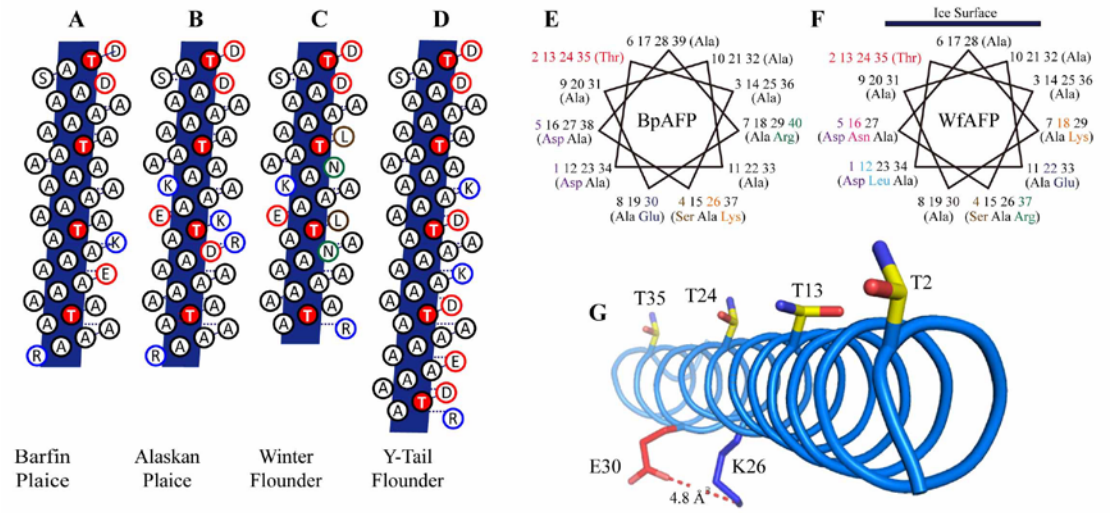

Figure 2.6.
Helical net and helical wheel representation of bpAFP and other right eye flounder type I AFPs. Helical net representation of (A) bpAFP, (B) Alaskan plaice, (C) winter flounder and (D) yellow-tail flounder. The helical wheel representation of (E) bpAFP and (F) wfAFP. The monomeric α-helical model structure of bpAFP constructed with EasyModeller 4.0 (Kuntal et al., 2010) and PyMOL.

Dependence of the Ice Plane Specificity on the Concentrations of bpAFP and rbpAFP

Chapter: 3

3.1 Summary

Abstract

Antifreeze protein (AFP) molecules specifically adsorbed onto the embryonic ice crystal surfaces to arrest their growth. This specificity of their adsorption onto different planes plays the important role to regulate their ice shaping and antifreeze acitivites. Consequecntly, determination of the target surfaces of any AFP on the ice crystal has considered as an essential part for characterization of AFPs. This essential information could be obtained from the Fluorescence-based ice plane affinity (FIPA) analysis, a widely used teachnique that visualize the ice plane specificity of fluorescently tagged AFP molecules. The FIPA images of native and resombinnat bpAFP showed that they interminably bind to ice crystal in a concentraton-dependent mannar. BpAFP can adsorb onto multiple planes including basal planes at 0.1 $mg \cdot mL^{-1}$ protein concentartion. Such interminable binding of bpAFP alters the ice crystal morphology from hexagonal trapezojhedron to lemon shaped. On the other hand, the nfeAFP6 failed to adsorbed onto the basal planes even at 0.2 $mg \cdot mL^{-1}$ of protein concetration, which is the typical properties of all moderate active AFPs. Here, it is notable that it is the first report of the concentration-depemdent FIPA analysis of any AFP.

Outlines

In this chapter the author described the contents of an unpublished manuscript entitled "Concentration-dependent oligomerization of an α-helical polypeptide makes it hyperactive" by Sheikh Mahatabuddin, Yuichi Hanada, Yoshiyuki Nishimiya, Ai Miura, Hidemasa Kondo, Peter L Davies and Sakae Tsuda. The authors contributions are S.M. and S.T. designed research; P.L.D. contributed new analytic tools; S.M., Y.H., Y.N., A.M., and H.K. performed Research and analyzed data; S.M., P.L.D., and S.T. wrote the paper. It also contains the data of another unpublished manuscript entitled "Introduction to critical ice shaping concentration (CISC): A new parameter to evaluate the activities of antifreeze proteins" by Sheikh Mahatabuddin, Yoshiyuki Nishimiya, Ai Miura, Hidemasa Kondo and Sakae Tsuda. The authors contributions are S.M. designed the research; S.M., Y.N., A.M., and H.K. performed Research and analyzed data; S.M. and S.T. wrote the manuscript.

3.2 Introduction

The ligand of Antifreeze proteins (AFPs), the embryonic ice crystal, encompass with different patterns of oxygen atoms that presented on the surface of distinct planes defined by Miller-Bravais indices (see details in the sections 1.5.1 and 3.4). Among these numerous planes AFPs can recognize the patterns in prism, pyramidal and basal surfaces of ice crystal and get specifically adsorbed on them. Hyperactive AFPs has the ability to bind onto all of these planes whereas moderately active species bound specifically onto prismatic and/or pyramidal planes of the ice crystals (Jia and Davies, 2002). Therefore, investigation of the particular ice planes on which AFP molecules specifically adsorbed become an indispensable information for the characterization of these unique ice-crystal modifiers.

Adsorption of the AFPs onto the ice crystal surfaces has been undoubtedly demonstrated by Raymond and DeVries (1977). Afterwards, the binding of AFP molecules were suggested onto the faces parallel to *a*-axes depending on the match between the spacing of potential hydrogen-bonding side chains in some AFPs and the spacing of the water molecules on respective ice planes (DeVries and lin, 1977; DeVries, 1984). However, these findings cannot provide specific information about the adsorption planes of respective molecules though it advances the knowledge about adsorption of AFPs onto the ice crystals. In contrast, understanding the crystallography of adsorption become a vital subject to elucidate the structure-function relationships of AFP molecules. In 1991 Knight et al. introduced a simple and robust method for the determination of specific planes on which AFP molecules specifically get adsorbed to alter the morphology and ice crystal growth kinetics. This method of determination of AFP adsorbed ice planes was named as ice-etching technique.

The ice-etching technique was based on the theory that, when supercooling is sufficient to force growth on an adsorption plane, the adsorbed molecules must be incorporated *in situ* within the growing ice crystal, rather than being pushed along with the moving interface. The ice-etching patterns of wfAFP and Alaskan plaice AFP showed that these α-helical peptides bound onto the (20-21) pyramidal planes whereas another α-helical peptide sculpin AFP adsorbed onto the (2-1-10) secondary prism planes (Knight et al., 1991). It also showed that the type III AFP from ocean pout adsorbed onto several ice planes including the planes covered by wfAFP and sculpin AFP (Antson et al., 2001). This technique has recently been improved by using fluorescently labeled proteins instead of the normal protein solution (Garnham et al., 2010). Incorporation of fluorescent tags with the peptide molecules facilitated direct visualization of the AFP bound planes onto the ice crystal hemispheres under UV light. Such visualization eradicate the necessity of sublimation of the water molecules from the outer surface of the AFP bound single ice hemispheres which was indispensable for observation of AFP bound planes in ice-etching technique. This modified method was denoted as fluorescence-based ice plane affinity (FIPA) analysis. It effectively

reproduced the ice-etching pattern obtained for type III AFP from ocean pout and wfAFP (Antson et al., 2001, Garnham et al., 2010, Basu et al., 2013).

The FIPA images of hyperactive AFPs, such as *Mp*AFP, *Tm*AFP, *col*AFP and Maxi, visualized complete fluorescent ice hemispheres that suggesting the adsorption of the peptide molecules onto multiple planes including basal plane (Basu et al., 2013, Sun et al., 2014; Hanada et al., 2014). On the other hand, the moderately active AFPs, such as wfAFP, type III AFP and type II AFP, cannot adsorbed onto the basal planes to visualize entirely fluorescent ice hemispheres (Basu et al., 2013). These results supported the hypothesis that describes basal plane binding is indispensable for hyperactivity of AFPs (Scotter et al., 2006). Recently, an intermediate active AFP from a fly, MidgeAFP, has been identified. It was reported that this AFP adsorbed onto the pyramidal planes intermediate between the prism and basal planes (Basu et al., 2016).

In this chapter, the author describe about the concentration-dependent ice plane affinity of native, recombinant bpAFP and nfeAFP6, a recombinant protein of the defective isoform identified from Notched-fin eel pout. The concentration-dependent interminable ice plane binding was observed only for native and recombinant bpAFP. To date, the bpAFP is the only known type I AFP that bind onto the basal planes of the ice crystals.

3.3 Materials and methods

Preparation of single ice crystals

The single ice crystals were prepared according to the method described by Basu et al. (2013). In brief, light film of vacuum grease was applied on to the notched surface ring of each mold (Fig. 3.1A), notches were kept open carefully for entering waters into it. The molds were then placed onto a metal pan for sealing the notched greased surface in such a way that notches oriented away from the center of the pan. Afterwards, 0.22 μm filtered and degassed cooled (4 °C) milliQ water to the center of the pan, but outside of the molds carefully so that no bubbles formed inside the pan. When water levels became approximately 7-8 mm deep, the water started to enter inside the mold through the notch. The water level inside the molds were kept 5-6 mm deep. After that, the pan containing the molds kept inside a temperature controlled ethylene glycol bath cooled to -0.5°C and kept it perfectly balanced by adding blast weight to the side of the pan if necessary. After approximately one and half hour later a seed ice crystal was placed in the middle of the pan, outside of the molds. It act as a nucleator and propagate the ice inside the molds through the notched spaces. The diameter of the notch allowed only one ice crystal to propagate through it, resulting single ice crystals in each mold. It was incubated for overnight for completion of the freezing of all the water molecules previously entered inside the mold (Fig. 3.1B). Over the next three days 15 mL of cooled milliQ water (4°C) was added to each mold once a day and the temperature of the ethylene glycol bath was dropped -0.3°C per day after addition of new layer of water. At the day four the molds completely filled with ice.

After complete freezing the mold containing the single ice crystals were pulled out from the pan and the ice crystals were pushed out carefully from the molds. These ice crystal placed onto a clean surface and kept in -20°C refrigerator for one hour. The singularity and orientation of the axes were determined by observing the crystals between two crossed polaroids in a freezer room (temperature of the room was -1°C). Absence of any discontinuity or cracks to change the direction of the light proved the singularity of the ice crystal. On the other hand, when *c*-axis is exactly parallel to the incident light, no lights should be passed through the crystal and when *c*-axis tilted slightly from the parallel position, a uniform multicolor spectrum of light is transmitted through the crystal when it is rotated between the polaroids. The basal plane of the hexagonal ice crystal is normal to the *c*-axis and most commonly it is normal to the circular plane of the cylindrical ice crystal (Fig. 3.1C).

Growing a hemispherical single ice crystal in the presence of fluorescently labeled AFP

These single cylindrical ice crystals were cut down into desired orientation shown in figure 3.1D and E. The orientation of the *a*-axes in this cylindrical ice crystal (Fig. 3.1Ea) were determined through ice pitting (Knight, 1966) as described by Basu K et al. (2013). The desired oriented ice crystals were then mounted onto the frosty probe through the previously bored cavity on its flat surface, the temperature of the frosty probe was kept -0.7 °C. This single ice crystal mounted to the frosty probe then immerged in the cooled degassed milliQ water in a hemispherical cup in such a way that the level of water and the upper surface of the crystal remain in same height. Afterwards, the temperature of the frosty probe set to -4 °C and covered the cup and the frosty probe with insulation box. After approximately 45 minutes the ice crystal converted to a small hemisphere (Fig. 3.1F). It was then immerged into the fluorescently labeled AFP solution (25-30 mL) in the same cup and similar way of the previous step (Fig. 3.1F). In this stage the temperature of the frosty probe kept -8°C for next 40 minutes of which the solution was stirred after every 20 minutes. Then the temperature of the frosty probe changed -1°C per 20 min of time interval and allow the ice crystal to grow for next 1 hour. After formation of a golf ball size (approximate diameter 2.5-3 cm) ice crystal it was pull out from the solution with the frosty probe (Fig. 3.1H). It was then detached from the frosty probe by gradual increase of the temperature of the probe to 0.1°C. The detached ice crystal was then wiped with Kimwipe® and put onto a plastic pane in flat side down state. It was kept into a -20°C freezer for at least 20 minutes. Finally, this ice crystal was kept on a UV-lamp to excite the fluorescent molecules and photographed with a camera that can filter the emission of nonspecific light.

Preparation of fluorescently labeled native and recombinant bpAFP

40 μL of 5 $mg{\cdot}mL^{-1}$ Rhodamine [5(6)-TAMRA-X, SE (6-(Tetramethylrhodamine-5-(and-6)-Carboxamido) Hexanoic Acid, Succinimidyl Ester, mixed isomers] (Life Technologies) was added to 1 mL of 4 $mg{\cdot}mL^{-1}$ bpAFP solution

in 100mM $NaHCO_3$ (pH 8.0). This solution was mixed in a tube rotator for 4 hours at room temperature to ensure the attachment of fluorescent dye with the protein molecules. To remove unreacted reagent the reaction mixture was transferred into a Vivaspin 20 mL (2 kDa) centrifuge tube and 12 mL of 10 mM $NaHCO_3$ (pH 8.0) was added. This solution was concentrated to 1 mL and repeated this procedure for twice more times to wash out all unreacted dyes. Fluorescently labeled bpAFP was transferred to a 50 mL centrifuge tube and cooled degassed milliQ (4 °C) was added to prepare 0.1 $mg{\cdot}mL^{-1}$ solution of the protein. The 0.01, 0.02 and 0.03 $mg{\cdot}mL^{-1}$ concentrated solutions were prepared by successive dilution of 0.1 $mg{\cdot}mL^{-1}$ concentrated solution. Similar procedures was followed to prepare fluorescently labeled rbpAFP. For rbpAFP along with Rhodamine another dye pacific blue® (Succinimidyl ester) (Life Technologies) was used. Ice hemispheres in all these solutions were prepared and photographed according to the methodology described in previous section.

Preparation of fluorescently labeled nfeAFP6

50 μL of 5 $mg{\cdot}mL^{-1}$ Rhodamine [5(6)-TAMRA-X, SE (6-(Tetramethylrhodamine-5-(and-6)-Carboxamido) Hexanoic Acid, Succinimidyl Ester, mixed isomers] (Life Technologies) was added to 1 mL of 8 $mg{\cdot}mL^{-1}$ nfeAFP6 solution in 100mM $NaHCO_3$ (pH 8.0). This solution was mixed in a tube rotator for 4 hours at room temperature to ensure the attachment of fluorescent dye with the protein molecules. To remove the unreacted dyes the reaction mixture was dialyzed using Spectra/Por®3 dialysis membrane against 10 mM $NaHCO_3$ (pH 8.0) for 10 hours. This fluorescently labeled proteins was then transferred to a 50 mL falcon tube and adjusted the volume to 40 mL by adding cooled degassed milliQ (4 °C) to adjust the final protein concentration to 0.20 $mg{\cdot}mL^{-1}$. The 0.10 and 0.02 $mg{\cdot}mL^{-1}$ concentrated rhodamine labeled nfeAFP6 solution were prepared by successive dilution of 0.20 $mg{\cdot}mL^{-1}$. Ice hemispheres in all these solutions were prepared and photographed according to the methodology described in previous section.

Size exclusion chromatography

Size exclusion chromatography was carried out using Suparose® 12 (Mr = 1-300 kDa) column of Amershem Biosciences. The column was calibrated using blue dextran, bovine γ-globulin, haemoglobin, lysozyme and vitamin B12 of molecular weight 200-kDa, 158-kDa, 64-kDa, 14.3-kDa and 1.35-kDa respectively. The blue dextran was used to determine the void volume which was 8.0 mL for that column. The injection volume of all the standard as well as analytes was 250 μL. All the solutions were prepared using milliQ as solvent and centrifuged before injection to the column to sediment the undissolved particles (if any). The 0.15 M NaCl and 0.05 M Na_2HPO_4 (pH 7) buffer was used as mobile phase for SEC with 0.2 $mL{\cdot}min^{-1}$ flowrate. The stock solutions of bpAFP and rbpAFP were prepared at the concentration 10 $mg{\cdot}mL^{-1}$ and successively diluted to prepare 0.5-5.0 $mg{\cdot}mL^{-1}$ solutions with milliQ.

Analytical ultracentrifugation (AUC)

A Beckman Optima XL-I Analytical ultracentrifuge (Beckman Coulter) was used for sedimentation velocity measurements at 40,000 rpm at 4 °C with 2.5 mg of bpAFP in 0.5 mL AFP of 10 mM sodium phosphate (pH 7.9). Double sector charcoal-Epon cells equipped with quartz windows were used and concentration distributions were determined by absorbance optics. Sedimentation coefficient distributions were determined using standard methodology.

3.4 Results

The hexagonal ice crystal consists numerous crystallographic ice planes defined by Miller-Bravais indices. Only a few of them are known to be intractable planes for known AFP molecules (Wathen et al., 2003; Basu et al., 2013), such as (0001) basal plane, (1-100) primary prism plane, (2-1-10) secondary prism plane, (20-21) pyramidal plane (Fig. 3.2). The FIPA analysis was carried out to investigate the interacting ice planes on a single macroscopic crystal of bpAFP and rbpAFP. The ice hemisphere grown in 0.01 $mg{\cdot}mL^{-1}$ concentrated bpAFP and rbpAFP solutions with the orientation of *c*-axis parallel to the frosty probe illumination from the fluorescently tagged protein near the periphery of the ice hemisphere (Fig. 3.4Ba and 3.5Ba). When the hemispheres oriented at the right angle to this direction, with the *c*-axis of the ice mounted perpendicular to the frosty probe, six of twelve ellipses were illuminated on the equator of the hemisphere (Fig. 3.3Aa and 3.5Ba) indicating the bpAFP and rbpAFP binding planes. Winter flounder AFP (wfAFP) showed a similar but not identical pattern of ellipses oriented in the same direction (Basu et al., 2013; Knight et al., 1991). Its binding surfaces were (20-21) pyramidal planes with clear breaks between the surfaces on opposite sides of the equatorial division. However, the pyramidal planes bound by bpAFP are less well separated as though they bind to a pyramidal plane that is closer to the primary prism surface. At these low concentration there were no sign of bpAFP or rbpAFP binding to the (0001) basal plane.

With increasing bpAFP or rbpAFP concentration the ice hemisphere became illuminated over its entire surface, partially obscuring the plane-specific signals seen at one tenth the highest concentration tested (Fig. 3.3A, b-d; 3.4B, b-d; 3.5b-d and 3.6B, b-d). These observations suggest that bpAFP is capable of binding to multiple ice planes of an ice crystal in a concentration-dependent manner. The bpAFP-binding to a basal plane was clearly evidenced by illumination at the center of the ice hemisphere mounted with its *c*-axis normal to the frosty probe (Fig. 3.4Bd and 3.6Bd). Widespread binding over the ice hemisphere has generally been observed with hyperactive AFPs at the concentration of 0.1-1.0 $mg{\cdot}mL^{-1}$ (Basu et al., 2013; Hanada et al., 2014).

This concentration-dependent ice crystal binding affect the ice crystal sizes grown in the presence of bpAFP (Fig. 3.3B). Interminable binding of these peptide molecules onto the ice surfaces decreased the length of the ice crystals along c-axis from 35-4 μm with increasing concentration 0.5-50 $mg{\cdot}mL^{-1}$. Concurrently, the ice

bipyramids became less faceted and rounded in shape, and finally changed to a tiny lemon shaped ice crystal. This alteration and shrinkage of the shape and size further supports the binding ability of bpAFP to multiple ice planes including basal planes, as the resultant lemon shaped ice crystals are only observed for hyperactive AFPs from insect and fish, such as Maxi (Bar-Dolev et al., 2012; Sun et al., 2014). However, the FIPA images of the moderately active AFPs visualized that they could not bind onto the basal planes of the ice hemispheres (Basu et al., 2013). This is the first report of concentration dependency of the ice plane specificity of any AFP. Therefore, FIPA analysis of a recombinant nfeAFP6 were carried out at the concentrations 0.02-0.20 $mg{\cdot}mL^{-1}$ (Fig. 3.7). It gives similar pattern at all the concentrations even at the double concentration of the highest concentration used for bpAFP i.e. 0.2 $mg{\cdot}mL^{-1}$ (Fig. 3.7c). The polar regions of the ice crystals (mounted *c*-axis normal to the frosty probe) were dark at all concentrations, which implies that it cannot bound onto the basal planes.

To see if bpAFP had any tendency to form oligomers in solution, the sample was examined by analytical ultracentrifugation. At a concentration 5 $mg{\cdot}mL^{-1}$, about 2.7% of the loaded bpAFP sedimented as a tetramer. There was no sign of a dimer or trimer, but a trace amounts of an octamer (Fig. 3.9). Oligomerization of rbpAFP was also supported by the results of size exclusion chromatography shown in figure 3.8.

3.5 Discussion

Type I AFPs inhibit ice growth by adsorbing onto the pyramidal or prism planes of the hexagonal ice crystal. Such binding of bpAFP to the pyramidal planes closer to the primary prism surface alter the shape of ice crystal to hexagonal trapezohedron with a fixed *c* to *a* axis ratio of 3.6:1 at lower concentrations. In contrast, wfAFP directed hexagonal bipyramid shape of ice crystal with a fixed *c* to *a* axis ratio of 3.3:1 (Dingyi and Laursen, 1992). With the increasing concentration bpAFP these crystal became less faceted and finally converted to lemon-shaped ice crystal which is one more indication of hyperactivity of BpAFP. It was initially proposed that this binding of the type I AFPs mediated by the hydrogen bonds formed between the hydroxyl groups of four regularly spaced threonines. This hypothesis has been examined by site specific mutation (Harding et al., 1999) that showed the removal of middle two threonines to valine caused no significant change in antifreeze activity. In contrasts, mutation of these threonines to a polar amino acid serine diminishes the antifreeze activity of that peptide. These results suggested that the methyl group of the threonine residues and the hydrophobic interaction of the ice binding residues are indispensable for antifreeze activity of type I AFPs.

At higher concentrations bpAFP molecules concurrently interact with multiple planes including basal planes. The basal plane binding of rod like wfAFP was absent even in the molecular dynamics simulation studies in which the hyperactive *Tm*AFP showed similar characteristics observed in experimental conditions (Wathen et al.,

2003), such as basal plane binding, busting along *a*-axes. Here, it is notable that *Tm*AFP displayed entirely fluorescent ice hemispheres, similar ice hemispheres were observed in the presence of natural and recombinant bpAFP at the protein concentrations 0.1 $mg \cdot mL^{-1}$. In hyperactive AFPs, for example *Tm*AFP, sbwAFP, *Mp*AFP (see details in section 1.4.2), a region containing two-dimensional arrays of threonines was initially assigned to IBS that orients the side-chain hydroxyl groups outward with remarkably similar spacing. Such IBS of these AFPs showed complementary space-match to multiple ice planes. The X-ray crystal structure of *Mp*AFP clarified the extensive ice like water array in anchored on the IBS where water molecules are anchored directly via hydrogen bonds to the peptide backbone and adjacent side chains (Granham et al., 2011). These anchored clathrate waters allowed a hypothesis that the clathrate water play an anchoring role to bind AFP to ice surfaces. On the other hand, the hyperactive AFP from an Antarctic sea ice bacterium, *col*AFP, and Maxi neither contain 2D-arrays of threonines nor the ice-like water arrays on their IBS. The hyperactivity of *col*AFP arises from its compound IBS that allow this molecule to contact with extensive area of an ice crystal (Hanada et al., 2014). In latter one, α-helical Maxi, form a four helix bundle structure, which coordinate ~400 waters into polypentagonal networks (Sun et al., 2014). Those polypentagonal water molecules fit into the ice lattice waters of multiple planes that also includes basal planes. Presence of Maxi-like four helix bundled oligomer has been observed for bpAFP. Both Maxi and bpAFP are largely composed of the 11-residue repetitive unit TX_{10} (where X is mostly alanine), and the repetitive unit of Maxi forms three helical turns with an average of 3.7 residues per turn, as opposed to 3.6 residues per turn in the classic α-helix (Sharp et al., 2014; Sun et al., 2014). As shown by the Maxi crystal structure this deviation in the peptide bond facilitates hydrogen bonding between the backbone carbonyl groups and the solvent water molecules. Moreover, the small size of the Ala side chain also helps water to access the peptide backbone. These two factors presumably contribute the extraordinarily high solubility of bpAFP.

The hydrophobicity of the ice-binding face of type I and other AFPs (1) was a key observation in formulating the clathrate water mechanism for adsorption of these AFPs to ice, first proposed by molecular modeling (Sharp et al., 2014; Sun et al., 2014). The hydrophobic groups can project water into a cage structure that matches waters in ice and quasi liquid layer immediately above the ice. Robust evidence for this ice-like water structure came from the X-ray crystallography (Garnham et al., 2011) with the added discovery that these clathrates are stabilized (anchored) to nearby hydrogen bonding groups on the peptide backbone (as in type I AFP) and hydrophilic side chains. Given that anchored clathrate waters on ice-binding site can merge with the quasi liquid layer they can also fuse with waters on another IBS. This compatibility is perhaps one reason why so many AFPs have crystallized with apposed IBSs that have obscured the full extent of water coverage (Sun et al., 2014). A striking example of water mediated fusion is the structure of Maxi, an extreme variant of type I wfAFP that forms a four-helix bundle structure held together by an internal network of clathrate waters (Sun et al., 2014). Tellingly, the ice-binding residues (Thr, Ala, Ala) project inwards to

organize the water network that binds the helices together. Despite this, Maxi has hyperactive ice-binding activity, which is explained by the water organization extending outwards from the interior to bind the AFP to many different planes of ice, including the basal planes.

It can be suggested that this same process is at work here with bpAFP. A small percentage of the monomer associates in a concentration-dependent manner through its ice-binding site to form a tetramer which, like Maxi, has a more extensive array of clathrate waters on its outer surface to match multiple planes of ice. This hypothesis explains why bpAFP has the properties of moderately active type I AFP at low concentrations, and hyperactivity at higher concentrations. Indeed, it is quite possible that Maxi evolved along these lines in order to help stabilize the beneficial associations of four helices. By extending the length of the helix through repeated gene duplication, and with folding into a heparin that can dimerize in an antiparallel way through clathrate waters, a more stable four-helix bundle structure would be achieved. We note that the antiparallel alignment of four bpAFP helices has neutralize the charges of the N- and C-terminal cap structures, with two positive and two negative charges at either end.

Figures

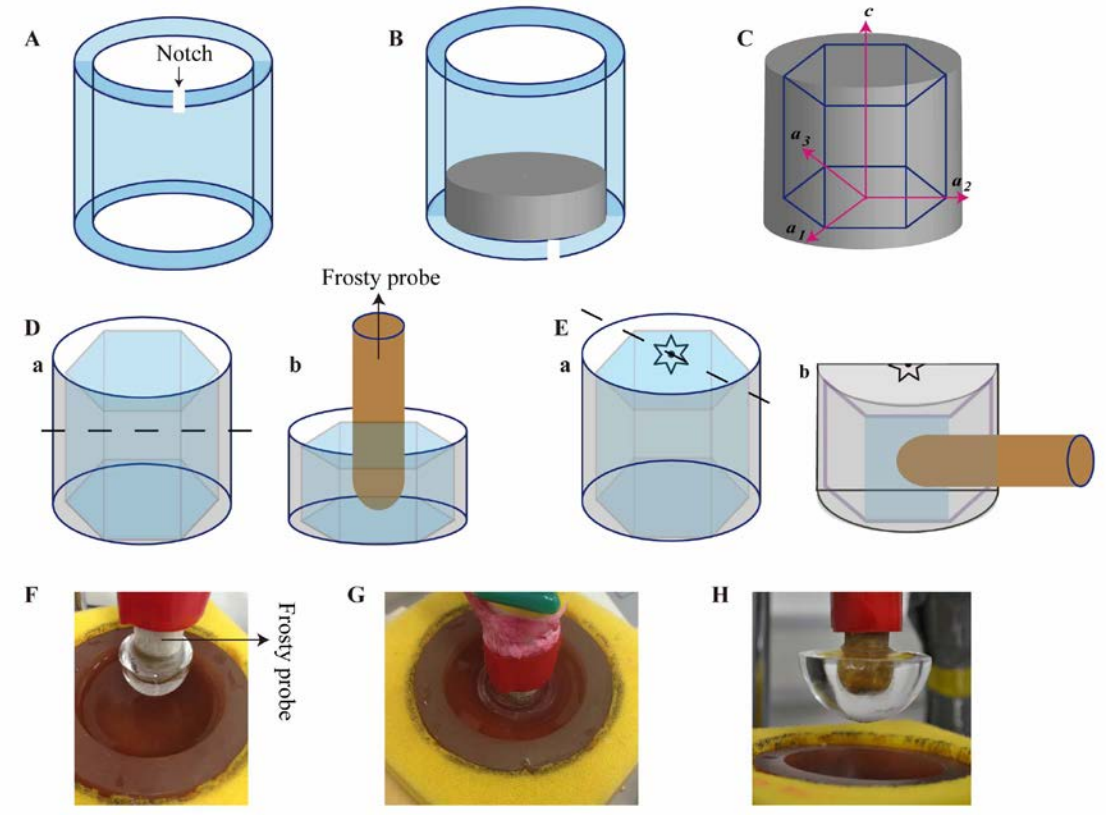

Figure 3.1.
Schematic representation of preparation of cylindrical and hemispherical hexagonal single ice crystals. Schematic representation of (A) a PVC cylindrical mold (4.5 cm diameter, 4 cm high and 4 mm thick) with a notch (1 mm wide and 2 mm height), (B) cylindrical seed single ice crystal formed with two basal planes on top and bottom, (C) the hexagonal single ice crystal, (D) the cylindrical ice crystals were cut along the dashed line (a) to mount that in the orientation in which the frosty probe is parallel to the *c*-axis (b), (E) the cylindrical ice crystals were cut along the dashed line (a) to mount that in the orientation in which the frosty probe is normal to the *c*-axis (b). (F) Preparation of small single ice hemisphere of known orientation by attaching the ice crystals (Db or Eb) on the frosty probe. (G) Immerging that single ice crystal in the solution containing fluorescently labeled AFPs. (H) A representative golf ball size ice hemisphere (diameter 2.5-3 cm) formed in fluorescently labeled AFP solution.

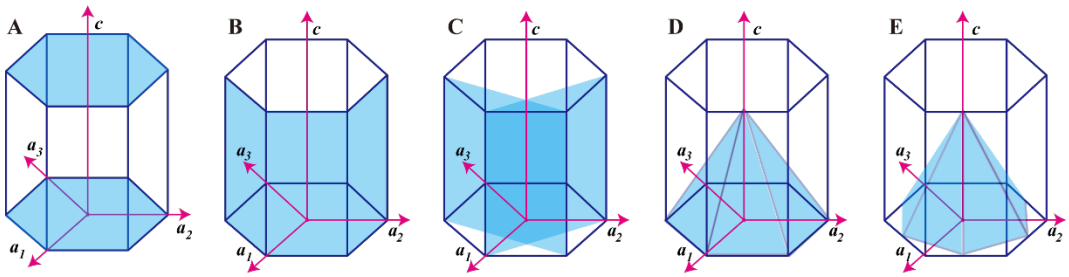

Figure 3.2.
Schematic representation of the ice binding planes of AFPs in a hexagonal ice crystal. Schematic representation of the (A) basal planes, (B) primary prism planes, (C) secondary prism planes, (D) pyramidal planes aligned with *a*-axes and (E) pyramidal planes offset of *a*-axes.

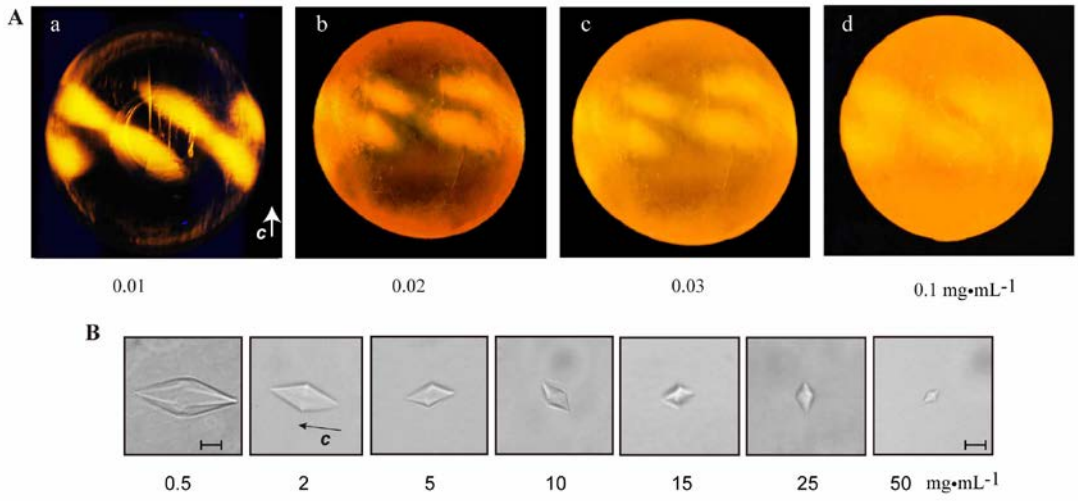

Figure 3.3.
Concentration-dependent interminable ice-binding and change in the ice crystal morphologies in the presence of bpAFP. (A) The UV-illuminated ice hemispheres grown in Rhodamine® labeled bpAFP at the concentrations 0.01-0.1 mg·mL^{-1}, all the ice crystals were mounted keeping their *c*-axis normal to the frosty probe. (B) Alteration of the ice crystal shape from hexagonal trapezohedron to lemon-shaped and concentration dependent change of the ice crystal size.

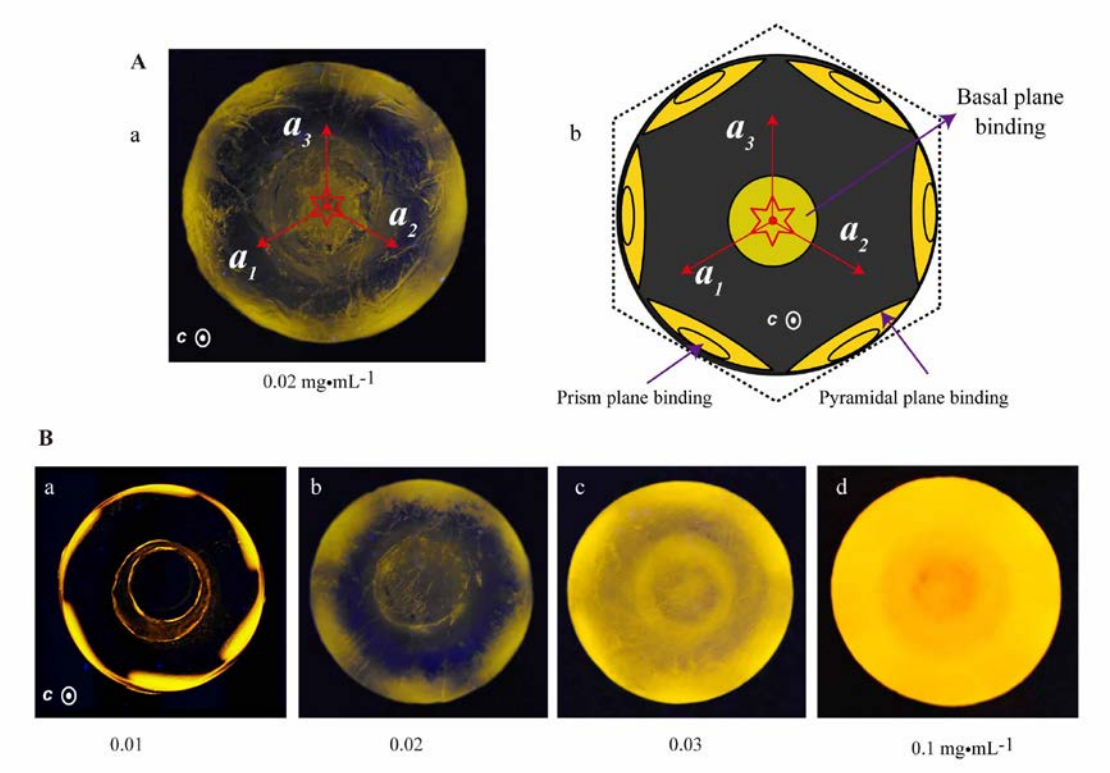

Figure 3.4.
Concentration-dependent interminable ice-binding of bpAFP. (A) The UV-illuminated ice hemisphere grown in Rhodamine® labeled bpAFP at the concentration 0.02 mg·mL^{-1} (a) and interpreted illustration of ice-binding planes of AFPs in this orientation of a hemispherical hexagonal crystal (b). (B) The UV-illuminated ice hemisphere grown in Rhodamine® labeled bpAFP at the concentrations 0.01-0.1 mg·mL^{-1}, all the ice crystals were mounted keeping their *c*-axis parallel to the frosty probe.

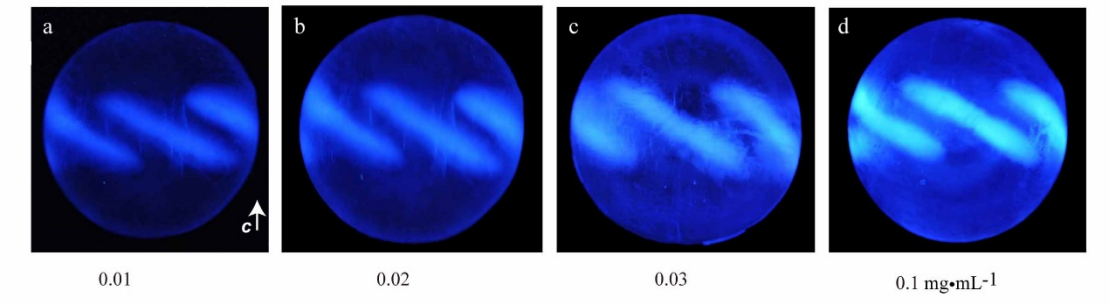

Figure 3.5.
Concentration-dependent interminable ice-binding of rbpAFP. (A) The UV-illuminated ice hemispheres grown in Pacific Blue® labeled rbpAFP at the concentrations 0.01-0.1 mg·mL^{-1}, all the ice crystals were mounted keeping their *c*-axis normal to the frosty probe.

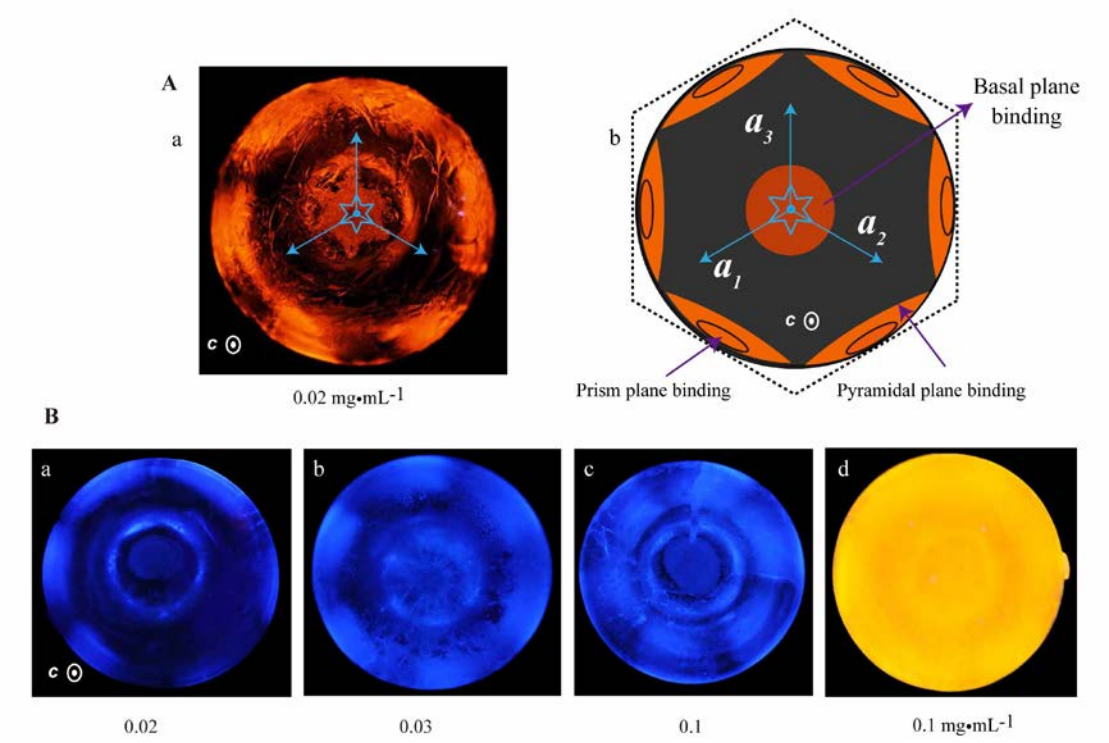

Figure 3.6.
Concentration-dependent interminable ice-binding of rbpAFP. (A) The UV-illuminated ice hemisphere grown in Rhodamine® labeled rbpAFP at the concentration 0.02 mg·mL^{-1} (a) and interpreted illustration of ice-binding planes of AFPs in this orientation of a hemispherical hexagonal crystal (b). (B) The UV-illuminated ice hemisphere grown in Pacific Blue® (a-c) and Rhodamine® (d) labeled rbpAFP at the concentrations 0.02-0.1 mg·mL^{-1}, all the ice crystals were mounted keeping their *c*-axis parallel to the frosty probe.

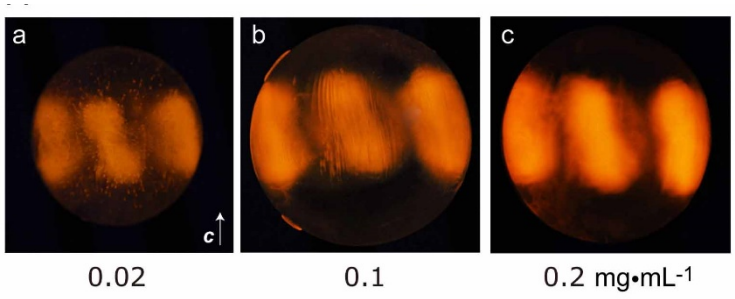

Figure 3.7.
Concentration-dependent FIPA images of nfeAFP6. The UV-illuminated ice hemispheres grown in Rhodamine® labeled nfeAFP6 at the concentrations 0.02-0.2 mg·mL^{-1}, all the ice crystals were mounted keeping their *c*-axis normal to the frosty probe.

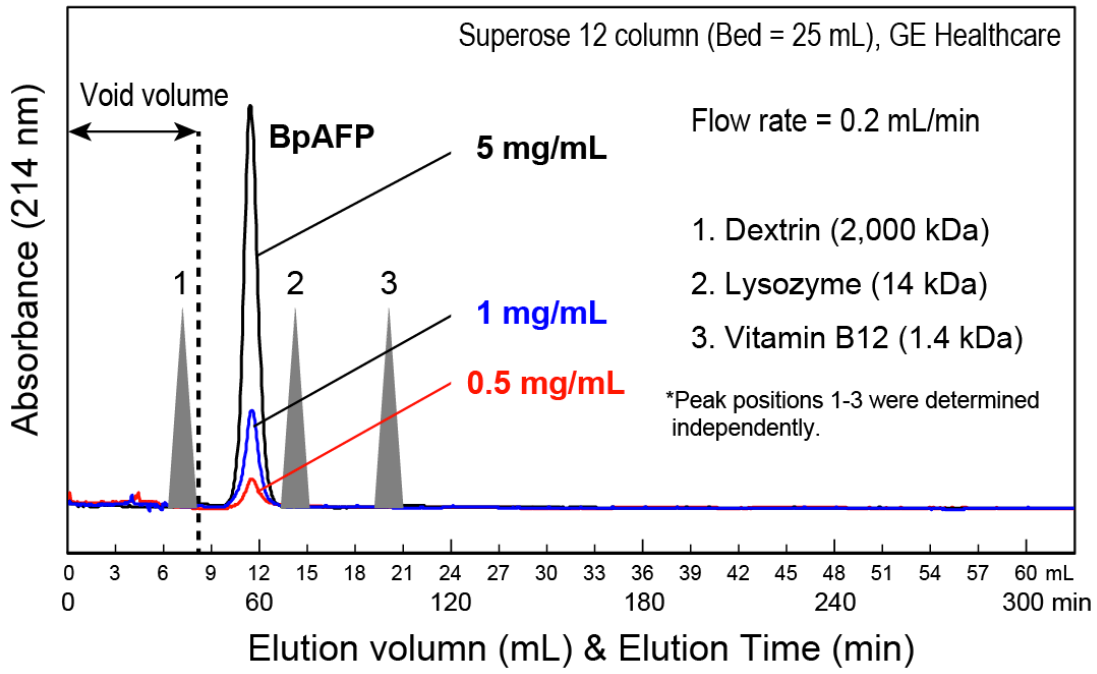

Figure 3.8.
Size exclusion chromatogram of rbpAFP. When 0.5 – 5 mg·mL^{-1} of the rbpAFP solutions (250 μL) were applied to one of the SEC columns (Superose 12), the protein was always eluted at a position between the peaks 1 and 2. If rbpAFP exists as a monomer (3.2 kDa), it should be eluted between the peaks 2 and 3. Our calibration using more data suggests that rbpAFP are assembled together to behave like an oligomer of ~30 kDa, regardless of its concentration.

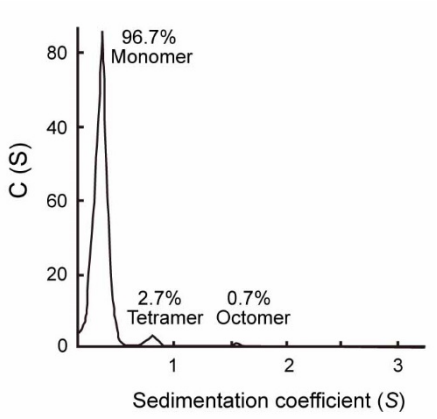

Figure 3.9.
Sedimentation profile of bpAFP from the analytical ultracentrifuge analysis.

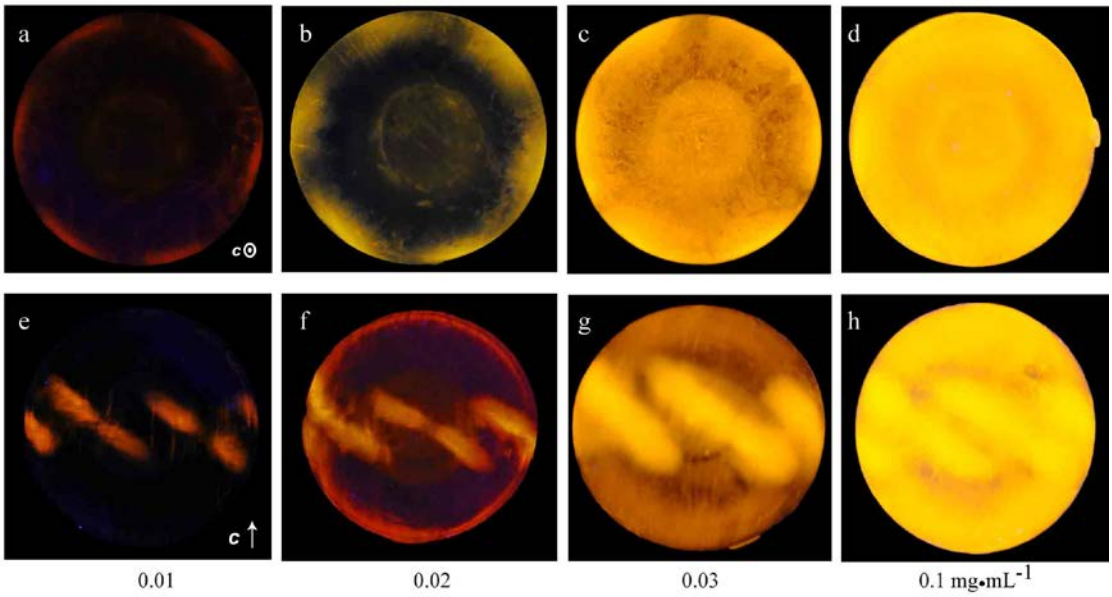

Figure 3.10.
Concentration-dependent interminable ice-binding of rbpAFP. The UV-illuminated ice hemisphere grown in Rhodamine® labeled rbpAFP at the concentration 0.01-0.1 mg·mL^{-1}, the orientation of the *c*-axis of upper and lower row are shown the figures a and c.

Thermal Hysteresis (TH) Activity and Effect of Temperature and solution pH on the TH

Chapter: 4

4.1 Summary

Abstract

Antifreeze proteins (AFPs) specifically bind to the ice surfaces to change the morphology of the ice crystals. Such biding depresses the freezing temperature in non-colligative manner, which is known as thermal hysteresis (TH) activity. The TH is a concentration-dependent parameter that used to evaluate the antifreeze activity of different AFPs. Here, the TH activity of the newly discovered antifreeze protein (bpAFP) and its recombinant protein (rbpAFP) have been determined. The TH activity is dependent on the concentration of the peptides as well as their conformation. The ice binding ability decreases upon denaturation of the AFPs. The denaturation of any protein largely depends on the temperature and solution pH. Consequently, temperature and pH of the solution affected on the TH activities of bpAFP and rbpAFP. The change in α-helical content at different temperature and pH has also been reported here. The experimental results suggests that (1) bpAFP can exhibit high TH activity at higher protein concentrations, (2) it forms a pH stable α-helix and can renature the secondary structure and activity after heating at 90 °C and (3) the busting pattern of bpAFP is also unique that represents both parallel and perpendicular to *c*-axis direction busting in a concentration-dependent manner.

Outlines

In this chapter the author described the contents of an unpublished manuscript entitled "Concentration-dependent oligomerization of an α-helical polypeptide makes it hyperactive" by Sheikh Mahatabuddin, Yuichi Hanada, Yoshiyuki Nishimiya, Ai Miura, Hidemasa Kondo, Peter L Davies and Sakae Tsuda. The authors contributions are S.M. and S.T. designed research; P.L.D. contributed new analytic tools; S.M., Y.H., Y.N., A.M., and H.K. performed Research and analyzed data; S.M., P.L.D., and S.T. wrote the paper. It also contains the data of another unpublished manuscript entitled "A super soluble 40-residual type I antifreeze protein consists an exceptionally pH stable and fully renaturable α-helix" by Sheikh Mahatabuddin, Yoshiyuki Nishimiya, Ai Miura, Tomoyasu Aizawa, Hidemasa Kondo and Sakae Tsuda. The authors contributions are S.M. and S. T. designed the research; S.M., Y.N., A.M., and H.K. performed Research and analyzed data; S.M. and S.T. wrote the manuscript.

4.2 Introduction

Antifreeze proteins (AFPs) are found in various psychrophilic organisms ranging from bacteria to fish. AFPs specifically adsorb onto the ice crystal surfaces to alter their morphology and stop their growth. Binding of AFPs slightly elevate the melting temperature (T_m) and depress the freezing temperature (T_f) in non-colligative manner of AFP bound ice crystal to create a gap between this two temperature (these two temperatures are similar in numerical values of the aqueous medium in the absence of AFP). This gap between melting and freezing temperature generated by adsorbed AFPs is denoted as thermal hysteresis (TH) (Fig. 4.1). It is a definitive measure to evaluate antifreeze activity.

The TH activity depends on the concentration, solution environment (i.e. pH) and conformation of the peptides. The AFPs can exhibit 0.5-1.0 ºC of TH at millimolar concentrations to ~6.0 ºC of TH at sub-millimolar concentrations. Former group of AFPs known as moderately active whereas the latter one is denoted as hyperactive AFP (Scotter et al., 2006; Middleton et al., 2012). Adsorption of AFPs on the ice surfaces decrease the surface energy through Gibbs-Thomson effect and convert the flat ice fronts to curved ice front (Knight et al., 1991). Such curvatures are energetically unfavorable for formation of new ice layers compared with the flat ice fronts and inhibit ice formation that defined as adsorption-inhibition mechanism (Raymond and DeVries, 1977). Most of the fish AFPs are adsorbs onto only a part of ice crystal. The α-helical fish AFPs (M W = ~ 3.5-kDa) with regularly spaced thr after every 11 amino acid residues are known as fish type I AFPs. All known type I AFPs showed moderate TH activity at their highest soluble concentrations. An α-helical bundle protein with high TH activity (2.21 ºC at 0.4 mg·mL^{-1} protein concentration) has been identified in winter flounder, Maxi. Which is a 33-kDa homodimer with hyperactivity (type Ih) (Marshall et al., 2005). X-ray crystallography showed that Maxi folds as a four-helix bundle with the erstwhile 'ice-binding' residues projecting inwards to help organize ~400 waters in its core that form a polypentagonal network and the four helices together (Sun et al., 2014). Another type Ih AFP that showed 2 ºC of TH activity at 0.4 mg·mL^{-1} protein concentration has been identified in another flounder fish American plaice (Gautheir et al., 2005). In addition, there are some defective isoforms of fish AFPs that failed show any significant TH activity even at 14 mg·mL^{-1} of protein concentration. For example, isoform 2 and 6 of Notched-fin eelpout AFP (nfeAFP2 and nfeAFP6) (Nishimiya et al., 2005; Takamichi et al., 2009).

It has been reported that the TH of α-helical AFPs is affected by different factors such as helix stability, the helix dipole and the arrangement of polar residues on the face of the helix (Davies PL and Hew, 1990; Chakrabartty and Hew, 1991; Gronwald et al., 1996; Patel and Graether, 2010). These factors are influenced by thermal denaturation or pH of the solution. The thermal denaturation of AFP9 (winter flounder), LS-12 (longhorn sculpin) and cunner AFP is reversible within the temperature range 1-60, 1-90 and 1-70°C, respectively (Chao et al., 1996; Deng and Laursen, 1998; Hobbs et al., 2011), while the antifreeze activities of these proteins after heating were not reported. By contrast, the AFP from from *Lolium perenne* grass (LpAFP) was active even after heating at 95°C (Middleton et al., 2012). The activity or identical CD profile after heating referred that these proteins are folded properly after thermal denaturation.

The pH of the solution also partially denature the peptides through changing the protonation state of the polar residue (Russo et al., 2012)). That change in protonation state alter the protein confirmation related to those residues. Such change deceases the TH activity at lower or higher limit of pH of two fungal AFP, TisAFP and AnpAFP (Xiao et al., 2010). The TH activities of these proteins fluctuated at least two fold at the same peptide concentration within the experimental pH range 2-8 and 2-13, respectively. On the other hand, the TH activity of wfAFP was not altered significantly within a pH range 3-11. Although the helical content of this AFP was changed within this pH range (Chakrabartty and Hew, 1991) for which helical contents were determined from the CD spectra at respective pH. However, pH of the solution can not completely nullify the helix concentent of this AFP even at very acidic or basic pH, which also evident from its significant TH activity at pH 1 or 13.

In this chapter, the author described about the TH activity of the native and recombinant bpAFP. The ice crystal bust, rapid growth of the AFP bund ice crystal at the lower range of TH, in the presence of these peptides has been observed. The effects of applied temperature and pH on the TH activity and helical content of these protein were also been examined at a fixed protein concentration.

4.3 Materials and methods

Measurement of TH activity

The TH activities of native and recombinant protein were measured using the photomicroscope system described by Takamichi et al. (2009) (Fig. 4.2). This photomicroscope system consists a Leica DMLB 100 photomicroscope equipped with Linkam LK600 temperature controller and a CCD camera. A 0.8 μL of desired concentrated peptide solution was frozen completely by cooling to -25^{o}C. Frozen samples were then thawed gradually to prepare a seed ice crystal and carefully observe its melting temperature T_m. After that the temperature of the solution again decreased gradually at the rate 0.1 ^{o}C·min^{-1} and the morphological change of that crystal was observed in the monitor. The temperature at which ice crystal started to grow up rapidly was recorded as the ice-initiation temperature (T_f). Difference between T_f and T_m was recorded as TH value at particular concentration. The 25 mM NH_4HCO_3 (pH 7.4) buffer was used as a solvent for preparation of protein solution with desired concentration. Al the experiments were carried out for minimum three times and final TH was the average value of these three individual measurements.

Effect of applied temperature on TH

A 100 μL of protein solution (12 mg·mL^{-1}) in 25 mM NH_4CO_3 (pH 7.4) buffer were heated for five minutes at desired temperature. After that the samples were allowed to cool down by keeping on ice for 3 minutes. TH activity was measured according to the method described in previous section. After heating at 80 and 100^{o}C the solutions became cloudy (Fig. 4.4E, F). The TH activity of the supernatants of the

precipitated solutions were measured after centrifugation for 1 min in a table top centrifuge machine. Al the experiments were carried out for minimum three times and final TH was the average value of these three individual measurements

Effect of pH on TH

A 40 μL of protein solution (10 mg·mL^{-1}) at different pH shown in table. 4.1. TH activity was measured according to the method described in previous section. Al the experiments were carried out for minimum three times and final TH was the average value of these three individual measurements.

Measurement of CD spectrum

Peptide solutions were prepared at 0.3 mg·mL^{-1} concentration in 10 mM sodium phosphate buffer of pH = 7.4. CD spectrum were recorded at the temperature range 0-90°C using JASCO J-725 CD spectrophotometer equipped with JASCO PTC-348WI temperature controller (Jasco Analytical Instruments, MD, USA). The pH dependence of the α-helix of native and recombinant protein was also measured at same concentration, the protein solutions were prepared at different pH using 10 mM sodium phosphate buffer for which pH was fixed by addition of 1M HCl or NaOH. The temperature during measurements of effect of pH were fixed at 20°C. CD data in degrees then converted to mean residue ellipticity (deg·cm^2·dmol^{-1}) using the following equation.

$$[\boldsymbol{\theta}]_{\boldsymbol{mrw},\lambda} = \frac{\boldsymbol{MRW} \times \theta_\lambda}{\boldsymbol{10} \times \boldsymbol{d} \times \boldsymbol{c}} \mathbf{deg}\, \boldsymbol{cm^2\, dmol^{-1}}$$

Where, $MRW = \frac{\text{Molecular Wight of protein in Da}}{\text{Number of amino acid (N)} - 1}$, θ_λ = CD data in degrees at λ wavelength, c = concentration in g·mL^{-1} unit.

Calculation of fraction of helix

The fraction helix was calculated from the mean residue ellipticity (deg·cm^2·dmol^{-1}) at 222 nm ($[\theta]_{222}$) for respective temperature and pH. The solution inside the cell in each temperature was retained for 5 minutes to confirm the temperature experienced by all of the peptide molecules. The fraction helix was calculated using the formula used by Greenfield and Fasman (1969). The formula was-

$$Fraction\ helix = \frac{[\theta]_{222}^{obs} - [\theta]_{222}^{coil}}{[\theta]_{222}^{helix} - [\theta]_{222}^{coil}}$$

The ellipticity of each peptide in 6.0M guanidine hydrochloride at 20 °C was assumed to represent 0% helix and its ellipticity at 222 nm was used as $[\theta]_{222}^{coil}$ for respective protein. The ellipticity for 100% helix formation was calculated from the equation described by Chen et al. (1974), $[\theta]^n = [\theta]^\infty(1 - {}^{k}/_{n})$; where, n and k are the chain length and wavelength−dependent factor, respectively (at 222 nm, k = 2.57 and $[\theta]^\infty$ = -39500).

Preparation of fluorescently labeled bpAFP

40 µL of 5 mg·mL^{-1} Rhodamine [5(6)-TAMRA-X, SE (6-(Tetramethylrhodamine-5-(and-6)-Carboxamido) Hexanoic Acid, Succinimidyl Ester, mixed isomers] (Life Technologies) was added to 1 mL of 8 mg·mL^{-1} bpAFP solution in 100mM $NaHCO_3$ (pH 8.0). This solution was mixed in a tube rotator for 4 hours at room temperature to ensure the attachment of fluorescent dye with the protein molecules. To remove unreacted reagent the reaction mixture was transferred into a Vivaspin 20 mL (2 kDa) centrifuge tube and 12 mL of 10 mM $NaHCO_3$ (pH 8.0) was added. This solution was concentrated to 1 mL and repeated this procedure for twice more times to wash out all unreacted dyes. Fluorescently labeled bpAFP was transferred to a 50 mL centrifuge tube and cooled degassed 10 mM $NaHCO_3$ (pH 8.0 (4°C) was added to prepare 0.2 mg·mL^{-1} solution of the protein. The 0.1 mg·mL^{-1} concentrated solutions with desired pH were prepared by successive dilution of 0.2 mg·mL^{-1} concentrated solution and required volume of HCl or NaOH. The cooled degassed 10 mM $NaHCO_3$ (pH 8.0) (4°C) was used as solvent for successive dilution. Latter the ice hemispheres in the presence of the AFP solutions (pH 6, 8 and 11.3) were grown up and photographed as described in section 3.3. The ice crystals were mounted keeping their basal planes normal to the frosty probe in all of the experiments.

4.4 Results

4.4.1 TH activities of natural and recombinant bpAFP

The concentration dependence profile of TH activities of both the natural and recombinant protein showed conventional hyperbolic profile (Fig. 4.3A), as obtained for other fish AFPs (Davies and Hew, 1990). The supersolubility of bpAFP and rbpAFP facilitated the TH measurements within a long range of concentration, 0.5-200 mg·mL^{-1}. The type I AFPs generally showed approximately 1 °C of maximal TH values obtained at 10-20 mg·mL^{-1} of peptide concentration, which also represents the dissolution limit of those peptides. Extrapolation of the hyperbolic TH profile of wfAFP (HPLC6) would put an upper limit of ~1.5 °C of TH if this was not limited by protein solubility (Marshall et al., 2004) (Fig. 4.3B). The native and recombinant bpAFP also produce approximately 1 °C of TH activity at the concentration of 10 mg·mL^{-1} whereas this value of TH increase to 2.5-3 °C with the increasing peptide concentration to 200 mg·mL^{-1}.

A TH activity of >2 °C is only one indication of hyperactivity. Such high TH value has only evaluated for the hyperactive AFPs (Scotter et al., 2006; Bar-Dolev et al., 2012; Hanada et al., 2014) and implying that bpAFP exerts a strong ability of ice-growth-inhibition at higher concentrations. This ability of ice-growth-inhibition further affects the busting patterns of the bpAFP bound ice crystals. The typical needle-shaped busting along the *c*-axis of the ice bipyramids occurred at lower concentrations of rbpAFP, such as 5 mg·mL^{-1} (Fig. 4.3C). By contrast, in the presence of highly

concentrated rbpAFP the ice crystal burst started from certain spot near the center of ice crystal and kept the crystal growth toward the direction normal to *c*-axis (Fig. 4.3D), similarly to hyperactive AFPs. This normal to *c*-axis ice crystal busting is another indication of concentration-dependent transition of hyperactivity of bpAFP.

4.4.2 Effect of temperature and pH on the TH of natural and recombinant bpAFP

Thermal denaturation of the AFPs affect their TH activities. For example, the hyperactive fish α-helical protein, Maxi, lost its TH activity even at room temperature (Marshall et al., 2005). Therefore, the effect of applied heat on the functional activities, TH activities, of the native and recombinant protein were observed at a fixed peptide concentration, 12 $mg \cdot mL^{-1}$. The TH activities of the heated samples were measured and plotted against their respective temperatures (Fig. 4.4A). It showed that, there are no significant change of the TH activities upon heating at 4-60 °C while it was lowered by further heating from 60-100 °C. This further heating aggregates the peptides (Fig. 4.4E, F), so that TH values estimated above 60 °C are attributed to the soluble active bpAFP or rbpAFP. It created an inflection point in the temperature dependent TH profile approximately at 70 °C that indicated the temperature at where the soluble fraction of these proteins becomes approximately 50% by heat treatment.

The dependence of the TH activities on the pH of the bpAFP and rbpAFP were examined. The activities of the 10 $mg \cdot mL^{-1}$ concentrated peptide solutions of both the native and recombinant bpAFP at a pH range 2 to 13 were measured. Approximately 0.6 °C of TH values were evaluated for both samples at neutral pHs, in which the native samples (isoform mixture) showed slightly more (about 10%) activity than the recombinant bpAFP (Fig. 4.4D). Their TH values were slightly decreased in both acidic (pH = 1-3) and basic (pH = 11-13), implies a stable nature of BpAFP against the pH change. A similar pH dependence was reported for wfAFP (Chakrabartty and Hew, 1991). It is notable that no aggregation was observed in the solutions within this range of pH.

4.4.4 Effect of temperature on the secondary structure of natural and recombinant bpAFP

The far-ultraviolet CD spectra of native and recombinant protein were resembled with the ordinary α-helical secondary structure (Fig. 4.4B and C). Their ellipticity minima were occurred at 222 and 208 nm. The negative value of this ellipticity minima were reduced with increasing temperatures similarly to sculpin AFP (Deng and Laursen. 1998). To compare the helicity of the native and recombinant peptide the ellipticity at 222 nm ($[\theta]_{222}$) was used, which is a reliable measure of α-helix formation and can be used directly to compare the helicity (Shoemaker et al., 1988). At 0 °C the fraction of the native and recombinant bpAFP contains 71 and 58 percent of α-helix, respectively (Table. 4.2). It was decreased with temperature and become 10 percent after heating at 60 °C, the TH activity after at this temperature was unchanged for both the natural and recombinant protein. Further heating at 70 °C the

helix content became 7-8 percent for which aggregation was observed at high concentration during TH measurements (Fig. 4.4E and F), while aggregated peptide was not observed during CD measurements even after heating at 90 °C. Lowering of the temperature from 90 °C to 0 °C results in restoration of 75 and 59 percent of helicity of bpAFP and rbpAFP, respectively. This values were almost identical before heating and implies completely reversible thermal denaturation of these peptides within the temperature range 0-90 °C. The helix content of wfAFP and sculpin AFP were reported 75 and 60 percent near 0 °C (Chakrabartty and Hew, 1991; Deng and Laursen. 1998).

4.4.5 Effect of pH on the secondary structure of natural and recombinant bpAFP

The helix formation of natural and recombinant protein was also affected by pH. The pH titration of the helix contents (Table. 4.2) showed that these protein have similar helix content within the pH 4-10 while it decrease to 0.4 at acidic (pH 2) and basic (pH 12) pH. These results were in agreement with the functional activities, TH, within this pH range (Fig. 4.4D). The fraction of helix for native bpAFP at pH 2 was 0.4 which increase with increasing pH and become 0.51 at the pH 8. It was then started to decrease with increasing pH and became 0.41 again at pH 12. Similar values of helical content were observed for recombinant bpAFP at pH 2 and 12, while the highest helical content of this peptide was 0.46 at pH 10. It presumably arises from their slightly different amino acid sequences, as recombinant protein consists GSAM in the N-termini and G in the C-termini in addition to the bpAFP sequence. However, the pH titration did not cause any acid/base hydrolysis as they showed potential functional activities even at pH 13.

4.4.5 Effect of pH on the ice plane affinity of natural bpAFP

The native and recombinant bpAFP interminably bind on multiple ice crystal planes within the concentration range 0.01-0.1 $mg \cdot mL^{-1}$. The ice hemispheres grown in the solutions containing 0.1 $mg \cdot mL^{-1}$ of the labeled bpAFP visualized completely fluroscent ice hemispheres (Chapter 3) that implies bpAFP can bound onto multiple planes of an ice including the basal plane. The change of the helical contents with pH evoked the author to examine the effect of pH on the ice plane specificity of bpAFP. Therefore, FIPA analysis at three different pH was carried out. This experiments visualized entirely fluorescent ice hemispheres (Fig. 4.6) within the pH range 6-11.3. Hence, the solution pH cannot affect the ice plane specificity of native bpAFP at 0.1 $mg \cdot mL^{-1}$ at least within this range of pH.

4.5 Discussion

The hydroxyl groups of the four regularly spaced threonines form hydorogen bonds with the space matched water molecules on the ice surfaces. This was the original hypothesis of ice binding mechanism of type I AFPs. It was examined by site specific mutational analysis of wfAFP (Wen and Laursen, 1992, 1993; Zhang and Laursen, 1998; Harding et al., 1999). These mutational analysis showed (1) removal of the

middle two or four threonine's hydroxyl groups (substituted with Val) caused no significant loss of activity, (2) mutation of the middle two threonines to serines nullified the activity, and (3) A17L mutant was inactive, A21L was poorly active, while A19L and A20L had little effect on activity. There is also a tendency that alanines are conserved but polar residues are variable between the type I AFP sequences. These data enabled to assign the ice-binding site (IBS) to alanine-rich face including A^{17}, where methyl groups of the 4 threonines were speculated to have more importance for ice binding than their hydroxyl groups (Baardsnes et al., 1999; Davies et al., 2002; Graham et al., 2013). The alanine-assembled surface protruding 4 equally spaced threonines is the corresponding region (IBS) in bpAFP. This IBS of the bpAFP and rbpAFP enabled them to bind onto the multiple surfaces of the crystal.

The hydrophobicity of the ice-binding face of type I and other AFPs (Dvaies, 2014) was a key observation in formulating the clathrate water mechanism for adsorption of these AFPs to ice, first proposed by molecular modeling (Sharp, 2014; Nutt and Smith, 2008). The hydrophobic groups can project water into a cage structure that matches waters in ice and quasi liquid layer immediately above the ice. Robust evidence for this ice-like water structure came from the X-ray crystallography (Granham et al., 2011) with the added discovery that these clathrates are stabilized (anchored) to nearby hydrogen bonding groups on the peptide backbone (as in type I AFP) and hydrophilic side chains. Given that anchored clathrate waters on ice-binding site can merge with the quasi liquid layer they can also fuse with waters on another IBS. This compatibility is perhaps one reason why so many AFPs have crystallized with apposed IBSs that have obscured the full extent of water coverage (Sun et al., 2014). A striking example of water mediated fusion is the structure of Maxi, an extreme variant of type I wfAFP, that forms a four-helix bundle structure held together by an internal network of clathrate waters (Sun et al., 2014). The hyperactive ice-binding ability of Maxi is explained by these organized waters extending outwards from the interior to bind the AFP to many different planes of ice, including the basal plane. Similar binding ability of the bpAFP and rbpAFP onto the ice crystals generates a high TH gap of 2.5-3 °C. In addition, bpAFP altered the ice crystal morphology to hexagonal trapezohedron at lower concentration which loss its facets and gradually converted to tiny lemon shaped ice crystal at higher peptide concentrations. Such lemon shaped or hexagonal ice crystal with rounded vertices was ordinarily observed in the presence of hyperactive AFPs, such as Maxi, *Tm*AFP (Marshall et al., 2005; Granham et al., 2011). This lemon shaped ice crystals in the higher concentrated bpAFP solutions started to grow from a weakly-protected point at the temperatures below TH gap and propagated normal to *c*-axis, similarly to Maxi. By contrast, the ice crystals busted along *c*-axis similarly to the moderately active AFPs at the peptide concentrations below 75 $mg \cdot mL^{-1}$. These results categorized bpAFP as a sole AFP molecule that can concurrently exhibit the properties of both moderately and hyperactive AFPs in a concentration-dependent manner.

The identical TH values of the natural and recombinant protein after heating at 4-60 °C implies that the proteins can get back their secondary structure after heating at this range of temperature. It also implies that this heating cannot alter the solubility of bpAFP or rbpAFP. The change in the activity caused by the aggregated peptides after heating at 80 or 100 °C referred denaturation of some molecules followed by aggregation. This aggregation decreases the active concentration of AFP that reduce the TH values. While, the temperature dependent CD spectra showed that these peptides undergoes reversible thermal denaturation within the temperature range 0-90 °C. It was attributed from their helical contents at 0 °C before and after heating at 90 °C. The helical contents of bpAFP were 0.71, 0.52, 0.23 and 0.06 at the temperatures 0, 20, 40 and 90 °C, which is similar to the value observed for wfAFP (Ananthanarayanan and Hew, 1977). At 60 °C the helical content of both the bpAFP and rbpAFP were 0.1 that presumably be the threshold helicity required to prevent aggregation at higher concentrations i.e. 12 $mg{\cdot}mL^{-1}$, as aggregation started after heating at that temperature during TH measurements. Additionally, the CD spectrum at a fixed wavelength (at 208 nm) showed that both the bpAFP and rbpAFP undergoes gradual denaturation. On the other hand, the CD spectrum of these peptides slightly deviates from the classical helical spectrum in that, the mean residue ellipticity at 208 nm was of substantially lower in magnitude than that of 222 nm (Table. 4.4). Thus the $[\theta]_{222}/[\theta]_{208}$ ratio was larger than one, which is a typical feature of CD spectra of coiled-coil structures (Lau et al., 1984; Cooper and Woody, 1990; Zhou et al., 1992). While this ratio may suggest the presence of coiled-coil, it is better explained by the exceptional amino acid composition. The ratio of the ellipticity values ($[\theta]_{222}/[\theta]_{208}$) at these wavelengths were 1.18 and 1.0 at 4 and 20 °C, respectively. The value obtained at 4°C (1.18) for both the bpAFP and rbpAFP are significantly different from the value of ~1.05 reported for coiled-coils (Lau et al., 1984; Cooper and Woody, 1990), but it is in between the $[\theta]_{222}/[\theta]_{208}$ ratio of 1.24 (4 °C) and ~1.15 (1-5 °C) exhibited by Maxi (Marshall and Chakrabartty, 2005) and type I AFP (synthetic HPLC6) (Gronwald et al., 1996; Houston et al, 1998), respectively. It is notable that under these conditions the type I AFPs are monomeric. Albeit, remarkably similar CD spectra with high $[\theta]_{222}/[\theta]_{208}$ ratios were reported for other type I AFPs, including snailfish AFP (Evans and Fletcher, 2001) and artificial antifreeze polypeptides (comprised of KAAK motifs) (Zhang and Laursen, 1999), as do synthetic, capped and salt-bridged alanine-rich helical peptides (Merutka and Stellwagen, 1991; Merutka et al., 1991). Such high $[\theta]_{222}/[\theta]_{208}$ ratios have demonstrated as the general feature of the CD spectra of alanine-rich helical peptides (Wallimann et al., 2003). The structural basis for the anomalous CD spectra of alanine-rich helices is not clear, but it presumably be a structural variation in the α-helix itself. Thus, the $[\theta]_{222}/[\theta]_{208}$ ratio of bpAFP and rbpAFP inferred that their α-helical structure does not contain any

coiled-coil though the CD spectra showed a little higher ratio than normal α-helical peptides. In addition, the decrease in the ratio from 1.18 to 1 and less than 1 after upon heating of bpAFP or rbpAFP is consistent with the behavior of type I AFP (Gronwald et al., 1996), Maxi (Marshall and Chakrabartty, 2005) and other natural and synthetic alanine-rich peptides (Wallimann et al., 2003), inferring that the structural feature underlying the anomalous spectrum is favored at low temperatures. Therefore, this structural uniqueness facilitated reversible thermal denaturation of this protein within a long range of temperature (0-90 °C), which also displayed through the significant TH activities even after heating at 100 °C.

The $[\theta]_{222}/[\theta]_{208}$ ratios of bpAFP and rbpAFP at 20°C remain almost identical in the long range of pH, pH 4-10 for natural protein and 2-10 for the recombinant protein. This ratio decreased slightly at acidic/basic pH for the bpAFP and at only basic pH for rbpAFP. It probably be the reason for slightly higher TH activity displayed by the rbpAFP at acidic pH than bpAFP. Furthermore, the helical contents within the pH range 4-10 remain virtually unchanged that enabled these proteins to exhibit similar TH activities within this range. Their activities and helical contents were also decreased in acidic (pH 2) and basic (pH 12) conditions. Such transition of the TH activities and helical contents of both the bpAFP and rbpAFP at acidic pH presumably be arise from the ionization of two types of carboxylic groups involved in helix-stabilizing interactions similarly to wfAFP (Chakrabartty and Hew, 1991), namely, the β-carboxylate of D^{1} that might involve in a favorable interaction with the positive pole of the helix dipole and the γ-carboxylate of E^{30} (i) residues involved in salt bridge interaction with K^{26} (i+4, intrahelical salt bridges). Similarly, the alkaline transition (at pH 12) probably arise from ionization of two basic groups involved in helix stabilization. The first type is the ε-amino group of K^{26} involved in salt-bridge formation and the second type is the guanidinium group of R^{40} that could interact with the negative pole of the α-helix microdipole. However, these helical contents presumably be changed at negative temperatures during TH measurements by binding onto their ligands (ice crystals), which could be the reason for the identical trend of the TH profile at different pH of bpAFP and rbpAFP. It was also attributed from the entirely fluorescent ice hemispheres obtained at 0.1 $mg \cdot mL^{-1}$ of peptide concentration in the pH range 6-11.3.

Figures

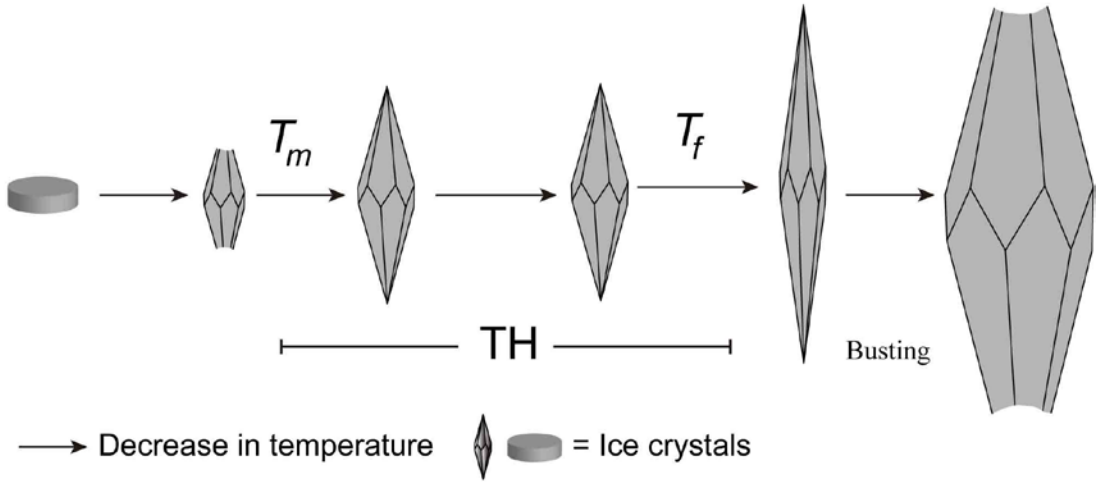

Figure 4.1.
Schematic representation of preparation of thermal hysteresis activity of AFPs.

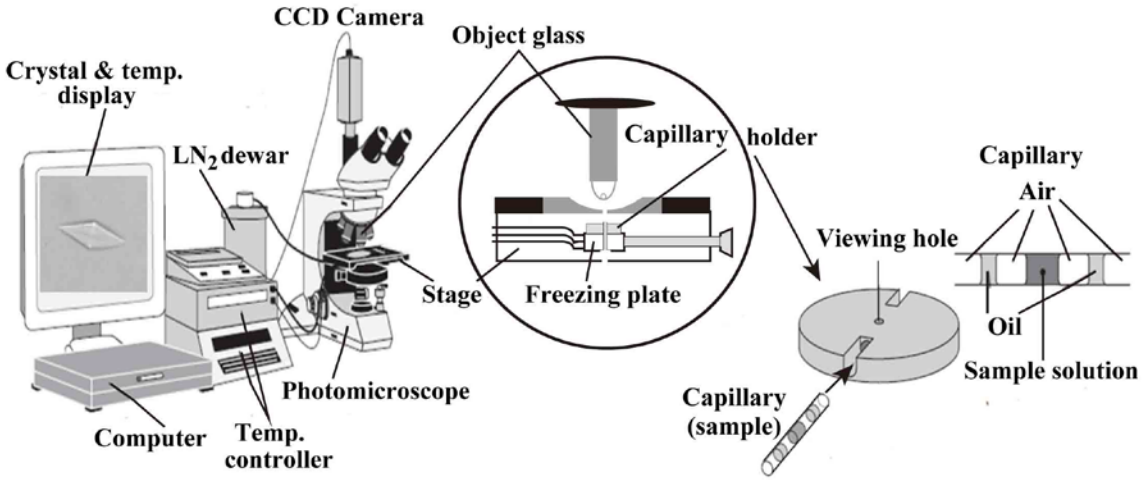

Figure 4.2.
Schematic representation of the procedure of determination of TH using the photomicroscope system. Scheme was modified from Takamichi et al. (2007).

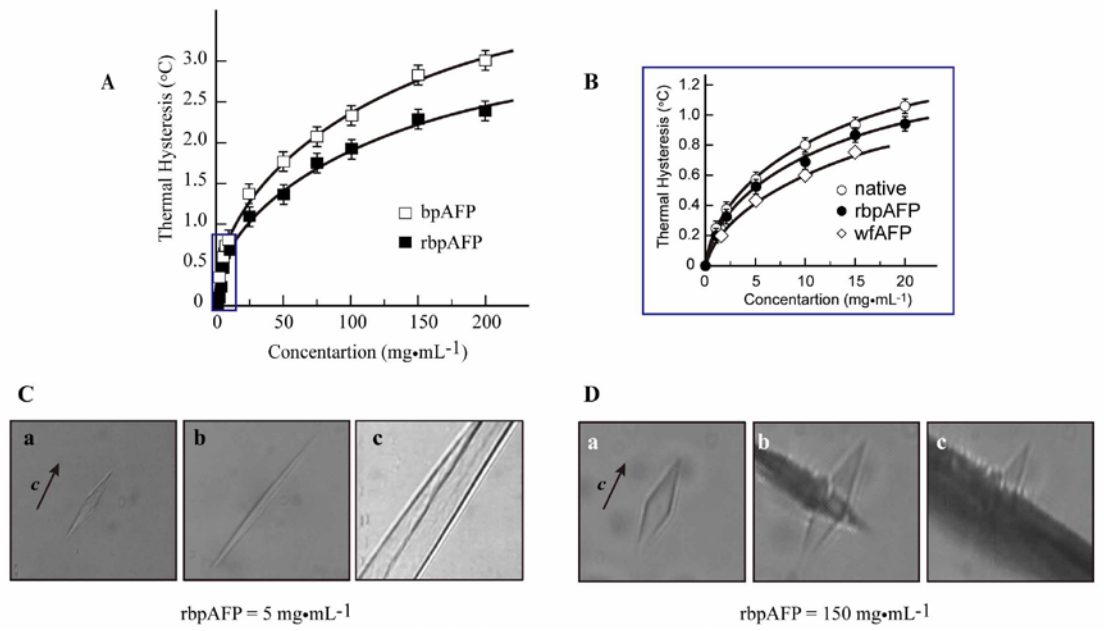

Figure 4.3.
Thermal hysteresis activity of bpAFP and rbpAFP. (A) Plot of TH as a function of the concentration of bpAFP and rbpAFP, of which the blue rectangular region is enlarged in (B). Busting ice growth along *c*-axis observed in the presence of 5 mg·mL^{-1} of rbpAFP. (D) Busting ice growth normal to *c*-axis observed in the presence of 150 mg·mL^{-1} of rbpAFP.

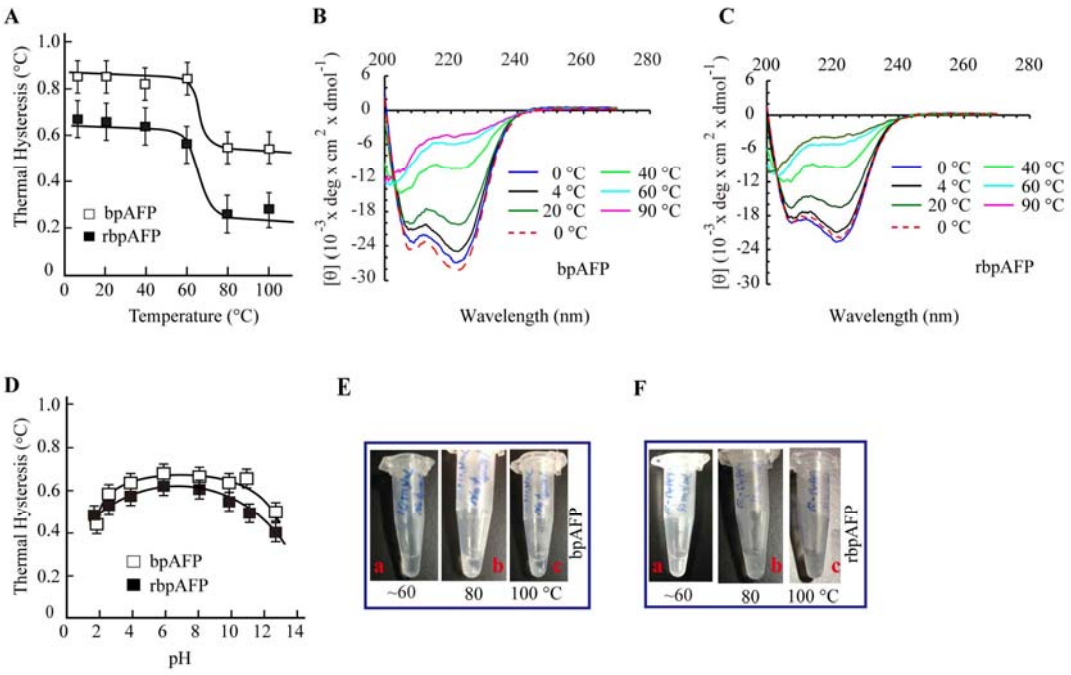

Figure 4.4.
Effect of pH and temperature on bpAFP and rbpAFP. (A) TH activity of 12 mg·mL^{-1} bpAFP and rbpAFP after heating to various temperature. (B) The CD spectra of 0.3 mg·mL^{-1} of bpAFP at different temperature, the dashed line represent spectrum after heating at 90 °C. (C) The CD spectra of 0.3 mg·mL^{-1} of rbpAFP at different temperature, the dashed line represent spectrum after heating at 90 °C. (D) TH activity of 10 mg·mL^{-1} bpAFP and rbpAFP at the pH between 2 and 13. The bpAFP(E) and rbpAFP (F) get precipitated during heating after 60 °C during measurement of effect of heat on TH activity.

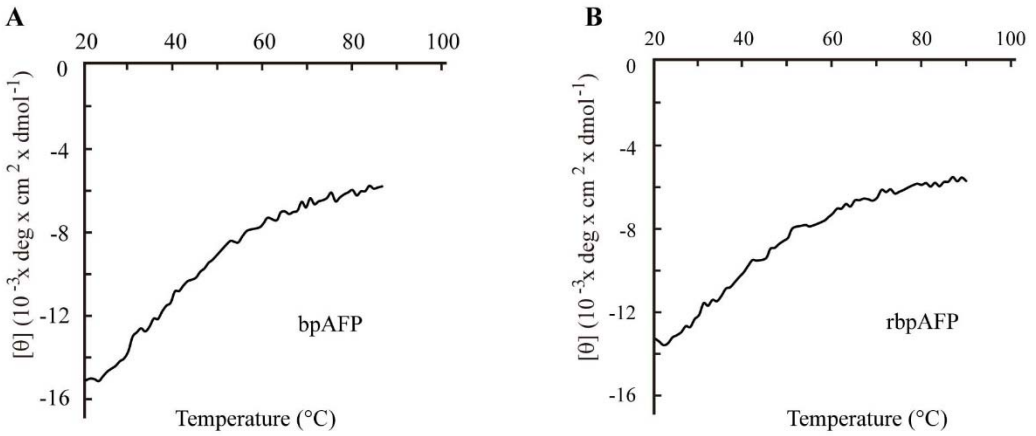

Figure 4.5.
Denaturation of bpAFP (A) and rbpAFP (B) with temperature. Concentration of the protein was 0.45 mg·mL^{-1} and the ellipticity values were at 208 nm.

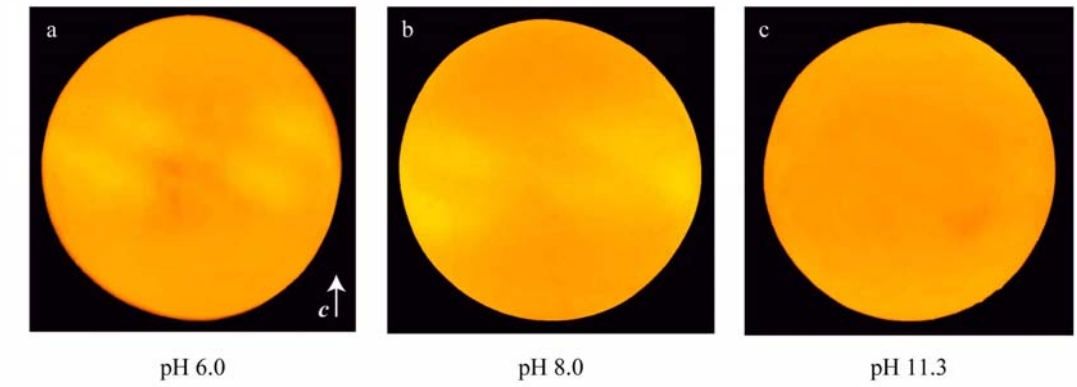

Figure 4.6.
pH dependent FIPA analysis of bpAFP. The UV-illuminated ice hemispheres grown in Rhodamine® labeled native bpAFP at the concentrations 0.1 mg·mL^{-1}, all the ice crystals were mounted keeping their *c*-axis normal to the frosty probe.

Tables

Table. 4.1: Buffers used in the measurement of effect of pH on TH

pH	Buffer
2.0	Glycine/HCl
3.0	Glycine/HCl
4.0	Sodium acetate/HCl
6.0	MES/NaOH
8.0	Tris/HCl
10	Arginine/NaOH
11	Arginine/NaOH
12.6	Arginine/NaOH

Table. 4.2: Helix content of the bpAFP and rbpAFP at different temperatures

Temperatures (°C)	Fraction of helix	
	bpAFP	rbpAFP
0	0.71	0.58
4	0.64	0.54
20	0.52	0.41
40	0.23	0.21
60	0.11	0.1
70	0.08	0.07
90	0.06	0.06
0 (after 90)	0.75	0.59

Table. 4.3: Helix content of the bpAFP and rbpAFP at different pH at 20°C

pH	Fraction of helix	
	bpAFP	rbpAFP
2	0.40	0.39
4	0.46	0.39
6	0.50	0.43
7	0.52	0.41
8	0.51	0.46
10	0.48	0.42
12	0.41	0.40

Table. 4.4: Ratio of the mean residue ellipticity at 222 and 208 nm at different temperatures.

Temp. (°C)	Mean residue ellipticity (deg·cm^2/dmol) × 10^3				$[\theta]_{222}/[\theta]_{208}$	
	bpAFP		rbpAFP		bpAFP	rbpAFP
	$[\boldsymbol{\theta}]_{\mathbf{222}}$	$[\boldsymbol{\theta}]_{\mathbf{208}}$	$[\boldsymbol{\theta}]_{\mathbf{222}}$	$[\boldsymbol{\theta}]_{\mathbf{208}}$		
4	-24.964	-21.042	-22.466	-19.079	1.18	1.18
20	-20.255	-20.053	-16.510	-16.474	1.01	1.00

Table. 4.5: Ratio of the mean residue ellipticity at 222 and 208 nm at different pH at 20°C temperature.

pH	Mean residue ellipticity (deg·cm^2/dmol) × 10^3				$[\theta]_{222}/[\theta]_{208}$	
	bpAFP		rbpAFP		bpAFP	rbpAFP
	$[\boldsymbol{\theta}]_{\mathbf{222}}$	$[\boldsymbol{\theta}]_{\mathbf{208}}$	$[\boldsymbol{\theta}]_{\mathbf{222}}$	$[\boldsymbol{\theta}]_{\mathbf{208}}$		
2	-16.206	-17.383	-15.628	-15.013	0.93	1.04
4	-18.229	-17.928	-15.667	-15.397	1.02	1.02
6	-19.482	-19.086	-17.011	-16.747	1.02	1.02
7	-20.256	-20.053	-16.510	-16.475	1.01	1.00
8	-19.764	-19.181	-18.191	-17.603	1.03	1.03
10	-18.746	-18.567	-16.615	-16.539	1.01	1.00
12	-16.545	-16.926	-15.899	-16.294	0.97	0.97

Expression and Purification of Mutant of bpAFP

Chapter: 5

5.1 Summary

Abstract

Antifreeze proteins (AFPs) specifically bind onto the ice surfaces to depress the freezing temperature in non-colligative manner, which is one of the functional activities of AFPs. Since discovery of AFPs in 1969 their structure function relationships have been studied from various aspects to elucidate the mechanism of antifreeze activities. Mutational analysis is an indispensable part of such studies. It facilitate the investigation of the role of respective amino acids in their functional activities as well as in structural stabilization. Therefore, threonine^{2} was mutated to Valine to investigate the role of that amino acid residue in the functional activity of the newly discovered AFP (bpAFP). Previous studies on the type I winter flounder AFP (wfAFP) showed that mutation of a threonine residue to valine does not alter the ice-binding properties of type I AFPs. By contrasts, the characteristic interminable ice-binding ability of bpAFP abolished in this single mutated bpAFP (T2V). It also altered the helical content and TH activity of this peptide significantly.

Outlines

In this chapter the author described the contents of an unpublished manuscript entitled “Point mutation of threonine at the C-terminal end to valine diminishes the basal plane binding ability of supersoluble hyperactive type I antifreeze protein, bpAFP” by Sheikh Mahatabuddin, Yuichi Hanada, Ai Miura, Hidemasa Kondo and Sakae Tsuda. The authors contributions are S.M. and S.T. designed research; S.M., Y.H., A.M., and H.K. performed Research and analyzed data; S.M. and S.T. wrote the paper.

5.2 Introduction

Antifreeze proteins (AFPs) have been discovered in an Antarctic fish in 1969. Since then AFPs are identified in various psychrophilic organisms ranging from bacteria to fish. These proteins specifically adsorb onto the ice crystal surfaces to alter their morphology and stop ice growth according to adsorption-inhibition model (Raymond and DeVries, 1977). The knowledge about their functional activities have been advanced from the contribution of the studies based on structure-function relationships of different AFPs. An essential part of this structure-function relationship studies is mutational analysis. Through which the role of the respective amino acid residues in the AFP sequence is investigated.

The AFPs adsorbed onto the specific ice planes, defined by Miller-Bravais indices, to decrease the freezing temperature. This depression of the freezing temperature is known as thermal hysteresis (TH), a concentration dependent parameter used to evaluate antifreeze activities of AFPs. Binding of AFPs converted the ice fronts to microcurvature. This binding mechanism of the AFPs have been studied for more than 4 decades (Raymond and DeVries, 1977). These studies proposed at least three different hypothesis regarding the binding of these peptides to ice surface. Yang et al. (1988) proposed that the hydrogen bonding of regularly spaced hydroxyl groups of four repetitive threonines in winter flounder AFP (wfAFP) is responsible for its ice binding property. This model further supported by Sicheri and Yang (1995) et al. by a series of docking models between refined structure of wfAFP and ice. While, mutation of these four threonines to valine cannot alter its ice plane specificity and TH activities. Additionally, replacement of central two threonines to serine diminishes the ice binding property of this peptide. Mutation of alanine to leucine gives different results based on their position, for example A17L mutant was inactive, A21L was poorly active, while A19L and A20L had little effect on activity (Wen and Laursen, 1992, 1993; Zhang and Laursen, 1998; Harding et al., 1999). These mutational analysis showed that there is a significant contribution to the mechanism of ice growth inhibition from the hydrophobic methyl group in threonine and valine. It also proposed a new ice binding face for type I AFPs that encompasses the conserved alanine-rich face and adjacent regularly spaced threonines (Baardsnes et al., 1999; Davies et al., 2002) (see detail in chapter 4). Hence, mutational analysis playing an important role to elucidate the ice binding mechanism of AFPs.

To investigate the mechanism and role of threonines mutational analysis of newly discovered bpAFP was carried out and described in this chapter. Mutation of threonine 2 to valine kept α-helicity and reversible thermal denaturation of that α-helix unchanged. By contrast, the interminable ice binding ability and TH activity was affected significantly by this point mutation.

5.3 Materials and methods

Expression and purification of T2V bpAFP

The DNA encoding bpAFP tagged with thrombin cleavage site followed by histidine (six) and thioredoxin tag in the N-terminal were extracted from the *Escherichia coli* (JM109) cells. Two partially overlapping DNA fragments were amplified by PCR using a forward primer (5'-GTCGCGAGCGATGCGGCTGCGGC-3'), a reverse primer (3'-ATCTACCGGAGAACCGCGTGGCACCAGACC-5') and the extracted DNA of wild type rbpAFP as a template. After two fragments were annealed, complete DNAs encoding the bpAFP mutant was constructed by DNA polymerase extension reaction. These PCR mixtures were ligated and transformed into *Escherichia coli* JM109 (Novagen) cells. The plasmid DNAs were prepared from resulting transfomants. Mutagenesis was performed using a KOD-plus mutagenesis kit (Toyobo, Osaka, Japan), and confirmed by DNA sequence analysis. These DNAs were then inserted in *Escherichia coli* BL21 (DE3) Rosetta2 (Novagen) to express T2V rbpAFP.

The Cells were cultivate in Luria-Bertani medium with 100 μgmL^{-1} ampicillin and expression of target protein was induced by 0.5 mM isopropyl-β-D-thioglactopyranoside (IPTG). Expression of the target peptide was confirmed by SDS-PAGE using 17% acrylamide gel. The cultivated cells were collected and suspended in 50 mL (per 1L culture medium) 50 mM Tris/HCl, pH 8.0. Cells were disrupted by sonication and centrifuged to remove insoluble fractions from this mixture. Supernatants of this centrifuged mixture were then applied to affinity chromatography using Ni-NTA column. Histidine tagged peptides were eluted with isocratic flow with 60% A buffer (50 mM Tris-HCl and 0.5 M NaCl) and 40% B buffer (10mM Tris-HCl, 0.5 M NaCl, 0.5 M Imidazole (Fig. 2.3C). Purification of T2V bpAFP from this Trx-tagged fusion protein described in results section.

Measurement of TH activity

The TH activities were measured using the photomicroscope system described by Takamichi et al. (2009) (Fig. 4.2). The photomicroscope system consists a Leica DMLB 100 photomicroscope equipped with Linkam LK600 temperature controller and a CCD camera. A 0.8 μL of desired concentrated peptide solution was frozen completely by cooling to -25 ^{o}C. Frozen samples were then thawed gradually to prepare a seed ice crystal and carefully observe its melting temperature T_m. After that the temperature of the solution again decreased gradually at the rate 0.1 $^{o}C \cdot min^{-1}$ and the morphological change of that crystal was observed in the monitor. The temperature at which ice crystal started to grow up rapidly was recorded as the ice-initiation temperature (T_f). Difference between T_f and T_m was recorded as TH value at particular concentration. 25 mM NH_4HCO_3 (pH 7.4) buffer was used as a solvent for preparation of protein solution with desired concentration. Al the experiments were carried out for minimum three times and final TH was the average value of these three individual measurements.

Measurement of CD spectrum

Peptide solutions were prepared at 0.3 mg·mL^{-1} concentration in 10 mM sodium phosphate buffer of pH = 7.4. CD spectrum were recorded at the temperature range 0-90 °C using JASCO J-725 CD spectrophotometer equipped with JASCO PTC-348WI temperature controller (Jasco Analytical Instruments, MD, USA). The pH dependence of the α-helix of native and recombinant protein was also measured at same concentration (in the chapter 4), the protein solutions were prepared at different pH using 10 mM sodium phosphate buffer for which pH was fixed by addition of 1M HCl or NaOH. The temperature during measurements of effect of pH were fixed at 20°C. CD data in degrees then converted to mean residue ellipticity (deg·cm^2·dmol^{-1}) using the following equation.

$$[\boldsymbol{\theta}]_{\boldsymbol{mrw},\lambda} = \frac{\boldsymbol{MRW} \times \theta_\lambda}{\boldsymbol{10} \times \boldsymbol{d} \times \boldsymbol{c}} \mathbf{deg}\, \boldsymbol{cm^2\, dmol^{-1}}$$

Where, $MRW = \frac{\text{Molecular Wight of protein in Da}}{\text{Number of amino acid (N)}-1}$, θ_λ = CD data in degrees at λ wavelength, c = concentration in g·mL^{-1} unit.

Calculation of fraction of helix

The fraction helix was calculated from the mean residue ellipticities (deg·cm^2·dmol^{-1}) at 222 nm ($[\theta]_{222}$) for respective temperature and pH. The solution inside the cell in each temperature was retained for 5 minutes to confirm the temperature experienced by all of the peptide molecules. The fraction helix was calculated using the formula used by Greenfield and Fasman (1969). The formula was-

$$Fraction\ helix = \frac{[\theta]_{222}^{obs} - [\theta]_{222}^{coil}}{[\theta]_{222}^{helix} - [\theta]_{222}^{coil}}$$

The ellipticity of each peptide in 6.0M guanidine hydrochloride at 20 °C was assumed to represent 0% helix and its ellipticity at 222 nm was used as $[\theta]_{222}^{coil}$ for respective protein. The ellipticity for 100% helix formation was calculated from the equation described by Chen et al. (1974), $[\theta]^n = [\theta]^\infty(1 - {}^{k}/_{n})$; where, n and k are the chain length and wavelength−dependent factor, respectively (at 222 nm, k = 2.57 and $[\theta]^\infty$ = -39500).

Preparation of fluorescently labeled T2V bpAFP

40 µL of 5 mg·mL^{-1} Rhodamine [5(6)-TAMRA-X, SE (6-(Tetramethylrhodamine-5-(and-6)-Carboxamido) Hexanoic Acid, Succinimidyl Ester, mixed isomers] (Life Technologies) was added to 1 mL of 4 mg·mL^{-1} T2V bpAFP solution in 100mM $NaHCO_3$ (pH 8.0). This solution was mixed in a tube rotator for 4 hours at room temperature to ensure the attachment of fluorescent dye with the protein molecules. To remove unreacted reagent the reaction mixture was transferred into a Vivaspin 20 mL (2 kDa) centrifuge tube and 12 mL of 10 mM $NaHCO_3$ (pH 8.0) was added. This solution was concentrated to 1 mL and repeated this procedure for twice

more times to wash out all unreacted dyes. Fluorescently labeled T2V bpAFP was transferred to a 50 mL centrifuge tube and cooled degassed 10 mM $NaHCO_3$ (pH 8.0 (4°C) was added to prepare 0.1 $mg{\cdot}mL^{-1}$ solution of the protein. Latter the ice hemispheres in the presence of the AFP solutions were grown up and photographed as described in section 3.3. The ice crystals were mounted keeping their *c*-axis parallel to the frosty probe in all of the experiments.

5.4 Results

5.4.1. Expression and purification of T2V mutated bpAFP

The effluents containing the peak (at 214 nm) in affinity chromatogram (similar to Fig. 2.3C) were collected and lyophilized after dialysis (against milliQ). This lyophilyzed Trx-tagged T2V bpAFP (50 mg) was then dissolved in 30 mL of PBS solution and allowed to be digested with thrombin protease (GE Healthcare) in the ratio 1 unit per 100 μg of fusion protein. This digested protein solution were applied through the Ni-NTA coulmn and the flow through fraction containing crude T2V mutant were collected and lyophilyzed after diyalysis. These lyophilyzed crude T2V mutants were further purified using reversed-phase HPLC.

15 mg of crude lyophilized protein was dissolved in 5 mL of PBS buffer (pH 7.4). This solution was applied for the reversed-hase HPLC using TSKgel ODS-80Ts column (TOSOH, Tokyo, Japan) with a linear gradient of 0-100% acetonitrile in 0.1% trifluoroacetic acid. Effluents containing pointed peak in the chromatogram (Fig.2.4 A) were collected and lyophilized after dialysis for 48 hours against milliQ. The purity of this lyophilized T2V bpAFP was confirmed with 15% Tris-Glycine native PAGE (Fig. 5.1C). The asparagus shape of the bpAFP bands are common feature of this AFP. This purified proteins can alter the ice crystal morphology of the ice crystal to hexagonal trapezohedron shape similarly to bpAFP and rbpAFP (Fig. 5.1D).

5.4.2. Antifreeze activity of T2V mutated bpAFP

The concentration dependence profile of TH activities of the T2V mutated protein showed conventional hyperbolic profile similarly to rbpAFP, as obtained for the fish AFPs (Davies and Hew, 1990). It also visualized that the TH activity of T2V mutant became ~70% of the recombinant and ~0.60% of the native protein at 10 $mg{\cdot}mL^{-1}$ of protein concentration. It is notable that, mutation of the threonines to valines did not affect the TH activities of wfAFP significantly (Chao et al., 1997; Haymet et al., 1998; Haymet et al., 1999). However, the typical needle-shaped busting along the *c*-axis of the ice bipyramids was observed in the presence of T2V mutated BpAFP (at 5 $mg{\cdot}mL^{-1}$ concentration) (Fig. 5.3C), which was similar to the busting pattern observed at lower concentrations of bpAFP and rbpAFP.

5.4.3. Secondary structure of T2V mutated bpAFP

The α-helical secondary structure of native and recombinant bpAFP were determined using CD spectroscopic techniques. The CD spectrum of T2V was also

visualized two minima at 208 and 222 nm, which represents the mutation did not change its secondary structure and protein folding. The dependence of the helicity of that mutant on temperature and pH was further examined by CD spectroscopy. The fraction of helix at 4 °C was measured 0.45 which is lower than both native and recombinant bpAFP (Table. 5.1). The $[\theta]_{222}/[\theta]_{208}$ ratio of this T2V mutant at this temperature was 1.12 also implies that it forms α-helical secondary structure as this value is near to the values obtained for type I synthetic antifreeze proteins (Gronwald et al., 1996; Houston et al, 1998). Further, heating decreases the helical content to zero or random coil gradually at the temperature 90 °C, whereas it showed similar ellipticity profiles and helical content (0.48) after cooling at 4 °C (Fig. 5.3B) to starting profile seen at 4 °C. Its helical content was also decreased at acidic and basic pH, while the helical content become high at pH 6 (near to the calculated pI value). However, the T2V mutant showed reversible thermal denaturation and pH stability of the secondary structure similar to bpAFP, while the helical contents were not identical to the native or rbpAFP.

5.4.4. Ice plane affinity of T2V mutant, natural and recombinant bpAFP

FIPA analysis was performed to determine the ice plane specificity of the T2V mutated bpAFP. A single macroscopic ice crystal was grown in the 0.1 mg·mL^{-1} of fluorescently labeled T2V mutated bpAFP, the *c*-axis of the crystal was parallel to the frosty probe. The image taken along *c*-axis (Fig. 5.4Aa) showed six distinct patches far from the center of the hemisphere and near to the periphery. The image of the same crystal from the oblique view (Fig. 5.4Ab) showed a clear central region of the crystal that implies protein cannot get adsorbed onto the basal planes of the ice crystal. The faint yellow circle near the center of the hemisphere (Fig. 5.4Aa) is an artifact arisen from the cuvette left by the frosty probe. This results implies that the basal plane of the ice hemisphere was left unbound by this mutated bpAFP. By contrast, the native and recombinant proteins showed concentration dependent interminable ice-binding ability within the concentration range 0.01-0.10 mg·mL^{-1} (see chapter three). At the lower limit of this concentration they adsorbed onto the pyramidal planes whereas at high concentration they provide completely fluorescent ice hemispheres (Fig. 3.4Ab, c, d and f). These entirely fluorescent ice hemispheres represents that they have the ability to bind to multiple planes including the basal plane.

5.5 Discussion

The site on the molecular surface of an AFP molecule which encompasses with the amino acids playing crucial role in ice-binding is known as ice binding site (IBS) of that molecule. The mutational analysis and molecular dynamics simulation studies on wfAFP showed that the IBS (IBS) of the α-helical type I AFPs consists the conserved alanine-rich face (including A^{17}) and adjacent regularly spaced four threonines (Wen and Laursen, 1992, 1993; Sicheri and Yang, 1995; Baardsnes et al., 1999; Haymet et al., 1999). These studies evoked us to predict the putative IBS of

bpAFP as the alanine assembled surface protruding four equally spaced threonines, for which an ability of binding to the pyramidal and prism planes of the ice crystal were detected. The oligomerization and/or molecular assembly presumably provided the basal plane binding ability to this IBS, which was absent in ordinary type I AFPs. The known type I AFPs commonly bind onto the prism (Sculpin AFP) or to the pyramidal planes (wfAFP) of the ice hemisphere (Knight et al., 1991). The pyramidal plane binding ability of wfAFP was showed to be arisen from the complementarity between the regularly spaced threonines (16.5 Å) and repeat spacing between the water molecules on the (20-21) pyramidal planes (16.7 Å) (Sicheri and Yang, 1995).

The role of these threonines was further examined by replacing them with valine or serine (Chao et al., 1997; Haymet et al., 1999). The two central threonines were replaced with valine and serine, of which serine mutant were virtually inactive while valine mutant showed 85% of activity to the wild peptide. On the other hand, the replacement of four threonines with valine and introducing one pair extra lysine and glutamate acid residues (VVVV2KE) in the first repetitive sequence at the N-terminal gives 100% activity while the SSSS (all Thr mutated to Ser) mutant as completely inactive though all of the mutants showed 100% helicity at 3°C. The author selected point mutation of the regularly spaced threonines to other amino acid residues instead of introducing valine/serine in two or four position simultaneously and determine the role of each threonine in interminable ice-binding of wfAFP. At the initial step the threonine^2 was mutated to valine (T2V bpAFP). The T2V mutant was expressed and purified for further studies.

The T2V mutant change the morphology of the ice crystals to hexagonal trapezohedron similarly to the native proteins. While, the mutant showed lower TH activities compared to the bpAFP and rbpAFP. It showed 70% of hysteresis of rbpAFP at 10 mg·mL^{-1} though the ice crystal busting pattern was identical to the native protein at lower concentrations. This activity was lower than the hysteresis observed for double valine (T13V and T24V) mutant of wfAFP (80% of hysteresis of native protein) (Harding et al., 1999, Chao et al., 1997)). This result suggests that threonine 2 has a significant role in ice growth inhibition of bpAFP. Additionally, the CD spectrum showed that the mutation of this threonine to valine did not alter the protein folding and α-helical structure of the peptide. The helical content of this mutant was 10% lower than bpAFP at 4 °C and it becomes zero at 90 °C. Both the natural and recombinant protein showed 6% helicity at the latter temperature. The $[\theta]_{222}/[\theta]_{208}$ ratio also determines its helical structure rather than coiled-coil (Gronwald et al., 1996; Houston et al, 1998). However, it attains the identical ellipticity profile after cooling at 4 °C (Fig. 5.3B) similarly to the bpAFP and rbpAFP. The change of the helicity depending on pH titration from pH 2 to pH 12 also showed similar pattern obtained for bpAFP and rbpAFP (table 5.2). Therefore, mutation of the threonine^2 to valine slightly lessen the ice growth inhibition ability, but the reversible thermal denaturation of this protein

within a long range of temperature (0-90 °C) and helical stability within long range of pH remain almost identical.

The ice plane specificity of T2V mutated bpAFP was drastically changed compared to bpAFP and rbpAFP. The unique interminable ice-binding ability of this protein disappeared after mutation. The FIPA images showed that the mutant failed to bind to the basal planes at 0.1 $mg \cdot mL^{-1}$ for which we detected multiple plane binding (including the basal plane) ability of bpAFP. The multiple plane binding was visualized entirely florescent ice hemispheres for both the bpAFP and rbpAFP at 0.10 $mg \cdot mL^{-1}$ of peptide concentration. Mutation of threonine^2 presumably diminished the ability of oligomerization which was predicted as driving force of bpAFP to bind on to the basal planes (see detail at chapter three). Further study on this mutant will provide more information about the exact role of threonine^2 for the functional activity of bpAFP. However, from the experimental results it is evident that threonine^2 has an important role on interminable ice-binding followed by functional activities of bpAFP.

Figures

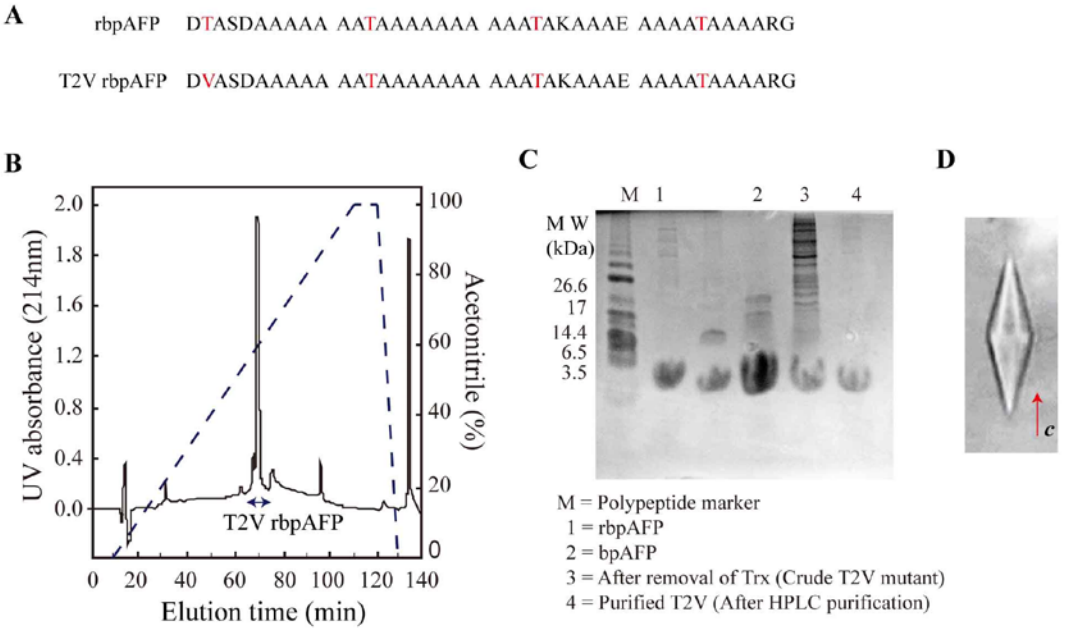

Figure 5.1.
HPLC purification of T2V mutant and ice crystal morphology in purified T2V bpAFP. (A) The sequence of bpAFP and T2V mutant. (B) The HPLC chromatogram containing separated peak of the purified T2V mutant, chromatogram was obtained from reverse phase HPLC using TSKgel ODS-80Ts column (TOSOH, Tokyo, Japan) with a linear gradient of 0-100% acetonitrile in 0.1% trifluoroacetic acid (blue dashed line) (C) Electrophoretogram of bpAFP, rbpAFP and crude and purified T2V bpAFP separated with 15% Tris-Glycine SDS-PAGE. (D) The hexagonal trapezohedron ice crystal observed in 1 mg·mL^{-1} of purified T2V bpAFP solution.

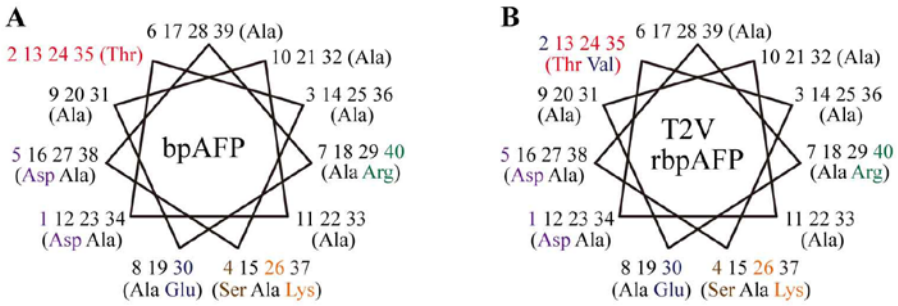

Figure 5.2.
Helical wheel representation of bpAFP and T2V mutant. The helical wheel representation of (A) bpAFP and (B) T2V mutant.

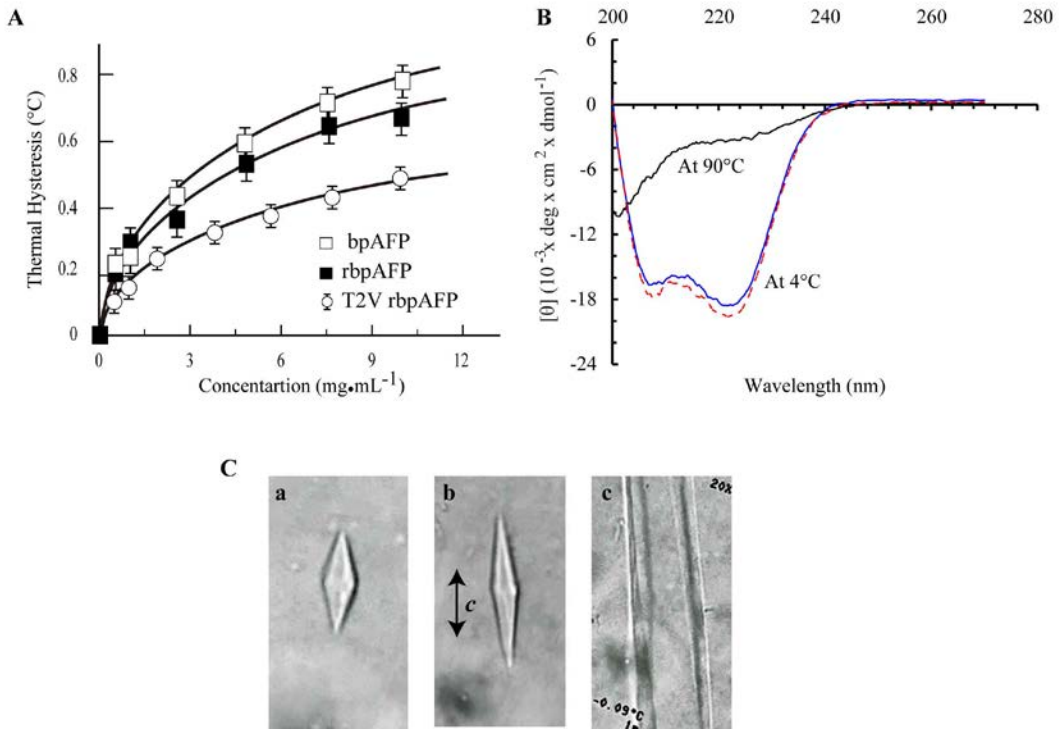

Figure 5.3.
Thermal hysteresis activity of and secondary structure of T2V mutant. (A) Plot of TH as a function of the concentration of bpAFP, rbpAFP and T2V mutated bpAFP. (B) The CD spectra of 0.3 mg·mL^{-1} of T2V bpAFP at different temperature, the dashed line represent spectrum at 4 °C after prior heating at 90 °C. (C) Busting ice growth along *c*-axis observed in the presence of 5 mg·mL^{-1} of T2V bpAFP.

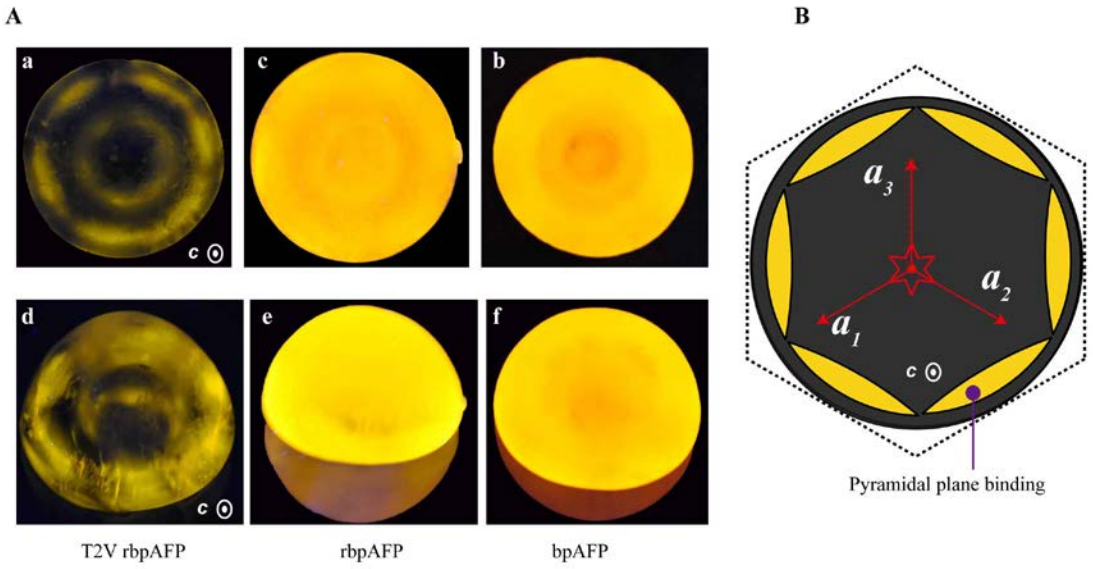

Figure 5.4.
Ice plane specificity of T2V bpAFP. (A) The UV-illuminated ice hemisphere grown in Rhodamine® labeled bpAFP and rbpAFP and T2V mutated bpAFP at the concentration 0.1 mg·mL^{-1}. (B) Interpretable illustration of ice-binding planes of T2V bpAFP at this concentration. All the ice crystals were mounted keeping their *c*-axis parallel to the frosty probe. The upper panels show the ice hemispheres photographed along the *c*-axis and the lower panels shows an oblique view of the same hemisphere.

Tables

Table. 5.1: Helix content of the native, recombinant and T2V mutated bpAFP at different temperatures

Temperatures (°C)	Fraction of helix		
	bpAFP	rbpAFP	T2V mutant
4	0.64	0.54	0.45
20	0.52	0.41	0.36
40	0.23	0.21	0.17
60	0.11	0.1	0.04
70	0.08	0.07	0.02
90	0.06	0.06	00
0 (after 90)	0.75	0.59	0.48

Table. 5.2: Helix content of the native, recombinant and T2V mutated bpAFP at different pH at 20°C

pH	Fraction of helix		
	bpAFP	rbpAFP	T2V mutant
2	0.40	0.39	0.32
6	0.50	0.43	0.56
7	0.52	0.41	0.36
12	0.41	0.40	0.31

Critical Ice Shaping Concentration (CISC): a New Parameter to Evaluate the Antifreeze Activities among Different AFPs

Chapter: 6

6.1 Summary

Abstract

The biological ice crystal modifiers, antifreeze proteins (AFPs), can bind onto the surface of ice crystals to alter their morphology and arrest their growth. These activities of ordinary AFPs have been evaluated using two concentration-dependent parameters, thermal hysteresis (TH) and ice recrystallization inhibition (IRI). However, it has not been subjected a parameter to correlate TH and IRI, which helps understanding of the ice-binding ability of AFPs including defective species that cannot perfectly arrest the ice crystal growth. Here we examined a new parameter named "critical ice shaping concentration (CISC)", a minimum concentration of an AFP species necessary to alter the shape of the ice crystals. We evaluated the CISC for three different types of fish AFPs including a defective AFP isoform, and examined the correlation between CISC and IRI. The obtained results showed for the first time that effective IRI concentrations of these AFPs are approximately double of their CISCs.

Outlines

In this chapter the author described the contents of a published manuscript entitled "Critical ice shaping concentration: A new parameter to evaluate the activity of antifreeze proteins" by Sheikh Mahatabuddin, Yoshiyuki Nishimiya, Ai Miura, Hidemasa Kondo and Sakae Tsuda. The authors contributions are S.M. designed research; S.M., Y.H., Y.N., A.M., and H.K. performed Research and analyzed data; S.M. and S.T. wrote the paper. It also contains the data of another unpublished manuscript entitled "Introduction to critical ice shaping concentration (CISC): A new parameter to evaluate the activities of antifreeze proteins" by Sheikh Mahatabuddin, Yoshiyuki Nishimiya, Ai Miura, Hidemasa Kondo and Sakae Tsuda. The authors contributions are S.M. designed the research; S.M., Y.N., A.M., and H.K. performed Research and analyzed data; S.M. and S.T. wrote the manuscript.

2 Introduction

Modification of ice crystal morphology and controlling their growth-kinetics are the major scientific challenges. The detrimental effects of ice growth are undesirable for both biological and materialistic processes. Biological systems require a plenty of liquid water to accomplish many reactions *in vivo* in cells and keep the fluidity of their body fluids. Formation of ice transfers the phase of water molecules from liquid to solid that disrupts such fluidity and creates pseudo-scarcity of liquid water threating the life of any living organisms (Douct et al., 2009). Such freezing and glacial damage also creates considerable risks during the preservation of cells and organs at freezing temperatures (Pegg, 2010). Long time preservations of food items at these temperatures enhance the formation of large ice crystals that deteriorates their quality and texture (Petzold and Aguilera, 2009). Therefore, understanding the functional activities and physicochemical properties of the ice crystal growth modifiers could offer to develop innovative strategies for cryoprotection, cryopreservation (Pegg, 2010), hypothermic preservation (Kamijima et al. 2013), anti-icing and deicing technologies.

Organisms living in icy environments produce different ice crystal modifiers, such as ice binding proteins (IBPs) and polyols, to avoid glacial damages (Douct et al., 2009). Antifreeze proteins (AFPs) are one of the subset of IBPs discovered in 1969 from the Antarctic fish (DeVries and Wohlschlag, 1969). The AFPs change the ice crystal morphologies without altering the physicochemical properties of the water-based media. Therefore, these peptides gained promising interest as an additive for water-based materials instead of commonly used colligative antifreezes, such as salts and polyhydric chemicals. Since 1969 more than dozens of AFPs have been identified from various organisms (Griffith et al., 1992; Graether et al., 2000; Duman, 2001; Fletcher et al., 2001; Nishimiya et al., 2008; Davies, 2014). Among them, fishes living in the Polar region and its proximal temperature area are the potential source of the AFPs (Fletcher et al., 2001). To date, five class of fish AFPs have been reported: type I, α-helical alanine rich (Mw: 3.3-4.5-kDa) proteins; type II, ~14-kDa proteins having high level of structural similarities with C-type lectins; type III, ~7-kDa globular proteins containing short β-strands; type IV, predicted as helix bundle protein with 12-kDa molecular weight; type Ih, four helix bundle protein consisted of 65% alanines (Harding et al., 1999; Fletcher et al., 2001; Nishimiya et al., 2008; Sun et al., 2014). These AFPs can adsorb onto the embryonic ice crystals to modify their morphologies and growth kinetics irrespective of their structure or origin.

The adsorption of AFPs onto the embryonic ice crystals suppress their growth and facilitate the cold survival of respective organisms (Griffith et al., 1992; Graether et al., 2000; Duman, 2001; Fletcher et al., 2001; Nishimiya et al., 2008; Davies, 2014). AFPs are also found in the organisms that are inevitably frozen in the ice-laden environments (Griffith and Ewart, 1995; Duman 2001). For example, the plants, in which AFPs may help to control the size of the ice crystals (Sidebottom et al., 2000).

At several degree below the melting temperatures ice crystals increase in size at the expense of smaller crystals to increase average grain sizes. This process involves the grain boundary migration and termed as Ostwald ripening (Fig. 6.1). The grain boundary migration is a spontaneous process in all crystalline solids to decrease the grain boundary area per unit volume that decrease the total energy of the system (Knight et al., 1995). This recrystallization has detrimental effects on both biological and water-containing materials, for example foods and inks (Douct et al., 2009; Pegg, 2010; Zhao et al., 2006). AFPs bind to the ice surfaces to inhibit such migrations at the grain boundaries and display ice recrystallization inhibition (IRI) at very low concentrations (Knight et al., 1995).

The non-colligative depression of freezing temperature caused by the bound AFP molecules is defined as thermal hysteresis (TH), another concentration-dependent parameter used to evaluate the activity of different AFPs (Davies, 2014; Raymond and DeVries 1977; Knight et al. 1991). The common mechanism for binding of AFP molecules described that they organize ice-like waters on their ice binding surfaces that match and merge onto the ice surface (Sun et al., 2014; Basu et al., 2015). Such binding of AFPs converts the flat ice surfaces to energetically unfavorable micro-curvature that depresses the freezing temperature below the melting temperature according to Gibbs-Thomson effect. The TH vs concentration profile of fish AFPs is hyperbolic in nature and attains a plateau value at certain concentrations (Davies and Hew, 1990). Typically almost all fish AFPs exhibited significant TH activities at the minimum concentration of approximately 0.5 $mg{\cdot}mL^{-1}$. In contrast, there are some AFPs, such as isoform 2 and 6 of AFP from Notched-fin eelpout (nfeAFP6, nfeAFP2), has no significant TH activities even at 14 $mg{\cdot}mL^{-1}$ concentration (Nishimiya et al., 2005). Nevertheless, they can adsorb onto the planes of the hexagonal ice crystals to create crystal facets to convert them to bipyramid shapes unlike other fish AFPs. It is notable that Notched-fin eelpout produce at least 13 isoforms of AFPs (nfeAFP). The isoforms such as nfeAFP13 or nfeAFP8 exhibited significant TH activities (Nishimiya et al., 2004). Therefore, TH is not a universal measure to compare the functional activities of AFPs. In addition, there is no established concentration-dependent parameter to correlate IRI and TH, although both of them represent the functional activity of the same biomolecule. Hence, it could be beneficial to introduce a new assessable parameter that can be used for comparative studies between various AFPs and correlate their TH and IRI activities.

In this chapter, the author examined a new concentration-dependent parameter, critical ice shaping concentration (CISC), which could be used for any kind of AFPs either defective or effective. The CISC is the minimum concentration of AFPs necessary to modify the ice crystal morphology to a characteristic shape: i.e. bipyramid or lemon shape. Here we note that, the shaping of an ice crystal into an equilibrated morphology obtained at CISC is a preliminary step of the TH activity measurement. Therefore, the ice shaping concentration, CISC, is directly related to the TH activities of the AFPs. The author examined the effective IRI concentrations (C_{eff}) based on time

lapse images of AFP containing 30% (W/V) glucose solutions to clarify the correlation between CISC and C_{eff} of type I, II, III fish AFPs and their recombinant proteins including a mutant.

6.3 Materials and methods

Expression and purification of AFPs

The native bpAFP was purified from fish muscle homogenate of barfin plaice (Fig. 6.2A) (see detail in chapter 2). The purity of the lyophilized natural protein was confirmed with glycine-SDS PAGE (Fig. 6.3). Its recombinant protein, rbpAFP, expressed and purified according to the procedure described in chapter 2. The purity of the protein was examined in a native PAGE show in figure 6.3. The T2V mutant was expressed and purified in similar method described in chapter 5.

The type II (lpAFP) from *Brachyopsis rostratus* (longsnout poacher) was provided from Nichirei Foods Inc. (9-Shinminato, Mihama-ku, Chiba-shi, Chiba 261-8545, Japan). The purity of the sample was confirmed by SDS-PAGE (Fig. 6.3). It was used without further purification.

The type III AFP (nfeAFP) was purified from fish muscle homogenate of *Zoarces elongatus Kner* (Notched-fin eelpout) according to the procedure described by Nishimiya et al. (2005). In brief, the fish muscle homogenate was centrifuged and the supernatant was dialyzed against 50 mM sodium acetate buffer (pH 3.7). The AFP containing solution was loaded onto a high-S column (1.0 × 5.0 cm; Bio-Rad, Hercules, CA, USA) after removal of precipitates formed during dialysis. The column-bound AFPs were eluted with linear NaCl gradient (0-0.5 M) in 50 mM sodium acetate buffer (pH 3.7). Dialysis and lyophilization of the eluents provided the purified isoform mixture of natural nfeAFP (Fig. 2). The recombinant isoform nfeAFP6 were purified by reverse-phase HPLC using the similar procedure described by Nishimiya et al. (2005). It is notable that type I AFP (~3.7–kDa) always gives an asparagus-like band and nfeAFP (~7–kDa) visualized a band appearing at a greater mobility (smaller molecular weight) position than the calculated one (Fig. 6.3).

Observation of ice crystal morphology

The ice crystal morphology was observed using a photomicroscope system consisting of a Leica DMLB 100 photomicroscope equipped with a Linkam LK600 temperature controller and a CCD camera. The sample solution was placed as a droplet (≈1 μL) on a circular cover slip (13 mm diameter) and then sandwiched using another cover slip. This sandwiched sample was then placed on the stage of the microscope and frozen to -20 °C at a rate 40 °C/min and incubated for two minutes. It was heated to -1 °C at the same rate. After that, it was slightly warmed up at the rate of 5 °C/min to create small ice crystals. After formation of the small crystals, it decreases the temperature to just below the melting temperature and kept holding for observation of the equilibrated shape (hexagonal bipyramid or lemon) of ice crystals. The observed ice crystal was then photographed using the CCD camera. The AFP concentration at

which small circular disk shape ice crystals converted to bipyramid (Fig. 6.4A) or lemon-shaped one at a temperature just below the melting temperature is recorded as CISC of respective AFP. To determine the CISC of the AFPs, AFP solutions of different concentrations were applied. For each AFP, 1 mg/mL concentrated stock solution was prepared using 10 mM ammonium hydrogen carbonate buffer (pH=7.4). AFP solutions of desired concentrations were prepared by successive dilution of the stock solutions with the same buffer. We note that, each experiments were carried out at least three times to ensure the reproducibility (Olijve et al., 2016b). We also avoided formation of any ice crystal in the vicinity of the focused one to minimize the detrimental effects arisen from them.

Measurement of IRI activity

The IRI activity was measured using sucrose-sandwich-splat assay as described by Smallwood et al. A 1 μL of 30% (W/V) sucrose solution was sandwiched between the coverslips of 13 mm diameter. This sandwiched sample was then placed on the stage of a photomicroscope system consisting of a Nikon ECLIPSE E600 photomicroscope equipped with a Linkam LK600 temperature controller and a CCD camera. The temperature of the samples was decreased to -40 °C at the rate of 20 °C/min and incubated for 2 minute. It was then warmed to -6°C at the rate of 10 °C/min for incubation and incubated at this temperature for 40 minutes, which was selected from the observation of 120 min incubation of the experimental sample (Fig. 6.4B). The Ice crystals were viewed using a 50× objective in the microscope and photographed after every 10 minutes. AFP concentration at which the time-lapse images showed no visual change in ice crystal size within the holding time is recorded as C_{eff}. AFP containing 30% sucrose solutions were prepared using 1 mg/mL concentrated AFPs in milliQ water as the stock solution. A 18 mg/mL glucose solution in 30% sucrose was used as a control sample. All the experiments were repeated three times to ensure reproducibility (Olijve et al., 2016b) of our experimental results.

6.4 Results

6.4.1. CISC of bpAFP, rbpAFP, T2V mutated rbpAFP, lpAFP, nfeAFP and nfeAFP6

The threshold concentrations required for modification of the ice crystals into the distinctive shapes (Fig. 6.5A) have been examined for native type I-III AFPs, recombinant type I (rbpAFP), III (nfeAFP6) and mutant of type I (T2V rbpAFP). The native samples bpAFP, lpAFP and nfeAFP consist of 6 (at least), 2 and 13 isoforms of type I, II and III AFP, respectively (Nishimiya et al., 2005, 2008). The recombinant protein of the 6th isoform of type III AFP, nfeAFP6, is denoted as defective isoform as it cannot perfectly halt the ice growth (Takamichi et al., 2009). In the absence of these AFPs, the shape of an ice crystal was circular disk-shaped (Fig. 5.5Aa). In the presence of AFPs, however, adsorption of the peptides impeded the uniform growth that results in the bipyramidal (bpAFPs and nfeAFPs) or lemon shaped ice crystals (lpAFP) (Fig. 6.4A). This morphological change from circular disk to bipyramid with increasing type I AFP concentrations are shown in figure 6.4A. BpAFP and nfeAFP could not

sufficiently suppress the growth of the ice crystals to convert them to bipyramid shape at the concentration of 0.04 mg·mL^{-1} (Fig. 6.5Ba and Fa). An infinitesimal increase of the concentration of these peptides to 0.05 mg·mL^{-1} while changed the ice crystal morphology (Fig. 6.5Bb and Fb). Similarly, 0.1, 0.15, 0.03 and 0.15 mg·mL^{-1} were threshold peptide concentrations to generate lemon shaped and bipyramid ice crystals in the presence of rbpAFP, T2V mutated rbpAFP, lpAFP and nfeAFP6, respectively (Fig. 6.5Cb, Db, Eb and Gb). Here the author note that, 0.05 mg·mL^{-1} (Fig. 6.4 Ae) of bpAFP cannot create significant TH gap, while at 0.50 mg·mL^{-1} (Fig. 6.4Ag) concentration it showed ~0.20 °C of TH activity. Which implies that, 0.45 mg/mL (0.50-0.05) of type I AFP is offering this amount of TH. In the presence of 0.1 mg·mL^{-1} nfeAFP6 (Fig. 6.5Ga) or 0.045 mg·mL^{-1} bpAFP (Fig. 6.4Ad) the transient ice crystal morphologies are tend to shape a bipyramid while a slight decrease in temperature resulted ice crystal growth in all directions, in a manner similar to buffer control (Fig. 6.5Aa). Similar tendency was observed for other AFPs at the concentrations below CISC. These results also indicated that nfeAFP6 required a higher concentration to alter ice crystal morphology than the reaming AFPs tested. This phenomenon implies that, a sufficient amount of AFP molecules are necessary to modify the ice crystal shape. In summary, the CISC of bpAFP, rbpAFP, T2V mutated rbpAFP, lpAFP, nfeAFP and nfeAFP6 were evaluated to 0.05, 0.10, 0.15, 0.03, 0.05 and 0.15 mg·mL^{-1}, whose molar concentrations are 13, 26, 40, 2, 7 and 21 μM, respectively, evaluated based on their molecular weight (Table 6.1) (type I = 3.7-kDa, nfeAFP, nfeAFP6 = 7-kDa (Nishimiya et al. 2005), and lpAFP = 13.8-kDa (Nishimiya et al., 2008).

6.4.2. IRI of bpAFP, rbpAFP, lpAFP, nfeAFP and nfeAFP6

The method of sucrose-sandwich-splat assay developed by Smallwood et al. (1999) are widely used for determination of IRI activities. It allows inclusion of a high concentration of solute that ensures the avoidance of boundary inhibition. In the present study, the IRI activities were assessed near the concentrations of CISC for natural type I, II, III AFPs and their recombinant proteins (Fig. 6.6).

In the absence of AFPs, 30% sucrose and 18 mg/mL (10 mM) monosaccharide (10 mM D-glucose in 30% sucrose) solutions cannot inhibit the ice recrystallization within the holding period (Figs. 6.6A and B). The size of ice crystals in these control solutions were larger than those created in the presence of trace amount of AFPs even at 0 minute of holding period. We note that even at the AFP concentrations below CISC, the ice crystals were infinitesimally small compared with the solutions without AFPs at the end of holding time (Fig. 6.5).

The images captured after 40 minutes of holding time of the solutions containing CISC concentrations of bpAFP, rbpAFP, lpAFP and nfeAFP visualize the large grain of ice crystals (Fig. 6.6C, D, E and F). In the solutions containing 0.08 mg·mL^{-1} bpAFP and nfeAFP the ice grains increase in size though it was the concentration above their CISC (Fig. SI A and D). At the concentration double to CISC i.e. at 0.1 mg/mL no

significant change in ice crystal size were visualized within the observation period (Fig. 6.6D, and F). Similar results were obtained for 0.20 and 0.06 mg·mL^{-1} of bpAFP and lpAFP, respectively, which was also the 2 fold concentration of their CISC. Therefore, our experimental results showed that the effective concentrations for appreciable IRI activity C_{eff} for AFPs native bpAFP, rbpAFP (type I), type II (lpAFP), and III (nfeAFP) are 0.1 (26 μM), 0.2 (52 μM), 0.1 (14 μM) and 0.06 (4 μM) mg·mL^{-1}, respectively.

In contrast, the defective isoform of nfeAFP, nfeAFP6, failed to restrict grain boundary migrations even at four fold higher concentration of its CISC (Fig. 6.6C). Analogous to the other AFPs, in the nfeAFP6 concentrations below, above or at the CISC, it forms very fine grains of ice crystals at initial time of incubation. While during incubation the size of the ice crystals was increased in all examined concentrations. It is notable that the size of the ice crystals observed after 40 minutes of incubation was smaller than the control solutions (Fig. 6.6A, B and SI B). These results suggest that, although nfeAFP6 failed to offer significant TH activity, it has the ability to restrict the grain boundary migration to some extent.

6.5 Discussion

The unit structure of an ice crystal is hexagonal (I_h) at one atmospheric pressure (Davies, 1990). The hexagonal structure possesses different patterns of oxygen atoms on the surface of distinct planes defined by Miller indices (Hobbs, 1974). Uniform growth of all of these planes except for the basal planes in water is responsible for a circular disk-shaped crystals, as observed without any ice crystal modifiers such as AFP. In the presence of AFPs, however, the formation of hexagonal crystal is hindered by their adsorption to specific planes. The AFP adsorbed plane is converted to the one that contains many curved fronts between the ice-bound-AFPs, which are energetically unfavorable for ice formation. These growth-terminated surfaces become crystal facets, which is a sign of growth inhibition effect of AFPs (Davies, 1990). The type I and III AFPs typically adsorb onto the pyramidal and/or prism planes of embryonic ice crystals (Basu et al., 2014). Therefore, ice crystal growth along these planes is impeded compared to the basal planes of the ice crystals. Such altered formation of consecutive basal planes modifies the ice crystal morphology from disc to bipyramid (Davies et al., 1990). Similarly, adsorption of lpAFP onto the prism and pyramidal plane (Nishimiya et al., 2008) changed the morphology of the ice crystals to lemon shape.

The experimental results suggested that, there is a certain concentration barrier for the AFPs to successfully alter the morphology of an ice crystal as well as effectively inhibit IR. With the increase in peptide concentration, the number of adsorbed AFP increased on the ice surface. Therefore, hexagonal ice crystal converted to the typical bipyramid, lemon or any specific shapes at that minimum concentrations. This concentration is denoted as CISC. Nevertheless, CISC was not sufficient to halt the ice growth for long time (Fig. SI E and F). Moreover, this concentration of AFPs was also insufficient to stop grain boundary migration effectively while it was effectively

suppressed at the AFP concentrations double of their CISC. Additionally, to exhibit significant TH activities effective AFPs required at least 5-10 fold higher concentration of CISC.

Question may arise why it is necessary to have more AFPs, though CISC amount of AFP is sufficient to change the ice crystal morphology by arresting its growth along AFP-bound surfaces? To answer this question, it may help a two-step binding mechanism of AFP molecules proposed by Takamichi et al., which originally explained the enhancement of the TH activities of nfeAFP8 induced by annealing time (Takamichi et al., 2007). They proposed that, the slower secondary binding of AFPs onto the convex ice front shrunken the growth area that might leads to higher TH activity without changing the AFP concentrations. This slower adsorption kinetics was also proposed by Dori et al. (2014), which was due to special microfluidic experiments with fluorescently labeled AFPs. We hence propose that, AFP molecule becomes adsorbed onto the ice crystal in two different adsorption processes, namely primary adsorption and secondary adsorption (Fig. 6.6). In the presence of AFPs, as the embryonic ice crystal forms the AFP molecules get adsorbed onto it simultaneously to halt its growth by forming comparatively curved ice fronts between two adsorbed AFP molecules. This primary adsorption is very fast process, and it requires a threshold number of adsorbed AFP molecules (minimum concentration equal to CISC) to stop the crystal growth sufficiently to create crystal facets. This impedimental growth along certain surfaces results an equilibrated shape of ice crystal (bipyramid (Fig. 6.7B) or lemon). The experimental results of Dori et al. (2014) were also suggested such very fast initial adsorption of AFPs.

The primarily adsorbed AFP molecules are insufficient to arrest the overall crystal growth or grain boundary migration to exhibit significant TH or effective IRI activities. Therefore, new AFP molecules get adsorbed onto the curved ice fronts created by the primarily adsorbed molecules that further decrease the surface energy and generate more infinitesimally small curved fronts depending on their concentration, secondary adsorption (Fig. 6.7C). These adsorbed AFPs further decrease the surface energy and covert the ice fronts more infinitesimally small curved. This secondary adsorption process is slower than the primary adsorption (this could be one of the reason for enhancement of TH by annealing time). Some defective AFPs, such as nfeAFP6 or nfeAFP2 presumably have the lower ability to bind onto the curved surfaces through this secondary adsorption process, hence nfeAFP6 cannot create significant TH gap (Nishimiya et al., 2005). This might also be a reason for poor IRI activities at even four fold higher concentrations of CISC of nfeAFP6. Regarding such adsorption of AFPs Kubota (2011) proposed an equation based on the Langmuir adsorption mechanism to correlate the AFP's surface coverage with time, $\sigma = \sigma_{max}(1 - e^{-(t/\tau)})$, where σ and σ_{max} are the coverage and its maximum value, t is time for ice formation and τ is time-constant for accumulation. Such maximum surface coverage and extent of the secondary adsorption presumably caused the plateau state of the TH profiles (Fig. 4.3A in this thesis, Davies et al., 1990) at which ice surfaces are saturated with the

secondarily adsorbed AFPs. Other models have also been proposed to describe kinetics of AFP-ice interactions (Sander and Tkachenko, 2004; Knight and DeVries, 2009).

In conclusion, the new parameter CISC is interrelated for the first time with the IRI and TH activity. Type I, II, III fish AFPs and their recombinant proteins can exhibit effective IRI at two fold concentrations of their CISC, for which the author made the assumptions that 1) CISC of AFP is a measure of primary adsorption ability onto the ice crystal surfaces to cause ice-shaping, while 2) IRI and TH are related with more AFP concentrations needed for both primary and secondary adsorptions to halt the ice crystal growth. It will be interesting to examine the correlation between IRI and TH through CISC.

Figures

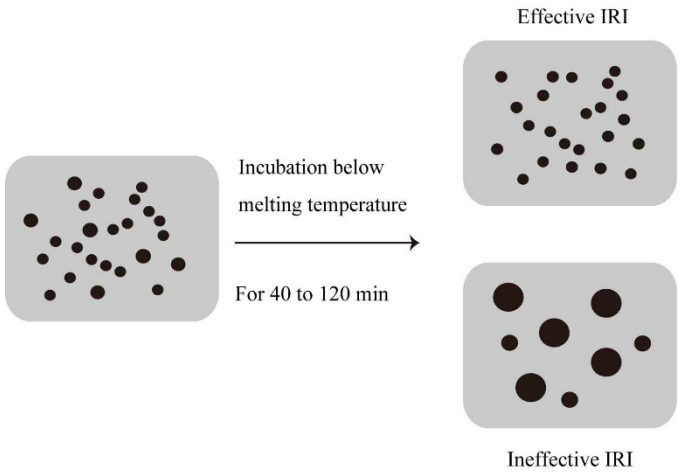

Figure 6.1.
Schematic representation of ice recrystallization inhibition.

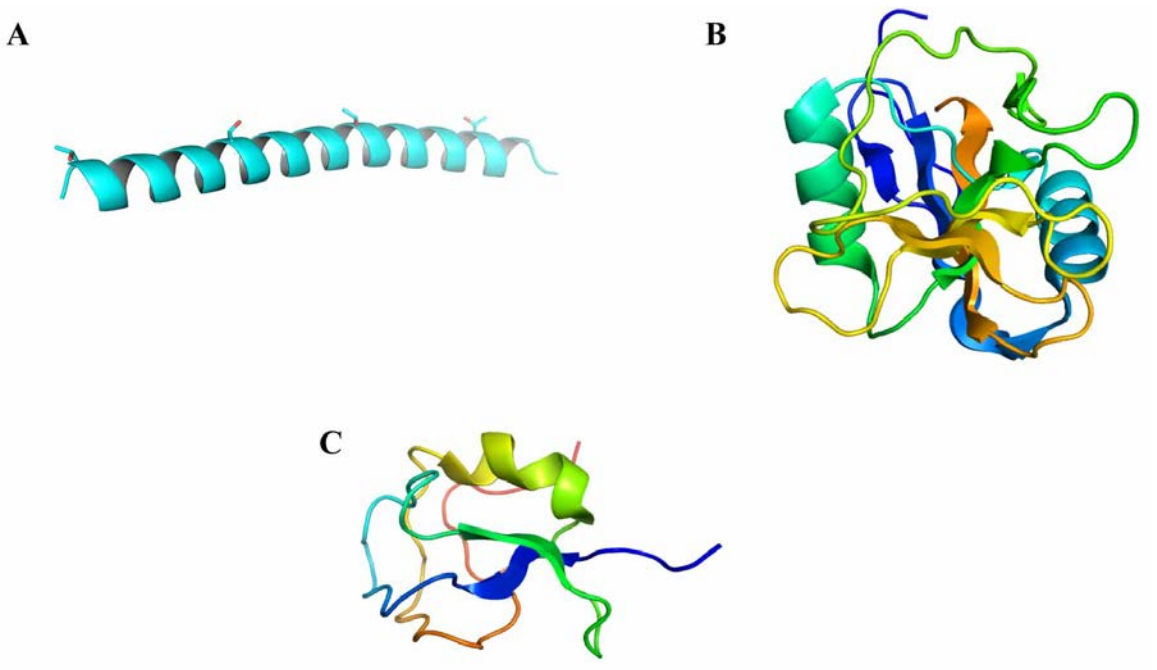

Figure 6.2.
AFPs used in this study and their source fishes. (A) Predicted model structure of bpAFP. (B) Calcium independent type II AFP (lpAFP) from *Brachyopsis rostratus* (regenerated from PDB ID: 2ZIB). (C) Type III AFP (nfeAFP) from *Zoarces elongatus Kner* (regenerated from PDB ID: 2LX3). These structures were regenerated using PyMOL.

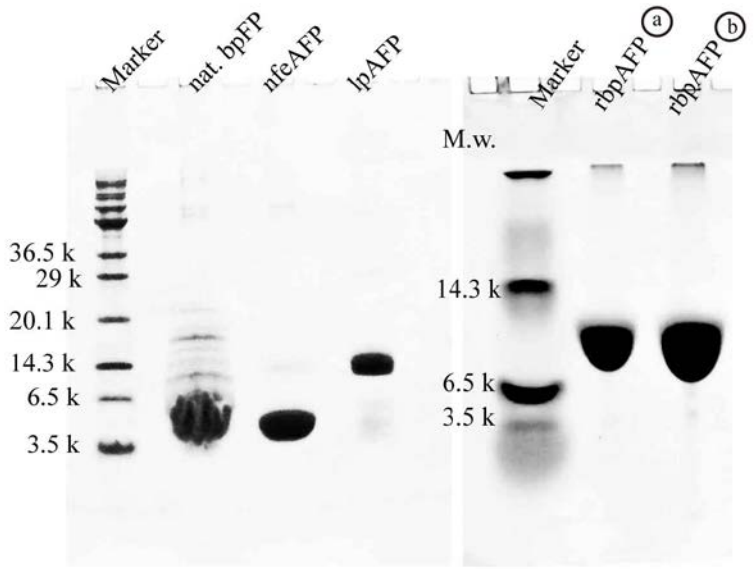

Figure 6.3.
Electrophoretogram obtained from 15% glycine-SDS gel and native gel. Here, a and b represents 5 and 10 mg·mL^{-1} of purified rbpAFP.

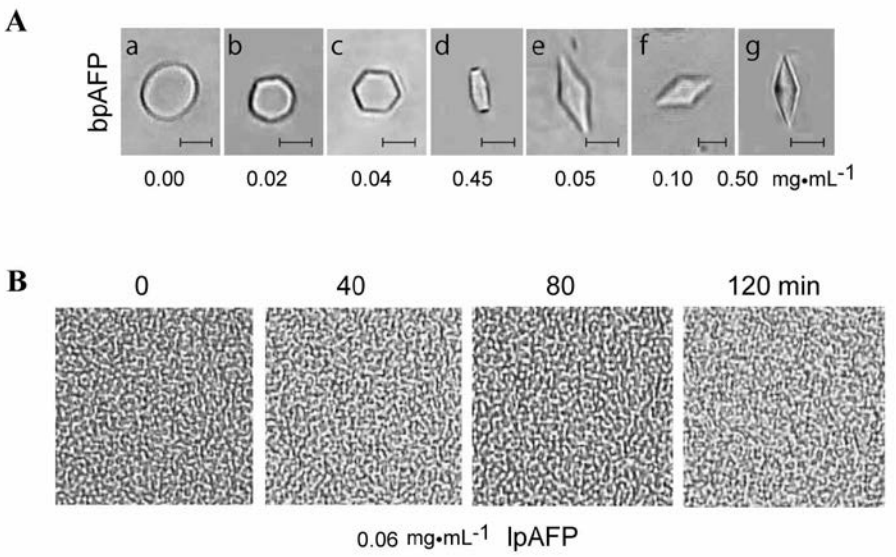

Figure 6.4.
Transition of the circular disk shaped to bipyramidal shape of an ice crystal (A) and time-lapse images of effective IRI of lpAFP for 120 minutes (B).

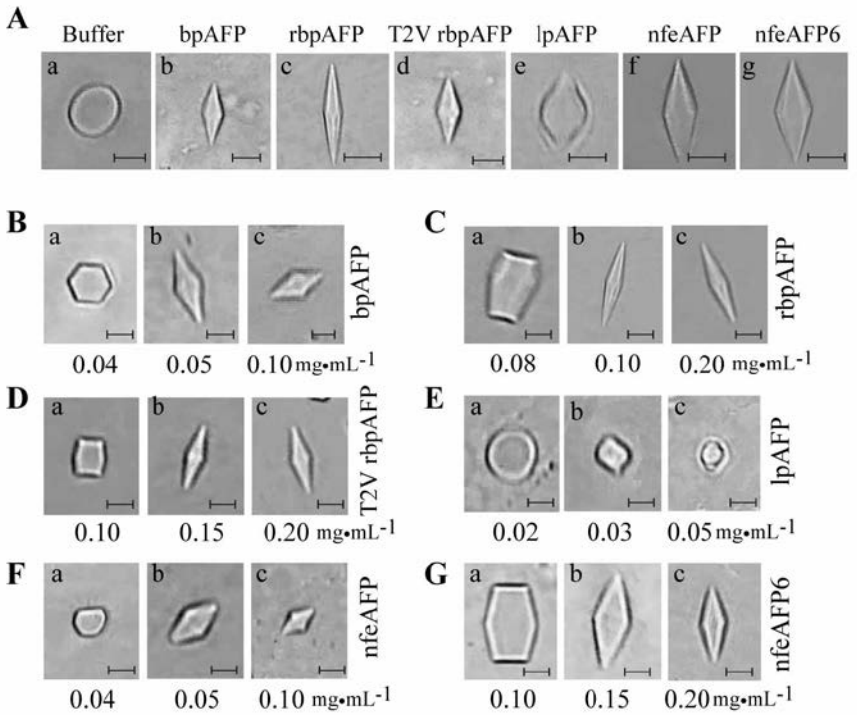

Figure 6.5.
Ice crystal morphologies in the absence and presence of AFPs. (A) Ice crystal morphologies in (a) 10 mM ammonium bicarbonate (ABC) buffer, (b) 2 mg·mL^{-1} native bpAFP, (c) 0.5 mg·mL^{-1} rbpAFP, (d) 2 mg·mL^{-1} T2V bpAFP, (e) 0.5 mg·mL^{-1} lpAFP and (f) 1 mg·mL^{-1} nfeAFP, and (g) 1 mg·mL^{-1} nfeAFP6. Determination of CISC values for native bpAFP (B), rbpAFP (C), T2V bpAFP (D), lpAFP (E), nfeAFP (F), nfeAFP6 (G). Scale bar represents 20 μm- length.

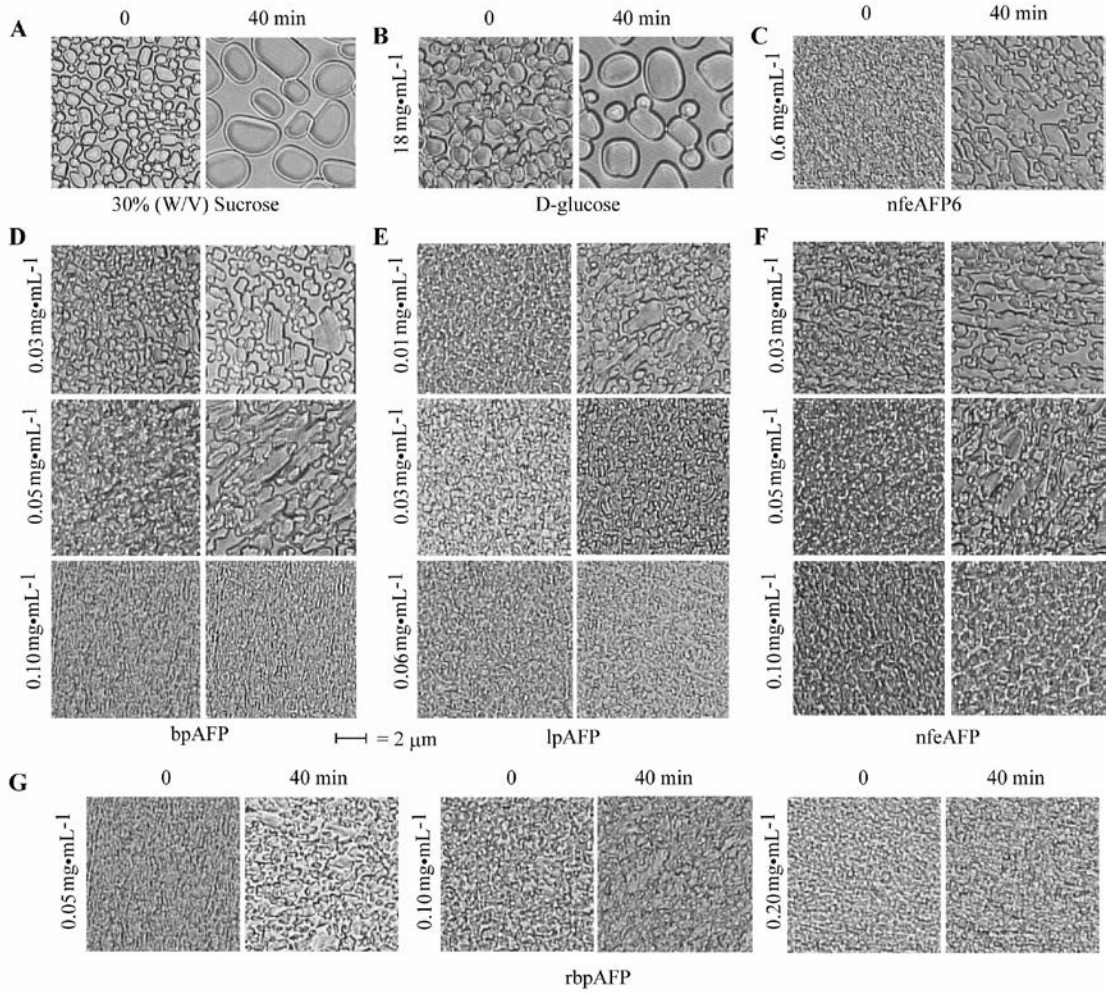

Figure 6.6.
Ice recrystallization inhibition in absence and presence of AFPs. Time lapse image of IRI of (A) 30% (W/V) sucrose solution, (B) 18 mg·mL^{-1} glucose, (C) 0.6 mg·mL^{-1} nfeAFP6, (D) different concentration of natural bpAFP, (E) different concentrations of lpAFP, (F) different concentrations of nfeAFP and (G) rbpAFP. All the experimental solutions prepared in 30% (W/V) sucrose.

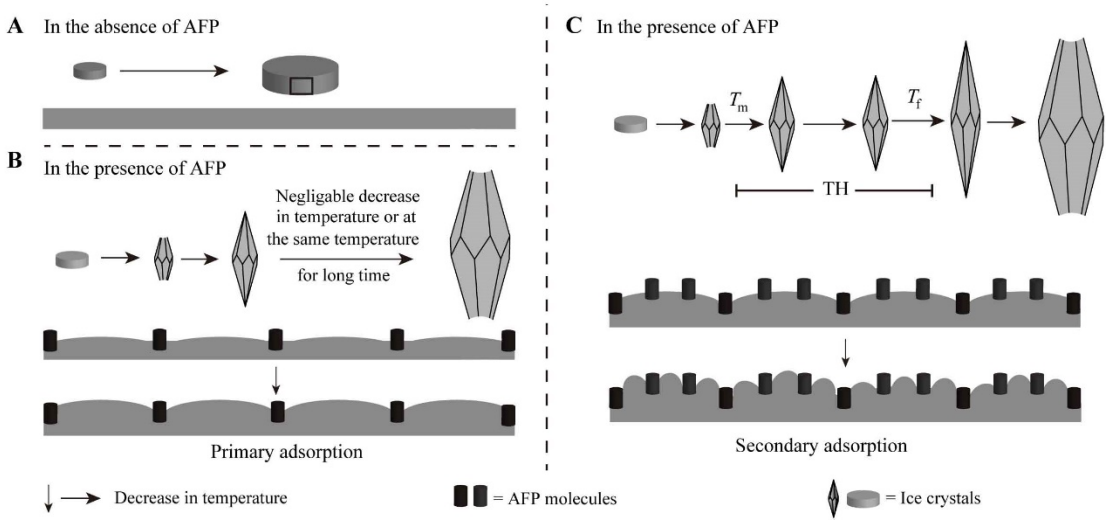

Figure 6.6.
Schematic representation of proposed two step adsorption of AFP molecules. Ice crystal growths in the (A) absence of AFPs, (B) presence of very low concentration of AFPs such as CISC and (C) presence of higher concentrations of AFPs

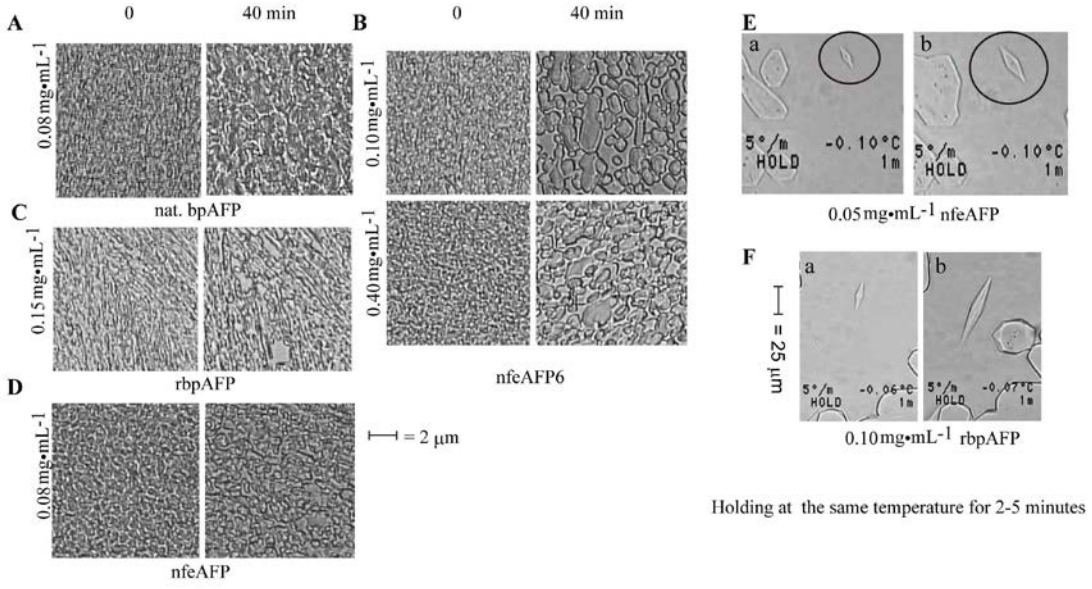

Figure SI.
Ice recrystallization inhibition and ice crystal growth in presence of AFPs. Time lapse image of IRI (A) in 0.08 mg·mL^{-1} natural bpAFP, (B) in 0.1 and 0.4 mg·mL^{-1} nfeAFP6 (C) 0.15 mg·mL^{-1} rbpAFP and (D) 0.08 mg·mL^{-1} nfeAFP. Enlargement of bipyramid ice crystal in the presence of (E) 0.05 mg·mL^{-1} nfeAFP and (F) 0.10 mg·mL^{-1} rbpAFP in 10 mM ABC buffer.

Tables

Table. 6.1: CISC and effective ice recrystallization inhibition concentrations (C_{eff}) for different AFPs.

AFPs	CISC		C_{eff}	
	Concentrations		Concentrations	
	$mg \cdot mL^{-1}$	μM	$mg \cdot mL^{-1}$	μM
bpAFP	0.05	13	0.1	26
rbpAFP	0.10	26	0.2	52
T2V bpAFP	0.15	40	Not performed	
lpAFP	0.03	2	0.06	4
nfeAFP	0.05	7	0.10	14
nfeAFP6	0.15	21	0.6 (ineffective)	84

General Discussion

Chapter: 7

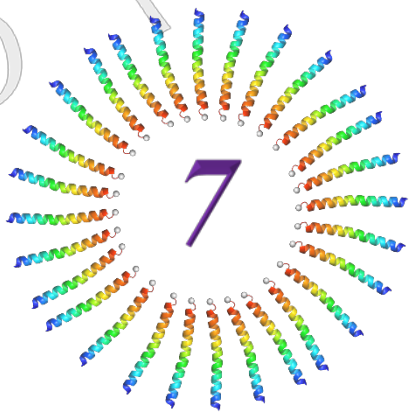

7.1 Summary

The biological ice crystal modifiers, antifreeze proteins (AFPs), can bind onto the surface of ice crystals to alter their morphology that assist certain organisms to survive at ice-laden environments. The mechanism of function of these peptides and their evolution have been studied by Biologists, Biochemists, Biophysicists and Molecular Biologists for past few decades. Their tremendous efforts led us to identify these proteins in various organisms ranging from bacteria to fish, since the discovery of AFP in 1969. Discovery of new species and their characterization advanced our knowledge regarding their mechanism of action, structural diversity and evolutionary precursors. In the ***Chapter two*** the identification and mass purification of a new AFP has been reported that showed supersolubility in milliQ water. The large-scale purification methodology of this protein (bpAFP) from fish muscle homogenate was established. Its determined sequence and secondary structure suggested this 40-residual peptide is the alanine richest isoform of type I AFP that composed of 3 tandem repeats of the 11-residue consensus sequence TX_{10} (where X is mostly alanine). Except the regularly spaced thronines and C-terminal arginine it contain just five polar amino acids (D^{1}, S^{4}, D^{5}, K^{26}, E^{30}) and rest of the residues are alanines. While, other type I AFPs have more polar residues to acquire more amphipathic nature of their α-helices. This simplicity of the sequence construct an extremely regular surface of this molecule. A recombinant protein consisting this sequence (rbpAFP) was expressed in *E. coli* and purified for further characterization of this AFP. Both the native and recombinant bpAFP changed the morphology of ice crystal to hexagonal trapezohedron. This protein is the only known AFP that showed both the moderate and hyperactivity in a concentration-dependent manner. To date, bpAFP is the AFP which solubilized at very high concentrations that might exposed the prospect to utilize this protein in myriad research fields. In addition the developed mass purification method of this AFP (in this dissertation) facilitate the studies that require mass amount of AFPs, such as cell or organ preservation.

It is widely recognized that, the unit cells of the ice crystals formed at atmospheric pressure are mainly hexagonal (Hobbs, 1974). These hexagonal ice crystal contains numerous planes defined by Miller-Bravais indices in which different patterns of oxygen atoms are presented on the surface of distinct planes. The ice-binding specificities of AFPs on those planes are one of the major factor that governs their activities. Therefore, understanding the crystallography of adsorption become a vital subject to elucidate the structure-function relationships of AFP molecules. In 1991 Knight et al., introduced a simple and robust method for the determination of specific planes onto which AFP molecules specifically get adsorbed to alter the morphology and ice crystal growth kinetics. This method was named as ice-etching technique. This technique has recently been improved by using fluorescently labeled proteins instead of the normal protein solution (Garnham et al., 2010). Incorporation of fluorescent tags with the peptide molecules facilitated direct visualization of the AFP bound planes onto the ice crystal hemispheres under UV light. Such visualization eradicate the necessity

of sublimation of the water molecules from the outer surface of the AFP bound single ice hemispheres which was indispensable for observation of AFP bound planes in ice-etching technique. This modified method was denoted as fluorescence-based ice plane affinity (FIPA) analysis. In order to get insight of the AFP concentrations on the ice plane specificity the author performed FIPA analysis of bpAFP, rbpAFP and nfeAFP6 in the ***Chapter three***. The FIPA images visualized that nfeAFP was unable to show any concentration-dependent ice plane specificity within the concentration range 0.02-0.2 $mg{\cdot}mL^{-1}$. While, native and recombinant bpAFP displayed concentration-dependent interminable ice-binding specificity within concentration range 0.01-0.1 $mg{\cdot}mL^{-1}$. At lower concentrations ([bpAFP] ≤ 0.02) it showed similar but not identical FIPA pattern obtained for wfAFP (Basu et al., 2014) caused by the ice plane specificity of bpAFP towards prism and pyramidal planes. The AFP surmounted areas on the ice hemispheres increases with increasing protein concentrations. Thus, entirely fluorescent ice hemispheres were obtained at the latter concentration (0.10 $mg{\cdot}mL^{-1}$) of bpAFP, such hemispheres were obtained in the presence of hyperactive species, for example *Mp*AFP, *Tm*AFP, sbwAFP and *col*AFP (Basu et al., 2014; Hanada et al., 2014). These entirely fluorescent ice hemispheres implies the multiple ice-plane (including basal plane) binding of bpAFP in a concentration-dependent manner. This interminable ice-binding further affects the ice crystal size and shapes obtained in bpAFP solutions. The ice crystal shape converted to hexagonal trapezohedron to lemon-shaped and the size decreases to 35-5 μm in the presence of 0.5-25 $mg{\cdot}mL^{-1}$ of bpAFP. The basal plane binding of this rod like α-helical protein presumably be originated from the self-assembly or oligomerization of this peptide similarly to the Maxi (Sun et al., 2014). However, as far as author knows, this is the first AFP that bind onto the ice crystal planes in a concentration dependent-manner and this dissertation (and the manuscript ii) is the first report of such concentration dependency of ice plane specificity of any AFP.

It is well-known that, the target ligand of AFPs is the embryonic ice crystals. The AFP molecules specifically get adsorbed on to these embryonic ice crystals that elevates slightly the melting temperature and depresses the freezing temperature of respective crystal in non-colligative manner. It creates a gap between the melting and freezing temperature of the ice crystals formed in the presence of AFPs that denoted as thermal hysteresis (TH) activity. The TH is a concentration-dependent parameter that widely used for characterization of the activities of AFPs. The AFPs can exhibit 0.5-1.0^{o}C of TH at millimolar concentrations to ~6.0^{o}C of TH at sub-millimolar concentrations. Former group of AFPs known as moderately active whereas the latter one is denoted as hyperactive AFPs (Scotter et al., 2006; Middleton et al., 2012). The adsorption followed by inhibition is widely accepted mechanism for the TH caused by AFPs (Raymond and DeVries 1977). However, the mechanism of such adsorption of AFPs onto the ice surfaces are still under investigation. At least three different hypothesis have been proposed to explain the adsorption mechanism of AFPs, namely hydrogen bonding hypothesis (Yang et al., 1988), hydrophobic effect (Wen and

Laursen, 1992; Haymet et al., 1998; Baardsnes et al., 1999) and anchored clathrate hypothesis (Nutt and Smith, 2008). The latter one is the one of the major hypothesis employed to explain the mechanism of AFP adsorption in recent years. The presence of the semi-clathrate (Sun et al., 2014) and/or the anchored clathrate waters (Garnham et al., 2011) in AFPs emphasis this hypothesis. Further experimental evidences and studies on the structure-function relationships could enrich and establish a concrete adsorption mechanism of AFPs to ice surfaces. From this standpoint, the author examined the TH activities and factors affecting TH activity of bpAFP and rbpAFP in the ***Chapter four***. The concentration-dependent TH profile of this newly identified AFP displayed ordinary hyperbolic nature similarly to other fish AFPs (Davies and Hew, 1990). While, the bpAFP and rbpAFP showed a very high TH activity (2.5-3°C) compared to the known moderately active AFPs at higher protein concentrations. Remarkably, its interminable ice binding also altered the ice crystal busting, rapid growth of the AFP bound crystal at its freezing temperature, in concentration dependent manner. The typical needle-shaped busting along the *c*-axis of the ice bipyramids occurred at lower concentrations of bpAFP, such as 5 $mg \cdot mL^{-1}$. By contrast, in the presence of highly concentrated bpAFP the ice crystal burst started from certain spot near the center of ice crystal and kept the crystal growth toward the direction normal to *c*-axis, similarly to hyperactive AFPs (75-200 $mg \cdot mL^{-1}$ protein concentration). These characteristics concurrently categorize bpAFP as both the moderately and hyperactive AFP. This presumably be play a role to correlate and/or investigate the grounds that are responsible for such distinctive activities of AFPs though they are originated to serve same physiological function or environmental stress. However, the TH activities of bpAFP and rbpAFP were not significantly affected within a long range of pH (pH 3-10) and temperature (~60°C). Additionally, the α-helix of these peptide undergoes reversible denaturation within a temperature range 0-100°C. Such pH and temperature stability of this supersoluble peptide evoke its applicability in myriad scientific fields that includes *in vivo* or *in vitro* modification of the growth kinetics and morphology of the ice crystals.

The role of different amino acid residues of AFP sequence on their functional activities has been investigated through mutational analysis and advanced our knowledge about mechanism of action of AFPs. It helped to elucidate the role of hydrogen bonding and other amino acids except regularly spaced threonines in ice-binding of wfAFP (Wen and Laursen, 1992, 1993; Sicheri and Yang, 1995; Baardsnes et al., 1999; Haymet et al., 1999). These studies have been determined the ice binding site (IBS) of the α-helical type I AFPs consists the conserved alanine-rich face (including A^{17}) and adjacent regularly spaced four threonines. However, to date the individual role of two terminal threonines (Thr 2 and 35) of type I AFPs was not examined. From this perspective, the author mutated the threonine of the C-terminal end to valine (T2V) and characterized in the ***Chapter five***. This point mutation did not significantly affect the α-helical secondary structure or its thermal reversibility and pH stability. By contrast, this mutation reduced 30% of the TH activity and eradicate the

basal plane binding ability of bpAFP. These results pointed out the important role of threonine[2] for the functional activities of bpAFP.

It is acknowledged that the modification of ice crystal morphology and controlling their growth-kinetics are the major scientific challenges. The detrimental effects of ice growth are undesirable for both biological and materialistic processes. Biological systems require a plenty of liquid water to accomplish many reactions *in vivo* in cells and keep the fluidity of their body fluids. Formation of ice transfers the phase of water molecules from liquid to solid that disrupts such fluidity and creates pseudo-scarcity of liquid water threating the life of any living organisms (Douct et al., 2009). Such freezing and glacial damage also creates considerable risks during the preservation of cells and organs at freezing temperatures (Pegg, 2010). Long time preservations of food items at these temperatures enhance the formation of large ice crystals that deteriorates their quality and texture (Petzold and Aguilera, 2009). Therefore, understanding the functional activities and physicochemical properties of the ice crystal growth modifiers could offer to develop innovative strategies for cryoprotection, cryopreservation (Pegg, 2010), hypothermic preservation (Kamijima et al. 2013), anti-icing and deicing technologies. The biological ice crystal modifiers, antifreeze proteins (AFPs), can bind onto the surface of ice crystals to alter their morphology and arrest their growth. These activities of ordinary AFPs have been evaluated using two concentration-dependent parameters, thermal hysteresis (TH) and ice recrystallization inhibition (IRI). However, it has not been subjected a parameter to correlate TH and IRI, which helps understanding of the ice-binding ability of AFPs including defective species that cannot perfectly arrest the ice crystal growth. In the ***Chapter six***, the author introduced a new parameter named "critical ice shaping concentration (CISC)", a minimum concentration of an AFP species necessary to alter the shape of the ice crystals. The CISC and effective IRI concentrations (C_{eff}) of natural and recombinant type I, II and III fish AFPs were also examined in this chapter. The new parameter CISC is interrelated with the IRI and TH activity. Type I, II, III fish AFPs and their recombinant proteins can exhibit effective IRI at two fold concentrations of their CISC, for which the author made the assumptions that 1) CISC of AFP is a measure of primary adsorption ability onto the ice crystal surfaces to cause ice-shaping, while 2) IRI and TH are related with more AFP concentrations needed for both primary and secondary adsorptions to halt the ice crystal growth. The assumption of secondary binding of AFPs have also been made by Takamichi et al. (2007) and Dori et al. (2014). The adsorption mechanism and surface coverage of AFPs have been proposed by Kubota (2011) and the author (i and in this thesis). The relationship between the two functional activities of AFPs (TH and IRI) is highly debated (Sidebottom et al., 2000; Yu et al., 2010; Singh et al., 2014; Capicciotti et al., 2015). A recent study has been reported that there are no significant correlation between TH and IRI activity of AFPs (Olijve et al., 2016). While, the relationship of CISC with TH and IRI could correlate this two widely used concertation dependent parameters at least in their staring effective concentrations. It will be interesting to examine the correlation between IRI and TH through CISC.

7.2. Conclusion

The mechanism of action and structure-function relationship of AFPs have been studied for several decades to construct a concrete knowledge about their activities and evolution. Such knowledge have been enriched from the contribution of discovery of new AFP species and their characterization. This dissertation have provide the information of discovery a new AFP and describe its detailed characterization. This supersoluble AFP (bpAFP) consists 40 amino acid residues and three 11-residue consensus sequence TX_{10} (Where X is mostly alanines). This sequence and secondary α-helical structure categorized this peptide as type I fish antifreeze protein. To date, bpAFP is the only known type I AFP that offer (2.5-3°C) of TH activities at higher concentrations. Such high TH activities were measured only for hyperactive AFPs. Its showed concentration-dependent interminable ice binding specificity and reported as sole type I AFP that can bind onto the basal planes of the ice crystal. The secondary structure of this protein displayed reversible thermal denaturation and extreme pH stability. It was also active within a long range of pH and after heating at 100°C. These characteristics of bpAFP offer an epoch to elucidate the ice binding mechanism and basis of functional activities of hyperactive and moderately active AFPs more closely. It also have the hypothermic cell preservation ability reported by Kamijima et al. (2013), but the mechanism of such cell protection abilities of AFPs is still unknown. For which, mass purification of bpAFP could play an important role to investigate the mechanism of this newly found function of AFPs.

On the other hand, the correlation between another two forms of functions of the AFPs, TH and IRI, is highly debated. In addition there are some AFP species that failed to offer significant TH. This means TH is not a good measure to evaluate ice-binding ability of various AFPs. The alternative measure is IRI, however its evaluation protocol is not unified, and it highly depends on the experimental settings that requires huge amount of sucrose (~30%). Additionally, there are no known concentration-dependent parameter to correlate IRI and TH and evaluate the activities of the defective isoforms, the isoforms that can only change the morphology but failed to offer effective TH. While, concentration based comparative studies of different AFPs have been utilized to understand their functions. The introduction of newly concentration-dependent parameter CISC can not only correlate the IRI but it can also be used for comparative studies between defective and effective isoforms of different AFPs. The results obtained in this research suggest two assumptions, firstly, CISC of AFP is a measure of primary adsorption ability onto the ice crystal surfaces to cause ice-shaping, and secondly, IRI and TH are related with more AFP concentrations needed for both primary and secondary adsorptions to halt the ice crystal growth.

References

A

Ananthanarayanan VS and Hew CL (1977) Structural studies on the freezing point-depressing protein of the winter flounder *Pseudopleuronectes americanus*. *Biochem Biophys Res Commun*, 74:685-89

Chakrabarty A and Hew CL (1991) The effect of a-helicity on the activity of a winter flounder antifreeze peptide. *Eur J Biochem*, 202:1057-1063

Antson AA, Smith DJ, Roper DI, Lewis S, Caves LSD, Verma CS, Buckley SL, Lilford PJ and Hubbard RE (2001) Understanding the mechanism of ice binding by type III antifreeze proteins. *J Mol Biol*, 305:875-889

B

Baardsnes J, Kondejewski LH, Hodges RS, Chao H, Kay C and Davies PL (1999) New ice-binding face for type I antifreeze protein. *FEBS Letters* 463:87-91

Berg JM, Tymoczko JL and Stryer L (2002) *Biochemistry* (W. H Freeman and Company, New York)

Bayer-Giraldi M, Uhlig C, John U, Mock T and Valentin K (2010) Antifreeze proteins in polar sea ice diatoms: diversity and gene expression in the genus Fragilariopsis. *Environ Microbiol*, 12:1041-1052

Bar-Dolev M, Celik Y, Wettlaufer JS, Davies PL, Braslavsky I (2012) New insights into ice growth and melting modifications by antifreeze proteins. *J. R. Soc. Interface*, 9:3249-3259

Basu K, Garnham CP, Nishimiya Y, Tsuda S, Braslavsky I and Davies PL (2013) Determining the ice-binding planes of antifreeze proteins fluorescence-based ice plane affinity. *J Vis Exp* E51185:1-10

Basu K, Graham LA, Campbell RL and Davies PL (2015) Flies expand the repertoire of protein structures that bind ice. *Proc Natl Acad Sci USA* 112:737-742

C

Chen Y-H, Yang JT and Chau KH (1974) Determination of the helix and b form of proteins in aqueous solution by circular dichroism. *Biochemistry*, 13(16):3350-3359

Chakrabartty A, Hew CL, Shears M and Fletcher G (1988) Primary structures of the alanine-rich antifreeze polypeptides from grubby sculpin, *Myoxocephulus aenaeus*. *Can J Zool*, 66:403-408.

Cheng CH and DeVries AL (1989) Structures of antifreeze peptides from antarctuc eel pout, *Austrolycicthys brachyeephalus*. *Biochem Biophys Acta*, 997:55-64

Cheng CC (1998) Evolution of diverse antifreeze proteins. *Current Opinion in Genetics and Development*, 8:715-720

Chakrabartty A, Ananthanarayanan VS and Hew CL (1989a) Structure-function relationships in a winter flounder antifreeze polypeptide: I. Stabilization of an α-helical antifreeze polypeptide by charged-group and hydrophobic interactions.

J Biol Chem, 264:11307-11312Chakrabartty A and Hew CL (1991) The effect of a-helicity on the activity of a winter flounder antifreeze polypeptide. *Eur J Biochem*, 202:1057-1063

Chakrabartty A, Ananthanarayanan VS and Hew CL (1989b) Structure-function relationship in a winter flounder antifreeze polypeptide: II. Alteration of the component growth rates of ice by synthetic antifreeze polypeptides. *J Biol Chem*, 264, 11313-11316

Cooper TM and Woody RW (1990) The effect of conformation on the CD interacting helices: a theoretical study of tropomyosin. *Biopolymers*, 30:657-676

Chakrabartty A and Hew CL (1991) The effect of a-helicity on the activity of a winter flounder antifreeze polypeptide. *Eur J Biochem*, 202:1057-1063

Chao H, Hodges RS, Kay CM, Gauthier SY and Davies PL (1996) A natural variant of type I antifreeze protein with four ice-binding repeats is a particularly potent antifreeze. *Protein Science*, 5:1150-1156

Chao H, Huston ME, Hodges RS, Kay CM, Sykes BD, Loewen MC, Davies PL and Sönnichsen FD (1997) A diminished role of hydrogen bonds in antifreeze protein binding to ice. Biochemistry, 36:14652-14660

Celik Y, Graham LA, Mok YF, Bar M, Davies PL and Braslavsky I (2010) Superheating of ice crystals in antifreeze protein solutions. *Proc Natl Acad Sci USA* 107:5423-5428

Capicciotti CJ, Poisson JS, Boddy CN and Ben RN (2015) Modulation of antifreeze activity and the effect upon post-thaw HepG2 cell viability after cryopreservation. *Cryobiology*, 70(2):79-89

D

DeVries AL and Wohlschlag DE (1969) Freezing resistance in some Antarctic fishes. *Science* 163:1073-1075

Duman JG and DeVries AL (1974) Freezing resistance in winter flounder *Pseudopleuronects americanus*, *Nature*, 247:237-238

DeVries AL and Lin Y (1977) The role of glycopeptide antifreezes in the survival of Antarctic fishes. *In Adaptation within Antarctic Ecosystems*, G A Liano, Gulf Publishing Co., Huston, TX, 439-458

DeVeries AL (1984) Role of glycopeptides and peptides in inhibition of crystallization of water in polar fishes. *Phiol Trans R Soc Lond B Biol Sci*, B304:575-588

Davies PL, Hew CL (1990) Biochemistry of fish antifreeze proteins. *FASEB J* 4:2460-2468

Dingyi Wen and Richard A Laursen (1992) A model for binding of an antifreeze polypeptide to ice. *Biophysical J*, 63:1559-1562

Duman JG and Olsen TM (1993) Thermal hysteresis protein activity in bacteria, fungi and phylogenetically diverse plants. *Cryobiology* 30:322-328

Deng G, Andrews DW and Laursen RA (1997) Amino acid sequence of a new type of antifreeze protein, from the longhorn sculpin *Myoxocephalus octodecimspinosis*. *FEBS letters*, 402:17-20

Deng G. and Laursen RA (1998) Isolation and characterization of an antifreeze proteins from the longhorn sculpin, *Myxocephalus octodeceimspinosis*. *Biochimica et Biophysica Acta* 1388:305-314

DeLuca CI, Davies PL, Ye Q, and Jia Z (1998) The effects of steric mutations on the structure of type III antifreeze protein and its interaction with ice. *J Mol Biol, 275:515*-525

Duman JG (2001) Antifreeze and ice nucleator proteins in terrestrial arthropods. *Annu Rev Physiol* 63:327-357

Davies PL, Baardsnes J, Kuiper MJ and Walker VK (2002) Structure and function of antifreeze proteins. *Philos Trans R Soc Lond B Biol Sci*, 357:927-935

Doucet D, Walker VK and Qin W (2009) The bags that came in form the cold: molecular adaptations to low temperature insects. Cell Mol Life Sci. 66(8):1404-18

Doucet D, Walker VK and Qin W (2009) The bags that came in form the cold: molecular adaptations to low temperature insects. *Cell Mol Life Sci*, 66(8):1404-1418

Do H, Lee JH, Lee SG and Kim HJ (2012) Crystallization and preliminary X-ray crystallographic analysis of an ice-binding protein (FfIBP) from *Flavobacterium frigoris* PS1. *Acta Crystallogr Sect F Struct Biol Cryst Commun*, 68:806-809

Davies PL (2014) Ice-binding proteins: a remarkable diversity of structures for stopping and starting ice growth. *Trends in Biochemical Sciences*, 39(11):548-555

Dori R, Celik Y, Davies P and Braslavsky I (2014) Ice-binding proteins that accumulate on different ice crystal planes produce distinct thermal hysteresis dynamics. *J R Soc Interface*, 11:20140526

E

Ewart KV and Fletcher GL (1990) Isolation and characterization of antifreeze proteins from smelt (Osmerus Mordax) and Atlantic herring (*Clupea harengus harengus*). *Can J Zool*, 68:1652-1658

Evans RP and Fletcher GL (2001) Isolation and characterization of type I antifreeze proteins from Atlantic snailfish (*Liparis atlanticus*) and dusky snailfish (*Liparis gibbus*). *Biochim Biophys Acta*, 1547:23-244

F

Fletcher GL, Addison RF, Slaughter D and Hew CL (1982) Antifreeze proteins in the Arctic sculpin (*Myoxocephulus scorpius*). *Arctic*, 35:302-306

Fletcher GL, Hew CL and Davies PL (2001) Antifreeze proteins of teleost fishes. *Annu Rev Physiol* 63:359-390

Feller G and Gerday C (2003) Psychrophilic enzymes: hot topics in cold adaptation. *Nature Reviews Microbiology* 1:200-208

Freeman CL, Harding JH, Quigley D and Rodger PM (2012) Protein binding on stepped calcite surfaces: simulations of ovocleidin-17 on calcite {31.16} and {31.8}. *Phys. Chem. Chem. Phys.* 14:7287-7295

G

Greenfield N and Fasman GD (1969) Computed circular dichroism spectra for the evaluation of protein conformation. *Biochemistry*, 8(10):4108-4116

Griffith M, Ala PI, Yang DSC, Hon WC and Moffat BA (1992) Antifreeze protein produced endogenously in winter ray leaves. *Plant Physiology* 100(2):593-596

Gurian-Sherman D and Lindow SE (1993) Bacterial ice nucleation: significance and molecular basis. *The FASEB Journal* 7:1338-1343

Gong Z, Ewart KV, Hu Z, Fletcher GL and Hew CL (1996) Skin antifreeze protein genes of winter flounder, *Pseudopleuronects americanus*, encode distinct and active polypeptides without the secretory signal and prosequences. *J Biol Chem*, 271(8):4106-4112

Gronwald W, Chao H, Reddy DV, Davies PL, Sykes BD and Sönnichsen FD (1996) NMR characterization of side chain flexibility and backbone structure in the type I antifreeze protein at near freezing temperatures. *Biochemistry*, 35:16698-16704

Graham LA, Liou YC, Walker VK and Davies PL (1997) Hyperactive antifreeze protein from beetles. *Nature* 388:727-728

Gauthier SY, Kay CM, Sykes BD, Walker VK and Davies PL (1998) Disulfide bond mapping and structural characterization of spruce budworm antifreeze protein. *Eur J Biochem* 258:445-53

Graether SP, DeLuca CI, Baardsnes J, Hill GA, Davies PL and Jia Z (1999) Quantitative and qualitative analysis of type III antifreeze protein structure and function. *J Boil Chem*, 274:11842-11847

Gerbaud V *et al*. (2000) Mechanism of calcite crystal growth inhibition by N-terminal undecapeptide of lithiostathine. *J Biol Chem*, 275(2):1057-1064

Graether SP et al. (2000) Beta-helix structure and ice-binding properties of a hyperactive antifreeze protein from an insect. *Nature* 406:325-328

Griffith M and Yaish MWF (2004) Antifreeze proteins in over wintering plants: A tale of two activities. *Trends in Plant Science*, 9(8):399-405

Graether SP and Sykes BD (2004) Cold survival in freeze-intolerant insects: the structure and function of beta-helical antifreeze proteins. *Eur J Biochem* 271:3285-3296

Graham LA and Davies PL (2005) Glycine-rich antifreeze proteins from snow fleas. *Science* 310:461

Gilbert JA, Davies PL and Laybourn-Parry J (2005) A hyperactive, Ca^{2+}-dependent antifreeze protein in an Antarctic bacterium. *FEMS Microbiol Lett* 245:67-72

Gauthier SY, Marshall CB, Fletcher GL and Davies PL (2005) Hyperactive antifreeze protein in flounder species the sole freeze protectant in American plaice. *FEBS J*, 272:4439-4449

Garnham CP, Gilbert JA, Hartman CP, Campbell RL, Laybourn-Parry J and Davies, PL (2008) A Ca^{2+}-dependent bacterial antifreeze protein domain has a novel β-helical ice-binding fold. *Biochem J* 411:171-180

Granham CP, Natarajan A, Middleton AJ, Kuiper MJ, Braslavsky I and Davies PL (2010) Compound ice-binding site of an antifreeze protein revealed by mutagenesis and fluorescent tagging. *Biochemistry*, 49:9063-9071

Gwak IG, Jung WS, Kim HJ, Kang SH and Jin ES (2010) Antifreeze protein in Antarctic marine diatom, *Chaetoceros noegracile*. *Mar Biotechnol*, 12:630-639

Garnham CP, Campbell RL and Davies PL (2011) Anchored clathrate waters bind antifreeze proteins to ice. *Proc Natl Acad Sci USA*, 108:7363-7367

Graham LA, Hobbs RS, Fletcher GL and Davies PL (2013) Helical antifreeze proteins have independently evolved in fishes on four occasions. *PLoS ONE* 8:e81285

H

Hobbs PV (1974) *Ice Physics* (Oxford University Press, London), pp 18-39

Hew CL, Slaughter D, Joshi SB, Fletcher GL and Ananthanarayanan VS (1984) Antifreze polypeptides from the Newfoundland ocean pout, *Macrozoarces americanus*: presence of multiple and compositionally diverse components. *J Comp Physiol B Biochem Syst Environ Physiol*, 155:81-88

Hew CL, Joshi S, Wang N-C, Kao M-H and Ananthanarayanan VS (1985) Structures of shorthorn sculpin antifreeze polypeptides. *Eur J Biochem*, 151:167-172

Hew CL and Yang DSC (1992) Protein interaction with ice. *Eur. J. Biochem.* 203:33-42

Haymet ADJ, Ward LG, Harding MM and Knight CA (1998) Valine substituted winter flounder antifreeze- preservation of ice growth hysteresis. *FEBS letter*, 430:301-306

Haymet ADJ, Ward LG and Harding MM (1999) Winter flounder 'antifreeze' proteins: synthesis and ice growth inhibition of analogous that probe the relative importance of hydrophobic and hydrogen bonding interactions. *J Am Chem Soc*, 121:941-948

Houston ME, Chao Heman, Hodges RS, Sykes BD, Kay CM, Sönnichsen FD, Loewen MC and Davies PL (1998) Binding of an oligopeptide to a specific plane of ice. *J Biol Chem*, 273(19):11714-11718

Harding MM, Ward LG and Haymet ADJ (1999) Type I antifreeze proteins structure – activity studies and mechanisms of ice growth inhibition. *Eur J Biochem*, 264:653-665

Hoshino T, Kiriaki M, Ohgiya S, Fujiwara M, Kondo H, Nishimiya Y, Yumoto I and Tsuda S (2003) Antifreeze proteins from snow mold fungi. *Can J Bot*, 81:1175-1181

Hobbs RS, Shears MA, Graham LA, Davies PL and Fletcher LG (2011) Isolation and characterization of type I antifreeze proteins from cunner, *Tautogolabrus adspersus*, order Perciformes. *FEBS Journal*, 278:3699-3710

Hakim A, Nguyen JB, Basu K, Zhu DF, Thakral D, Davies PL, Isaacs FJ, Modis Y and Meng W (2013) Crystal structure of an insect antifreeze protein and its implications for ice binding. *J Biol Chem*, 288(17):12295-12304

Hanada Y, Nishimiya Y, Miura A, Tsuda S and Kondo H (2014) Hyperactive antifreeze protein from an Antarctic sea ice bacterium *Colwellia sp*. has a compound ice-binding site without repetitive sequences. *FEBS* J, 281:3576-3590

J

Jia Z, Deluca CI, Chao H and Davies PL (1996) Structural basis for the binding of a globular antifreeze protein to ice. *Nature*, 384:285-288

Jia Z, and Davies PL (2002) Antifreeze proteins: an unusual receptor–ligand interaction. *Trends Biochem Sci*. 27:101-106

Janech MG, Krell A, Mock T, Kang JS and Raymond J A (2006) Ice-binding protein from sea ice diatoms. *J Phycol*, 42:410-416

Jung W, Gwak Y, Davies PL, Kim HJ and Jin E (2014) Isolation and Characterization of Antifreeze Proteins from the Antarctic Marine Microalga *Pyramimonas gelidicola*. *Mar Biotechnol*, 16:502-512

K

Knight CA (1966) Formation of crystallographic etch pits on ice, and its application to the study of hailstones. *J Appl Meteorol*, 5(5):710-714

Kerr RA (1986) Ice cap of 30 million years ago detected. *Science* 224:141-142

Knight CA, Cheng CC and DeVries AL (1991) Adsorption of α-helical antifreeze peptides on specific ice crystal surface planes. *Biophysical J*, 59:409-418

Knight CA, Wen D and Laursen RA (1995) Nonequilibrium antifreeze peptides and the recrystallization of ice. *Cryobiology*, 32:23-34

Kristiansen E, Pedersen S, Ramløv H and Zachariassen KE, (1999) Antifreeze activity in the cerambycid beetle *Rhagium inquisitor*. *J Comp Physiol B* 169:55-60

Kawahara H, Nakano Y, Omiya K, Muryoi N, Nishikawa J and Obata H (2004) Production of Two Types of Ice Crystal-Controlling Proteins in Antarctic Bacterium. *J Biosci Bioeng* 98:220-223

Knight CA, DeVries AL: Ice growth in supercooled solutions of a biological 'antifreeze', AFGP 1-5: an explanation in terms of adsorption rate for the concentration dependence of the freezing point, Phys Chem Chem Phys, **11**, 5749-5761 (2009)

Kuntal BK, Aparoy P and Reddanna P (2010) Easymodeller: A graphical interface to modeller. *BMC Res Notes*, 3:226

Kristiansen E et al. (2011) Structural characteristics of a novel antifreeze protein from the longhorn beetle *Rhagium inquisitor*. *Insect Biochem Mol Biol* 41:109-117

Kubota N (2011) Effects of cooling rate, annealing time and biological antifreeze concentration on thermal hysteresis reading. *Cryobiology*, 63:198-209

Koga Y (2012) Thermal adaptation of the archaeal and bacterial lipid membranes. *Archaea* 2012:AI 789652

Kondo H, Hanada Y, Sugimoto H, Hoshino T, Garnham CP, Davies PL and Tsuda S (2012) Ice-binding site of snow mold fungus antifreeze protein deviates from structural regularity and high conservation. *Proc Natl Acad Sci USA*, 109:9360-9365

Kamijima T, Sakashita M, Miura A, Nishimiya Y and Tsuda S (2013) Antifreeze Protein Prolongs the Life-Time of Insulinoma Cells during Hypothermic Preservation. *Plos One*, 8(9):e73643

Kuiper MJ, Morton CJ, Abraham SE and Gray-Weale A (2015) The biological function of an insect antifreeze protein simulated by molecular dynamics. *eLife*, 4:e05142

L

Lau SYM, Taneja AK and RS Hodges (1984) Synthesis of a model protein of defined secondary and quaternary structure – effect of chain length on the stabilization and formation of two-stranded a-helical coiled-coils. *J Biol Chem*, 259:13253-13261

Liou YC, Tocilj A, Davies PL, and Jia Z (2000) Mimicry of ice structure by surface hydroxyls and water of a beta-helix antifreeze protein. *Nature* 406:322-324

Li Y, Gong H and Park HY (2000) Purification and partial characterization of thermal hysteresis proteins from overwintering larvae of pine needle gal midge, *Thecodilosis japonesis* (Dipetra: cecidomiidae). Cryo Letters 21:117-124

Li C, Guo X, Jia Z, Xia B and Jin C (2005) Solution structure of an antifreeze protein CfAFP-501 from *Choristoneura fumiferana*. *Journal of Biomolecular NMR*, 32(3):251-256

Lee JK, Park KS, Park S, Park H, Song YH, Kang S and Kim HJ (2010) An extracellular ice-binding glycoprotein from an Arctic psychrophilic yeast. *Cryobiology*, 60:222-228

Lin FH, Davies PL and Graham LA (2011) The Thr- and Ala-rich hyperactive antifreeze protein from inchworm folds as a flat silk-like β-helix. *Biochemistry* 50:4467-4478

M

Merutka G and Stellwagen E (1991) Effect of amino acid ion pairs on peptide helicity. *Biochemistry*, 30(6):1591-1594

Merutka G, Shalongo W and Stellwagen E (1991) A model peptide with enhanced helicity. *Biochemistry*, 30(17):4245-4248

Marshall CB, Fletcher GL and Davies PL (2004) Hyperactive antifreeze protein in a fish: This plasma protein offers the winter flounder extra protection against ice polar waters. *Nature* 429: 153

Marshal CB, Chakrabarty A and Davies PL (2005) Hyperactive antifreeze protein from winter flounder is a very long rod-like dimer of a-helices. *J of Biol Chem*, 280:17920-17929

Momma K and Izumi F (2008) A three-dimensional visualization system for electronic and structural analysis. *J Appl Cryst*, 41:653-658

Mok YF et al. (2009) Structural basis for the superior activity of the large isoform of snow flea antifreeze protein. *Biochemistry* 49:2593-2603

Middleton AJ, Marshall CB, Faucher F, Bar-Dolev M, Braslavsky I, Campbell RL, Walker VK and Davies PL (2012) Antifreeze protein from freeze-tolerant grass

has a beta-roll fold with an irregularly structured ice-binding site. *J Mol Biol* 416:713-724

N

Ng NF, Trinh KY and Hew CL (1986) Structure of an antifreeze polypeptide precursor from the sea raven, *Hemitripterus americanus*. *J Biol Chem*, 261:15690-15695

Nishimiya Y, Sato R, Takamichi M, Miura A and Tsuda S (2004) Co-operative effect of the isoforms of type III antifreeze protein expressed in Notched-fin eelpout, *Zoarces elongatus Kner*. *FEBS J*, 272:482-492

Nishimiya Y, Sato R, Takamichi M, Miura A and Tsuda S (2005) Co-operative effect of the isoforms of type III antifreeze protein expressed in Notched-fin eelpout, Zoarces elongates Kner. *FEBS J*, 272:482-492

Nishimiya Y, Kondo H, Takamichi M, Sugimoto H, Suzuki M, Miura A and Tsuda S (2008) Crystal structure and mutational analysis of Ca^{2+}-independent type II antifreeze protein from longsnout poacher, *Brachyopsis rostratus*. *J Mol Biol*. 382:734-746

Nutt DR and Smith JC (2008) Dual function of the hydration layer around an antifreeze protein revealed by atomistic molecular dynamics simulations. *J Am Chem Soc*, 130:13066-13073

O

Olijve LLC, Meister K, DeVries AL, Duman JG, Guo S, Bakker HJ and Voets LK (2016a) Blocking rapid ice crystal growth thorough nonbasal plane adsorption of antifreeze proteins. *Proc Natl Acad Sci USA*, 113(14):3740-3745

Olijve LLC, Vrielink ASO, Voets IK (2016b) A simple and quantitative method to evaluate ice recrystallization kinetics using the circular Hough transformation algorithm. Cryst Growth Des, **DOI:** 10.1021/acs.cgd.5b01637

P

Pearce RS (2001) Plant freezing and damage. *Ann Bot* 87:417-424

Pentelute BL et al. (2008) X-ray structure of snow flea antifreeze protein determined by racemic crystallization of synthetic protein enantiomers. *J Am Chem Soc* 130:9695-9701

Petzold G and Aguilera JM (2009) Ice morphology: Fundamentals and technological applications in foods. *Food Biophys*, 4(41):378-396

Patel SN and Graether PS (2010) Increased flexibility decreases antifreeze protein activity. *Protein Science*, 19:2356-2365

Pegg DE (2010) The relevance of ice crystal formation for the cryopreservation of tissues and organs. *Cryobiology*, 60:S36–44

R

Raymond JA and DeVries AL (1977) Adsorption inhibition as a mechanism of freezing resistance in polar fishes. *Proc Natl Acad Sci USA*, 74-2589-2593

Raymond JA, Wilson P and DeVries AL (1989) Inhibition of growth of nonbasal planes in ice by fish antifreezes. *Proc Natl Acad Sci U.S.A.* **86,** 881-885

Raymond JA, Fritsen C and Shen K (2007) An ice-binding protein from an Antarctic sea ice bacterium. *FEMS Microbiol Ecol*, 61:214-221

Raymond JA, Christner BC and Schuster SC (2008) A bacterial ice-binding protein from Vostok ice core. *Extremophiles*, 12:713-717

Raymond JA and Janech MG (2009) Ice-binding proteins from enoki and shiitake mushrooms. *Cryobiology*, 58:151-156

Raymond, J. A., and Kim, H. J. (2012) Possible Role of Horizontal Gene Transfer in the Colonization of Sea Ice by Algae. *PLoS One*, 7:e35968

Russo NVD, Estrin DA, Marti MA and Roitberg AE (2012) pH-dependent conformational changes in proteins and the effect on experimental pK_as: The case of nitrophorin 4. *PLOS Comp Bio*, 8(11):e1002761

Raymond JA and Morgan-Kiss R (2013) Separate Origins of Ice-Binding Proteins in Antarctic Chlamydomonas Species. *PLoS One*, 8:e59186

S

Shackleton NJ et al. (1984) Oxygen isotope calibration of the onset of ice-rafting and history of glaciation in the north Atlantic region. *Nature* 307:620-622

Scott GK, Flether GL and Davies PL (1986) Fish antifreeze proteins: recent gene evolution. *Can J Fish Aquat Sci* 43-1028-1034

Schrag JD, Cheng CH, Panico M, Morris HR and DeVries AL (1987) Primary and secondary structure of antifreeze peptides from Arctic and Antarctic zoarcid fishes. *Biochim biophys Acta*, 915:357-370

Scott GK, Davies PL, Shears MA and Fletcher GL (1987) Structural variations in the alanine-rich antifreeze proteins of the Pleuronectinae. *Eur J Biochem*, 168:629-633

Scott GK, Hayes PH, Flether GL and Davies PL (1988) Wolffish antifreeze protein genes are primarily organized as tandem repeats that each contain two genes in inverted orientation. *Mol Cell Biol*, 8:3670-3675

Shoemaker KR, Fairman R, York EJ, Stewart JM and Baldwin RL (1988) *Peptides: chemistry and biology*, edited by Marshall GR, Escom, Leiden, pp:15-20

Sun X, Griffith M, Pasternak JJ and Glick BR (1995) Low temperature growth, freezing survival and production of antifreeze protein by the plant growth promoting rhizobacterium *Pseudomonas putida* GR12-2. *Can J Microbiol* 41:776-784

Sicheri F and Yang DSC (1995) Ice-binding structure and mechanism of an antifreeze protein from winter flounder. *Nature*, 375:427-431

Sönnichsen FD, DeLuca CI, Davies PL and Sykes BD (1996) Refined solution structure of type III antifreeze protein: hydrophobic groups may be involved in the energetics of the protein-ice interaction. Structure, 4(11):1325-1337

Sönnichsen FD, Davies PL and Sykes BD (1998) NMR structural studies on antifreeze proteins. *Biochem Cell Biology*, 76:284-293

Smallwood M, Worrall D, Byass L, Elias L, Ashford D, Doucet CJ, Holt C, Telford J, Lillford P and Bowles JD (1999) Isolation and characterization of a novel antifreeze protein from carrot (Daucus carota). *Biochem J*, 340:385-391

Sidebottom C, Buckley S, Pudney P, Twigg S, Jarman C, Holt C, Telford J, McArthur A, Worrall D, Hubbard R and Lillford P (2000) Heat-stable antifreeze protein from grass. *Nature*, 406:256

Snider CS, Hsiang T, Zhao G and Griffith M (2000) Role of ice nucleation and antifreeze activities in pathogenesis and growth of snow molds. *Phytopathology*, 90:354-361

Sander LM and Tkachenko AV (2004) Kinetic pinning and biological antifreezes. *Phys Rev Lett*, 93:128102

Scotter AJ, Marshall CB, Graham LA, Gilbert JA, Granham CP and Davies PL (2006) The basis for hyperactivity of antifreeze proteins. *Cryobiology*, 53:229-239

Schroeder HW and Lisa Cavacini L (2010) Structure and function of immunoglobulins. *Journal of Allergy and Clinical Immunology*, 125(2):S348

Sharp, K.A. (2011) A peek at ice binding by antifreeze proteins. *Proc Natl Acad Sci*, 108:7281-7282

Sun T, Lin F-H, Campbell RL, Allingham JS and Davies PL (2014) An antifreeze protein folds with an interior network of more than 400 semi-clathrate waters. *Science* 343:795-798

Sharp KA (2014) The remarkable hydration of the antifreeze protein Maxi: A computational study. J Chem Phys, 141(22):22D510

Singh P, Hanada Y, Singh SM and S. Tsuda (2014) Antifreeze protein activity in Arctic bacteria. *FEMS Microbiol Lett*, 351:14-22

T

Tyshenko MG, Doucet D, Davies PL and Walker VK (1997) The antifreeze potential of the spruce budworm thermal hysteresis protein, *Nature Biotechnol* 15:887-890

Takamichi M, Nishimiya Y, Miura A and Tsuda S (2009) Fully active QAE isoform confers thermal hysteresis activity on a defective SP isoform of type III antifreeze protein. *FEBS J*, 276:1471-1479

Takamichi M, Nishimiya M, Miura A and Tsuda S (2007) Effect of annealing time of an ice crystal on the activity of type III antifreeze protein. *FEBS J*, 274:6469-6476

U

Urrutia ME, Duman JG and Knight CA (1992) *Biochim Biophys Acta*, 1121:199-206

V

Vinnikov KA, Ivankov VN and Pitruk DL (2007) taxonomic relations of three flounder species of subfamily Pleuronectinae of the Sea of Japan. Russian Journal of Marine Biology, 33(2):98-109

W

Wen D and Laursen RA (1992a) A model for binding of an antifreeze polypeptide to ice. *Biophys J*, 63:1659-1662

Wen D and Laursen RA (1992b) Structure-function relationships in an antifreeze polypeptide: the role of neutral, polar amino acids. *J Biol Chem*, 267:14102-14108.

Wen D and Laursen RA (1992c) A Model for binding of an antifreeze polypeptide to ice. *Biophys J*, 63:1659-1662

Wen D and Laursen RA (1993a) Structure-function relationships in an antifreeze polypeptide - the effect of added bulky groups on activity. *J Biol Chem*, 268:16401-16405

Wen D and Laursen RA (1993b) Structure-function relationships in an antifreeze polypeptide - the role of charged amino acids. *J Biol Chem*, 268:16396-16400.

Worrall D, Elias L, Ashford D, Smallwood M, Sidebottom C, Lillford P, Telford J, Holt C and Bowles D (1998) A carrot leucine-rich-repeat protein that inhibits ice recrystallization. *Science*, 282:115-117

Wharton DA (2002) *Life at the limits: organisms in extreme environments* (Cambridge University Press, Cambridge)

Wallimann P, Kennedy RJ, Miller JS, Shalongo W and Kemp DS (2003) Dual wavelength parametric test of two-state models for circular dichroism spectra of helical polypeptides: anomalous dichroic properties of alanine-rich peptides. *J Am Chem*, 125:1203-1220

Wathen B, Kuiper M, Walker V and Jia Z (2003) A new model for simulating 3-D crystal growth and its application to the study of antifreeze proteins. *J Am Chem Soc*, 125:729-737

Wang S., Wen X., Nikolovski P., Juwita V., Arifin J.F. (2012) Expanding the molecular recognition repertoire of antifreeze polypeptides: effects on nucleoside crystal growth. *Chem Commun (Camb)* 48:11555-11557

X

Xu H, Griffith M, Patten CL and Glick BR (1998) Isolation and characterization of an antifreeze protein with ice nucleation activity from the plant growth promoting rhizobacterium *Pseudomonas putida* GR12-2. *Can J Microbiol* 44:64-73

Xiao N, Suxuki K, Nishimiya Y, Kondo H, Miura A, Tsuda S and Hoshino T (2010) Comparison of functional properties of two fungal antifreeze proteins from *Antarctomyces psychrotrophicus* and *Typhula ishikariensis*. *FEBS J*, 277:394-403

Y

Yang DSC, Sax M, Chakrabartty A and Hew CL (1988) Crystal structure of an antifreeze polypeptide and its mechanistic implications. *Natur*e, 333:232-237

Yeh Y and Feeney RE (1996) Antifreeze proteins: structures and mechanisms of function. *Chemical Reviews*, 96(2):601-618

Yamashita Y, Nakamura N, Omiya K, Nishikawa J, Kawahara H and Obata H (2002) Identification of an Antifreeze Lipoprotein from Moraxella sp. of Antarctic origin. *Biosci Biotechnol Biochem* 66:239-247

Yamashita Y, Miura R, Takemoto Y, Tsuda S, Kawahara H and Obata H (2003) Type II antifreeze protein from mid-latitude fresh water fish Japanese smelt (*Hypomesus niponensis*). Biosci Biotechnol Biochem, 67:461-466

Yu SO, Brown A, Middleton AJ, Tomczak MM, Walker VK and Davies PL (2010) Ice restructuring inhibition activities in antifreeze proteins with distinct difference in thermal hysteresis. Cryobiology, 61(3):327-334

Z

Zhou NE, Kay CM and Hodges RS (1992) Synthetic model proteins – positional effects of interchain hydrophobic interactions on stability of two-stranded α-helical coiled-coils. *J Biol Chem*, 267:2664-2670

Zhang W and Laursen RA (1998) Structure-function relationships in a type I antifreeze polypeptide – the role of threonine methyl and hydroxyl groups in antifreeze activity. *J Biol Chem*, 273:34806-34812

Zhang W and Laursen RA (1999) Artificial antifreeze polypeptides: α-helical peptides with KAAK motifs have antifreeze and ice crystal morphology modifying properties. *FEBS Lett*, 455:372-376

Zhang D-Q, Liu B, Feng D-R, He Y-M and Wang J-F (2004) Expression, purification, and antifreeze activity of carrot antifreeze protein and its mutants. *Protein Expression and Purification*, 35:257-263

Zhao C-L, Porzio S, Smith A, Ge H, Davis HT and Scriven LE (2006) Direct observation of freeze-thaw instability of latex coatings via high pressure freezing and cryogenic SEM. *JCT Res*, 3(2):790-793

Accomplishments

Original manuscripts:

(i) Mahatabuddin S, Nishimiya Y, Miura A, Kondo H and Tsuda S (2016) "Critical ice shaping concentration: A new parameter to evaluate the activity of antifreeze proteins". *Cryobiology and Cryotechnology*, 62 (02):95-103

(ii) Mahatabuddin S, Hanada Y, Nishimiya Y, Miura A, Kondo H, Davies PL and Tsuda S "Concentration-dependent oligomerization of an α-helical polypeptide makes it hyperactive" *Scientific Reports*, 7, 42501 (DOI: 10.1038/srep42501)

(iii) Mahatabuddin S, Nishimiya Y, Miura A, Kondo H and Tsuda S "Introduction to critical ice shaping concentration (CISC): A new parameter to evaluate the activities of antifreeze proteins" (Manuscript in preparation)

(iv) Mahatabuddin S, Hanada Y, Nishimiya Y, Miura A, Aizawa T, Kondo H and Tsuda S "A super soluble 40-residual type I antifreeze protein consists an exceptionally pH stable and fully renaturable α-helix" (Manuscript in preparation)

(v) Mahatabuddin S, Hanada Y, Miura A, Kondo H and Tsuda S "Point mutation of threonine at the C-terminal end to valine diminishes the basal plane binding ability of supersoluble hyperactive type I antifreeze protein, bpAFP" (Manuscript in preparation)

Other publications:

(vi) Arai T, Cheng J, Mahatabuddin S, Kondo H and Tsuda S (2015), Observation of inhibitory effect of antifreeze protein on progressive freeze-concentration, *Cryobiology and Cryotechnology*, 61 (02), 121-124

Conference presentations:

1. Mahatabuddin S, Hanada Y, Miura A, Kondo H, and Tsuda S: Ice-accumulation ability of an alpha-helical peptide shows a significant concentration dependence. *The 3rd International Life Science Symposium*, Conference hall of Hokkaido University, Sapporo, Japan; 26 November/2015. (Oral presentation)

2. Mahatabuddin S, Ishihara K, Hanada Y, Miura A, Kondo H and Tsuda S: Expression and Characterization of a New Type I Antifreeze protein from a Japanese Fish. *The 2nd International Life Science Symposium*, Conference hall of Hokkaido University, Sapporo, Japan; 23 October/2014. (Oral presentation)

3. Mahatabuddin S, Ishihara K, Hanada Y, Miura A, Kondo H and Tsuda S: Functional Analysis of a New Type I Antifreeze Protein from Barfin plaice, *Liposetta pinnifasciata. The 52nd Annual Meeting of Biophysical Society Japan (BSJ)*, Sapporo Convention center, Sapporo, Japan; 25-27 September/2014. (Poster presentation)

4. Mahatabuddin S, Ishihara K, Hanada Y, Miura A, Kondo H and Tsuda S: A 40-residue Type I Antifreeze Protein exhibited an extremely high thermal hysteresis activity. 2nd *International Ice-Binding Protein Conference*, Conference hall of

Hokkaido University, Sapporo, Japan; 04-08 August/2014. (Poster and oral presentation)

5. Mahatabuddin S and Tsuda S: "Introduction of a new parameter critical ice shaping concentration (CISC) for evaluation of the activity of antifreeze proteins" *The 4th International Life Science Symposium*, Conference hall of Hokkaido University, Sapporo, Japan; 18 November/2016. (Oral presentation)

6. Fukami D, Mahatabuddin S, Kondo H, Miura A and Tsuda S: "Activity modification by mixing of antifreeze proteins" *The 4th International Life Science Symposium*, Conference hall of Hokkaido University, Sapporo, Japan; 18 November/2016. (Oral presentation)

7. Rahman AT, Mahatabuddin S, Ohyama Y, Kondo H and Tsuda S: "Quantitative methods to evaluate ice recrystallization inhibition rate using Ferret's diameter" *The 4th International Life Science Symposium*, Conference hall of Hokkaido University, Sapporo, Japan; 18 November/2016. (Poster presentation)

8. Takeyama M, Mahatabuddin S, Miura A, Kondo H and Tsuda S: "Cell preservation mechanism of fish type III antifreeze protein using artificial lipid bilayer" The 89th Annual Meeting of the Japanese Biochemical Society, Sendai International Center, Tohoku University, Japan; 25-27 September/2016 (Oral and poster presentation)

Acknowledgements

The highest echelon of the degree-based education is PhD, which consists a set of training to train an ordinary human being to a recognized researcher. The vital role of an excellent supervisor to train me in the way of achievement of the PhD degree is cordially accomplished by my respected supervisor **Professor Sakae Tsuda**. I would like to express my sincere gratitude to him for his scholastic and patient supervision. He supports me continuously during easy and difficult periods in perusing PhD. I am thankful to him for his valuable discussions (anytime when I want to), endless supports and providing the great ideas to find out easiest solution of toughest problems. He always encouraged me to keep patience in the tough situations arise for last three years. His attitude and way of thinking will remain as a great source of inspiration and enthusiasm for me throughout my whole life as a scientist.

I would like to acknowledge associate professor Dr. Hidemasa Kondo for his instantaneous advices, solution of my problems and thoughtful suggestions, those help me to perform my research and show me the way to utilize new experimental techniques. I am thankful to him for his kind supports in my daily life here in Sapporo.

I am thankful to Professor Makoto Demura and associate professor Tomoyasu Aizawa for their kind assistance to measure CD spectra, an indispensable part of this dissertation.

I am grateful for the technical assistances and guidance from Dr. Yuichi Hanada, Kazunari Ishihara, Mami Sakashita. I am also thankful to Ms. Ai Miura for her fundamental and administrative supports.

I would like to especially thank Ms. Mari Igarashi of OIAS and Ms. Jing Cheng for their kind assistances to convert Japanese documents in English and filled up numerous documents necessary to stay here in Japan.

I want to thank all current and past members of FPRG research group who have been involved with me in this laboratory and teach me Japanese and so on.

I am sincerely grateful to the **IGP-RPLS (International Graduate Program for Research Pioneers in Life Sciences)** and **Monbukagakusho: MEXT** for providing me all kinds of financial support.

I am also thankful to my former research supervisor, Professor Md. Abu Bin Hasan Susan, Chemistry Department, University of Dhaka, Bangladesh for his encouraging words and supports to make me interested in research.

I would like to offer heartiest appreciation to my beloved daughters Mubassira and Maisha for their patience waiting up to late nights to meet with me (that recharge myself) and never obstacle me to come to laboratory for conducting my research work.

Last but not least, my heartiest acknowledgements go to my Parents who taught me how to walk through a difficult path without causing any harm to other pedestrians and to my spouse Nilufar Easmin, who hold me tight when I passed any of troughs in the path of my success by inspiring me to follow my dreams.

Finally, I am undoubtedly grateful to Almighty ALLAH who guide me always to meet all of the aforementioned valuable persons in my way of life to achieve Doctoral degree.